Dear Editor,

Please find the revised version of the article *egu-2023-2010.*
In this document, we have attached our responses to the four reviews. The track-change version of the article is also available at the end. Added text is shown in blue underlined, while removed text in shown in red strikeout.

Note that we have corrected some typos in the revised manuscript (shown in the track-change version) and updated the deposited source code, as we have added some optimizations in response to the comment of referee 2 on numerical cost.

Best Regards,
Kévin Fourteau on behalf of all co-authors

We are thankfull Richard Essery for his constructive review. Please find below our point by point response to the review. The comment of the referee are shown in blue and our response in black below. Proposed modifications of the manuscript are shown in green with page and line numbering corresponding to the preprint version of the article.

I greatly enjoyed reading this paper. The method for efficiently coupling the nonlinear surface energy balance to the linear subsurface heat conduction is a clever piece of matrix algebra, but it is not just that; it directly relates to a point of contention in the lively interactive discussions of Brun et al. (2022) and Potocki et al. (2022) concerning the mass balance of the Everest South Col Glacier.

There are limitations, however. Many processes are generally handled sequentially in snow models (Clark et al. 2015), but this paper only couples two of them. Only idealized test cases are shown and not full model performance in real applications.
We agree with the reviewer that two of the limitations of this work (which were also pointed out by other reviewers and the editor) are that: (i) we only tightly-couple two processes (the SEB and the internal heat equation) and leave others (such phase changes or liquid water percolation) sequentially treated and (ii) that we only treat idealized test cases. We were also aware of this potential limitation when doing this study, and wondered if more realistic cases should be analyzed. We eventually decided to leave them out.
Our motivation behind this choice is to allow to focus on a single topic, namely the efficient numerical coupling of the SEB to the internal heat budget in a FVM framework. We worry that introducing other tight-couplings (such as phase changes while solving the heat equation) might make the role of coupling the surface and internal energy budgets less clear, and thus renders this point less-readily available for current FVM models, such as Crocus or COSIPY. Likewise, we decided to focus on test cases without comparisons to direct observations, as it is not be possible to decipher errors due to the numerical implementations (which is the focus of our paper) from errors due to the assumed physics, parametrizations, and forcings (which we do not and cannot not address in this study). Therefore, we think that to meaningfully analyze numerical implementations in terms of cost, accuracy and robustness, the use of simplified test cases is appropriate. We however agree that the test cases should not be too unrealistic if we want their results to be informative of how a numerical scheme might behave in a realistic settings. That it is why we have used realistic forcings and initial conditions.

We now specify our intention more clearly in the text, and clearly explain that our simplifying assumptions are meant to ease the comparison of the numerical implementations of the surface-internal energy budgets, but that our toy-model should not be viewed as proper a snowpack/glacier model as many important components are lacking.

P12 - L330
“Two simple examples, showcasing the differences between numerical treatments, are presented below. We note that these simulations cannot be considered as fully realistic simulations of a snowpack or glacier surface, as many processes, such as the deposition of atmospheric precipitation (rain or snow) or mechanical settling, are lacking. The goal is rather to provide a simplified setting in which the impact of the numerical implementation of the SEB can be analyzed. In the same idea, we do not attempt to compare the simulation results to field observations. Indeed, it would not be possible to decipher errors due to the numerical discretization (the focus of this paper) from errors due to the assumed physics, parametrizations and atmospheric forcings. Nonetheless, in order for

the results to still be informative of how a given numerical implementation might behave in a more realistic setting, we use realistic atmospheric forcing, initial conditions, and physical parametrizations. The first simulation is meant to highlight the behavior of the numerical models when simulating the SEB on a snow-free glacier. The second one focuses on the impact of the model implementations on the simulation of the energy budget of a seasonal snowpack, during the melting period."

From the test case results, I could take contrary conclusions that the added complexity of coupling is not needed and the standard skin-layer formulation is fine as long the time step is not made too large, which is well known ("not too large" could still be prohibitively small for thin layers, though).

Indeed, very reasonable results can be obtained with the standard skin-layer formulation as long as the time step is kept short enough to avoid instabilities. The same conclusion could be made for the Class 1 model (no surface), as long as the top cell is kept thin enough. As all models solve the same equations, they converge to the "true" solution when the spatial and temporal resolution are refined, and the tightly-coupled approach is not expected to yield a different solution.
However, we believe the property of the tightly-coupled approach to accept both large time steps and mesh sizes, while keeping a similar numerical cost, motivates it use over the standard approaches. A numerical stability analysis is provided at this end of this response that shows that the coupled-surface scheme is unconditionally stable, contrary to the standard-skin layer formulation, and thus does not to require the implementation of an adaptative time step strategy. This is now discussed more clearly in the revised manuscript and the numerical stability analysis provided in an appendix.

P21 - L503
"The unstable nature of class 2 models can be shown with a linear stability analysis, provided in Appendix E. Such analysis shows that class 2 models are only conditionally stable, and confirm that instabilities are favored in the case of large time steps and small mesh sizes. We stress that these oscillations can appear even if the time integration of the internal energy budget relies on the Backward Euler method, known for its robustness against instabilities (Fazio, 2001, Butcher, 2008). Our understanding is that the sequential treatment of the standard skin-layer formulation breaks the implicit nature of the time integration by using "lagged" (in other words, explicit rather than implicit) terms. This, combined with the fact that the surface layer does not possess any thermal inertia and that its temperature can thus vary rapidly in time, permits large temperature swings if the time step is too large or the mesh size too small. On the other hand, it can be shown that the two schemes with a tightly-coupled SEB are unconditionally stable (Appendix E), in agreement with the absence of oscillations in their simulations. Notably, the unconditional stability of the coupled-surface scheme proposed in this article entails that the model does not need an adaptive time step size strategy depending on the mesh size. This ensures that it remains robust, regardless of the time step and mesh size.

P26 - L563
"Moreover, a tightly-coupled treatment of the SEB allows unconditional stability, while the standard skin-layer formulation can be unstable and displays large spurious oscillations with large time steps and small mesh sizes."

Specific comments:

Author list
"Brun Fanny" might like to have her name turned around.
We put Fanny's name in the good order.

Introduction

I don't recommend writing a comprehensive review of SEB formulations, but only giving recent examples of applications of a skin layer and no examples using a finite surface layer in the introduction, rather than original model development papers, gives a distorted view. An uncoupled skin layer has been in use for snow models at least as far back as Yamazaki and Kondo (1990). There is a snow surface layer temperature in Anderson (1968).
We added older model development papers in the revised manuscript. Notably we now provide references when discussing finite-top-layer models.

P1 - L20
"To reach this goal, the representation and evolution of the thermodynamical state (that is to say temperature profiles and phase changes) of snowpacks and glaciers are implemented in most numerical snowpack/glacier models (e.g. Anderson, 1976, Brun et al. 1989, Jordan, 1991, Bartelt and Lehning 2002, Liston and Elder, 2006, Vionnet et al. 2012, Sauter et al., 2020)."

P2 - L40
"On the other hand, some FVM implementations do not define a specific temperature associated with the surface, but rather use the temperature of the top-most numerical layer of the domain (i.e. the top layer of the simulated snowpack/glacier) for solving the SEB (Anderson, 1976, Brun et al., 1989, Jordan, 1991, Vionnet et al., 2012, van Kampenhout et al., 2017)."

22- There are many "numerical models" that are not snowpack/glacier models.

We reformulated the sentence to clearly state that by "most numerical models", we want to refer to snowpack/glacier models.

P1 - L20
"To reach this goal, the representation and evolution of the thermodynamical state (that is to say temperature profiles and phase changes) of snowpacks and glaciers are implemented in most numerical snowpack/glacier models "

32- The surface energy balance is described as "profoundly non-linear". Actually, this is a pretty benign nonlinearity in the field of nonlinear equations; it does not have multiple or chaotic solutions.
We removed the word "profoundly" to only state the problem is non-linear, and hence might requires some iterations for the proper solution to be computed.

49- The "infinitely small horizontal layer" would be better described as infinitely thin.
We replaced "small" with "thin".

While Eq. (1) is more generally applicable, it could already be emphasized that this is invariably implemented as a 1D model with T a function of z.

Consistently, with the remark of Reviewer 3, we now state that while the equation remains valid in 3D, we use it in a 1D set-up only as transitionally done in snowpack/surface-glaciers models.

P3 - L70

"In this article, we assume that the snowpack/glacier can be represented as 1D column, and therefore Eq. (1) should be understood as 1D equation."

I think that there will be very few exceptions to this "usually" of allowing snow temperature to exceed the fusion point before calculating melt, but there are examples of models with phase changes over a temperature range in Albert (1983) and Dutra et al. (2010).

As also pointed out by the review of Michael Lehning, several strategies have been proposed to handle phase change in snowpack/glaciers models. We modified the revised manuscript to clearly state that we rely on the method of exceeding the fusion point and then restoring thermodynamic equilibrium as it employed in the majority of snowpack/glacier models, but that alternatives exist. We now also stress that this method of "overshooting" is a form a sequential treatment, to which better treatments have been proposed in the recent literature. Building on this idea, we are currently working on the efficient tightly-coupled resolution of all internal thermodynamic processes, and will address it in a future work.

P3 - L82

"In this article, we follow this simple scheme as it is commonly employed in snowpack and glacier models. That being said, other, more complex, strategies have been proposed in the literature. This notably includes the use of a finite temperature-range over which melt/freezing occurs (e.g. Albert, 1983, Dutra et al., 2010), including melt/refreeze as an additional energy source term (e.g. Bartelt and Lehning, 2002, Wever et al., 2020), or the use of enthalpy as the prognostic variable (e.g. Meyer and Hewitt, 2017, Tubini et al., 2021)."

We have also estimated the sensitivity of our results to the treatment of these phase changes. We found that the conclusions of the article concerning the accuracy and stability of the different SEB schemes hold with a different treatment of phase changes (graphs provided in the response to the review of Michael Lehning). We now address this point in the revised manuscript:

P12 - L329

"Also, as some of the current snowpack and glacier models include the effect of internal phase-change while solving the internal heat equation (e.g. Bartelt and Lehning, 2002, Meyer and Hewitt, 2017), we quantified the sensitivity of our results to this specific treatment of melt/freeze. For that, we have also implemented versions of our three models that include such internal phase-changes in the heat equation."

P16 - L441

"Finally, using the versions of the models including phase-changes in the heat equation, we quantified the sensitivity of these observations to the treatment of the melt/refreeze. While the simulated temperature sometimes differ from our basic implementations (especially in the snowpack test case where melt occurs internally), the general behavior of the models, including the potential presence of instabilities in the Class 2 models, remain unchanged."

P20 - L493

"Finally, using the versions of the models including phase-changes in the heat equation, we verified that the conclusions of this convergence analysis remain valid in the case of a different treatment of the internal phase-changes"

136- "SNTHERM (Jordan, 1991), Crocus (Vionnet et al., 2012)"

The typo is corrected.

146- Another step is required if the calculated melt exceeds the available snow mass.

It is indeed important that the local calculated melt does not exceed the available snow mass. In our implementation, if the local melt exceeds the snow mass, layers are locally merged until the melt falls behind the available snow mass. This is now specified in the manuscript.

P12 - L323

"This remeshing step is also used to ensure that the melt of a layer cannot exceed its ice content. If such a case is encountered, the layer is merged with one of its neighbors before attempting melting. If the total melt exceeds the total mass, the simulations should be stopped. However, this last case did not arise in the simulations presented here."

234- LWout and H are given as examples of fluxes that are nonlinear in the surface temperature; L should also be mentioned as intrinsically nonlinear. H as defined by Eq. (B1) is only nonlinear if C_H is a function of surface temperature. It is, through Ri_b here, but models often neglect this nonlinearity because of the complexity of the resulting derivatives; it is not clear if that is done here. A supplement giving the elements of the Jacobian might be a useful addition.

We added L in the list of SEB terms that are non-linear with respect to the temperature.

In our implementation, we take into account the dependence of C_H to the surface temperature and include its impact on the Jacobian of the system (in order to have a true Newton method with quadratic convergence). Note that not taking this dependence in the Jacobian does not modify the solution of the non-linear system, but only the sequence of iterations and the convergence rate toward this solution.

To make our model readily-available we explicitly wrote the terms of the Jacobian in the new Appendix A.

P11 - L275

"The expressions of the matrices forming the block system are given in Appendix A, including the derivatives necessary for Newton's method."

261- I understand the problem, but I don't understand the benefit of returning the solution to the vicinity of the discontinuity.

The SEB should have a unique solution, but the Newton method is not guaranteed to find it. It can get trapped in a cycle of states around the solution. This situation can be diagnosed from the SEB, but I think that most models just give up and select the last iteration. Does the modified Newton method avoid this problem?

Yes, the goal of the truncation method is precisely to avoid the iterations to be stuck in a loop or to diverge and is quite adapted for the solving of the SEB with a fictitious variable. We've made a Figure as illustration below (the SEB non-linearity has been exaggerated for the illustration). In the case of the standard Newton method without truncation, the break in the slope can send the iterations far from the solution (or into loops depending of

the configuration). In the truncation case, the iteration is moved to the orange point after two truncations. At this point, the Newton scheme can converge normally to the solution.

P9 - L251

"The idea behind truncation is that the Jacobian (i.e. the derivative of the equations with respect to the unknowns to be solved for) computed on one side of a derivative discontinuity does not apply on the other side, and can therefore perturb the convergence towards the solution, typically leading to an endless iteration loop."

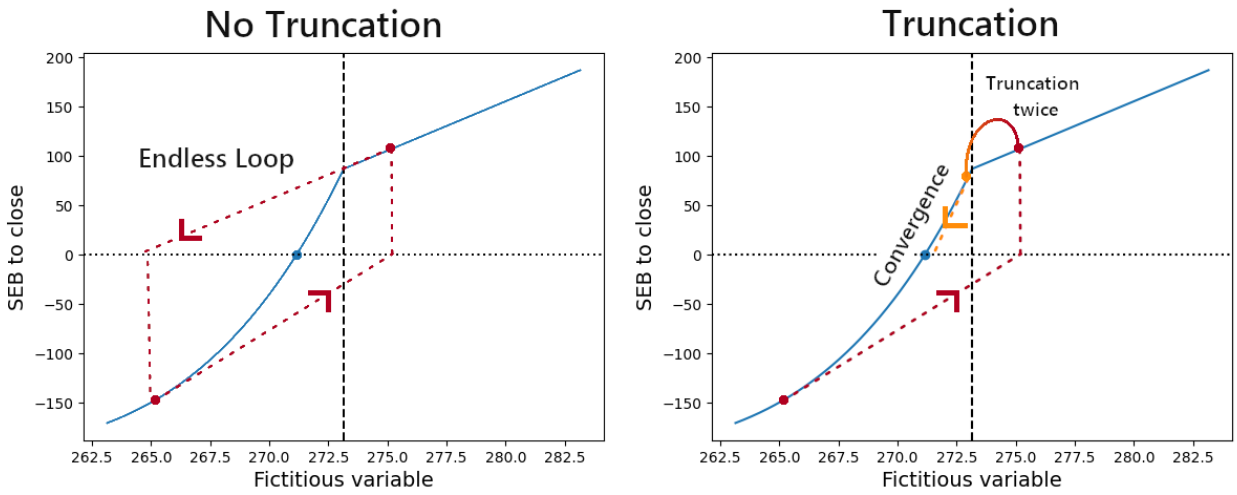

Figure – *Solving of a non-linear SEB with and without a truncation in Newton's method. In the truncation case, the estimation is brought from the red point to the orange point after two successive truncations.*

Note that Newton's method can be made even more robust by applying a truncation at the inflection points. However, this was not done in our case, as the SEB does not displays such inflection point with respect to the surface temperature.

265- Another solution in use, with its own numerical errors, is to linearize the SEB and solve it in one step without iteration (e.g. Best et al. 2011). This is essentially the Penman-Monteith method.
Equation (11) and following

Indeed, some models only solve the linear system with one iteration (for instance Crocus). However in this case, the obtained solution is not the actual backward Euler solution and does not have all its properties. We mention this point in the article.

P9 - L236

"We also note that some models made the choice of performing only a single iteration to solve this linear system of equations (with sometimes an extra iteration to handle specific cases, such as surface melting). However, we chose here to perform multiple iterations, in order to obtain the actual Backward Euler solution."

Be consistent in making diag, up and low superscripts or subscripts.

We corrected the manuscript consistently, with all diag, up, and low being subscripts.

284- "The above equation" is Eq. (13).

We modified the text to state that the "above equation" refers to Eq. (13) and that it allows one to solve the first temperature, as if they were solved with the complete system of Eq. (11).

P11 - L284

"The system of Eqs.(13) is a 2x2 non-linear system where only A_s and B_s need to be re-assembled at each non-linear iteration and whose solution for U_s is the same as the large system of Eqs. (11)."

286- "invert A_diag"

Following a comment of Reviewer 2 n the numerical efficiency of the method, we have proposed to partly rewrite the part of the article detailing the Schur-complement technique. This portion now reads:

P11 - L286

"[…] (ii) compute the products A_{diag}^{-1} B_{int} and A_{diag}^{-1} A_{up} (which is cheaper than directly inverting A_{diag}, (iii) iteratively [...]"

322- "cells which then become"

We wanted to write: "that merges adjacent cells when **they** become smaller than a given threshold". We modified the manuscript accordingly.

379- No refreeze in this test case.

Indeed, in the glacier test case, there is not refreeze as all water is sent to runoff. This will be mentioned in the text.

We still define the phase change rate in terms of melt and refreeze (general definition) and precise that in the glacier test case there is no refreezing.

P14 - L381

"Note that in this specific test case, no refreezing was observed (as melt occurs at the surface and is sent to runoff), meaning that the phase change rate directly corresponds to the melt rate."

421- "Concerning the glacier test-case, Fig. 3 shows"

We corrected the typo.

424- "by about 0.50 K"

We corrected the typo.

440- I have, indeed, seen time step oscillations like this in class 2 simulations. They are not the same as the well-known and catastrophic instability of the explicit Euler method with too large a timestep. Considering the wide use of class 2 models, a stability analysis to understand the origin of these oscillations (not necessarily for this paper) might be of interest.

To better explain the instabilities in Class 2 models we have performed a stability analysis, akin to the ones classically performed for the Forward/Backward Euler scheme. It is provided as the end of this response.

It shows that the standard skin-layer scheme is only conditionally stable, and that there is exist a maximum time step size. The presence of instabilities is favored in the case of large thermal conductivities or of a large derivative of the atmospheric fluxes with respect to the surface temperature in the SEB. On the contrary, these instabilities are hindered in the case of large cell sizes or large specific thermal capacity.

We believe this instability is of the same nature as the one observed with an explicit time-stepping, as it arises from the use of the first internal temperature from the previous time step in the computation of the subsurface heat flux. If the internal temperature from the

current time step is used instead (as in the scheme we propose), this instability is removed.

As mentioned above, the demonstration of the (un)conditional stability of the schemes is now presented in the new Appendix A and discussed in the text.

P21 - L503
"The unstable nature of class 2 models can be shown with a linear stability analysis, provided in Appendix E. Such analysis shows that class 2 models are only conditionally stable, and confirm that instabilities are favored in the case of large time steps and small mesh sizes. We stress that these oscillations can appear even if the time integration of the internal energy budget relies on the Backward Euler method, known for its robustness against instabilities (Fazio, 2001, Butcher, 2008). Our understanding is that the sequential treatment of the standard skin-layer formulation breaks the implicit nature of the time integration by using "lagged" (in other words, explicit rather than implicit) terms. This, combined with the fact that the surface layer does not possess any thermal inertia and that its temperature can thus vary rapidly in time, permits large temperature swings if the time step is too large or the mesh size too small. On the other hand, it can be shown that the two schemes with a tightly-coupled SEB are unconditionally stable (Appendix E), in agreement with the absence of oscillations in their simulations. Notably, the unconditional stability of the coupled-surface scheme proposed in this article entails that the model does not need an adaptive time step size strategy depending on the mesh size. This ensures that it remains robust, regardless of the time step and mesh size.

P26 - L563
"Moreover, a tightly-coupled treatment of the SEB allows unconditional stability, while the standard skin-layer formulation can be unstable and displays large spurious oscillations with large time steps and small mesh sizes."

460- "only marginally worse"
What we wanted to say here, is that sometimes the Class 2 model yield smaller error than the coupled-surface scheme, but when it do so it is only be small margin (which then justifies the use of a coupled-surface model in general). This was visibly not clearly phrased, as Micheal Lehning had the same remark. We rephrased the sentence to:

P17 - L458
"For almost all investigated time steps and in both test cases, the newly proposed scheme displays the lowest level of errors. Sometimes, the class 2 model yields the smallest error, but does so only by a small margin."

We have also re-formulated a similar sentence later in the manuscript.

P20 - L481
"Again, among the three implementations the tightly-coupled surface model yields the smaller errors for almost all investigated mesh refinements (as in the glacier test case, the class 2 model is however sometimes marginally better)."

490- Divergence of the class 2 model from the reference as the mesh is refined in the glacier test case (Fig. 10) is an odd result. I guess that this could happen if the time step in these mesh refinement tests is larger than in the reference. If so, this needs to be stated in the text.

We believe the increase of error with smaller mesh size st a result of numerical instabilities, that develop with small mesh sizes. This is now mentioned in the revised manuscript:

P20 - L490
"Finally, Fig. (10) reveals that in the glacier test case, the phase change rate errors of the class 2 tend to deteriorate with further mesh refinement past a certain point (here for an initial cell number above 90). We interpret this deterioration as a result of the appearance of numerical instabilities that develop with small mesh sizes."

Having said that, it is not apparent that the 225 cell simulation is worse than the one with 45 cells in Fig. 10c.
There are periods in Fig. 10c where the error in the 225 cells simulation is larger than the 45 cells. This is notably the case from mid-June to late-August.

504- "the backward Backward Euler method" sounds like it goes forward. Just one "backward" required.
Indeed. This is now corrected.

509- "mesh size too small"
We corrected the typo.

6.4- Having found G from the SEB, the obvious thing to do in a class 2 model is to use it as a flux boundary condition for the internal temperature calculations. Can any real class 2 model be found that uses the surface temperature as a Dirichlet boundary condition? If not, section 6.4, Fig. 14 and the last sentence of the conclusion should be deleted. A note that this would be the wrong thing to do will suffice.
The potentiality of using the surface temperature as a Dirichlet condition rather than the subsurface conduction flux was made aware to us from reading the publicly available COSIPY code (cosipy/modules/heatEquation.py files, last accessed 08/11/2023) and EBFM codes. However, we stress that these codes use a Forward Euler time stepping, and in this case the using the sub-surface conduction flux or a Dirichlet condition are equivalent.

We think it is important to mention and show that using a Dirichlet condition will lead to greatly deteriorated simulations, as the use of a Dirichlet condition actually numerically stabilizes the system (which can be seen with the absence of instabilities in the orange curve of Fig. 14 and can be demonstrated with a stability analysis, provided at the end of this document). However, this stabilization is at the detriment of accuracy and energy conservation.

We propose to better justify in the manuscript that the use of a Dirichlet condition might be tempting to obtain stability, but that it will produce large errors in response. We have also shorten the first part of the section:

P23 - L511
"As explained in Section 2.2, the heat conduction flux from the surface to the interior of the domain (i.e. G in Equation 3) needs to have the same value in the computation of the SEB and in the computation of the energy budget of the first interior cell. Inconsistencies in G between these two budgets lead to the violation of energy conservation and create an artificial energy source/sink near the surface. Such inconsistencies could be created when implementing the standard skin-layer formulation (class 2 models) due to the sequential

treatment of the surface and internal energy budgets. Indeed, after solving the SEB, one can either use the surface temperature or the subsurface heat flux G as a boundary condition for the computation of the internal temperatures. We note that the use the computed surface temperature as a boundary condition leads to an unconditionally stable numerical scheme (Appendix E). However, using such Dirichlet condition in order to stabilize the standard-skin layer formulation comes at the expense of energy conservation and deteriorates of the simulated results."

Search the text for ", that". In all but one case, it should be "that" or ", which".
This has been corrected.

Albert (1983): https://apps.dtic.mil/sti/pdfs/ADA134893.pdf

Anderson (1968): https://agupubs.onlinelibrary.wiley.com/doi/abs/10.1029/WR004i001p00019

Best et al. (2011): https://gmd.copernicus.org/articles/4/677/2011/

Clark et al. (2015): https://agupubs.onlinelibrary.wiley.com/doi/full/10.1002/2015WR017200

Dutra et al. (2010): https://doi.org/10.1175/2010JHM1249.1

Yamazaki and Kondo (1990): https://doi.org/10.1175/1520-0450(1990)029<0375:APMFSS>2.0.CO;2

We are grateful to the referee for their constructive review. Please find below our point by point response to the review. The comment of the referee are shown in blue and our response in black below. Proposed modifications of the manuscript are shown in green with page and line numbering corresponding to the preprint version of the article.

Summary:

This work proposes a methodological improvement to surface energy balance modeling over frozen ice surfaces by merging the benefits of two diverging current approaches to coupling air temperature and ice temperature. The coupling approach appears effective and insightful and is an important contribution to the field. The paper presents two case studies, one over snow and one over a glacier (with highly idealized implementations) as demonstrations of the accuracy. There is a well motivated exploration of the implementation's dependence on time and spatial resolution, which are not only practically important for anyone wishing to implement this method, but also provide the opportunity to discuss numerical stability.

General comments:

It is exciting to see this paper address both snowpack and glacier surface energy balance. It would be good to discuss (briefly) the physical similarities and differences (structure, air content) between the two.
We have added to the manuscript that snowpacks and glacier surfaces can be modeled in a similar framework as they share (i) the same fundamental governing equation (i.e. the energy conservation equation with heat conduction and shortwave absorption as a processes), and (ii) a first order phase change transition, where melt/refreeze occurs with latent heat. These similarities have already been used in the literature to treat snow and glacier ice in a unified framework, for instance in the model COSIPY. However, snowpacks and glacier surfaces present some differences that might complexify this unified treatment, for instance the fact that water does not percolate similarly in snow and glacier ice or that vapor movement plays a role significant role in snow but not in glacier ice.

We revised the manuscript to:

P3 - L60
"As snowpack and glaciers share many similarities and processes, such as heat conduction or the presence of a phase transition when the melt temperature is reached, they can be represented by the same type of equations. These similarities enable simulations mixing snow and glacier ice within a single framework (e.g. Sauter et al., 2020). Hence, for the sake of generality, the equations discussed in the following sections apply to both snow and glacier ice. That being said, snow and glacier ice present some differences, notably concerning liquid water percolation. As addressed later, this might require a differential treatment of glacier ice and snow when implementing the liquid water percolation scheme."

There is a consistent overuse of commas in the setup ',that' (many of which should be 'which' with no comma)
This was also pointed out by the review Richard Essery. This is now corrected.

The manuscript is clearly structured in introducing a new method to approach temperature and melt numerical modeling and then applying that method to two test cases. However, the test cases are very specific and thus convey limited information about the broader

application of the method – these limitations should be discussed, especially as a future goal would likely be to apply this numerical routine to more complicated cases.
This point was also stressed in the review of Richard Essery. We were also aware of this potential limitation when doing this study, and wondered if more realistic cases should be analyzed. We however decided to limit this study to simple idealized cases. Our goal behind this choice was to provide simple cases from which the impact of the numerical implementation can be clearly analyzed.

We also decided not to include comparisons with direct observations. Indeed, it would not be possible to decipher errors due to the numerical implementations (which is the focus of our paper) from errors due to the assumed physics, parametrizations, and forcings (which we do not and cannot not address in this study). Therefore, we think that to meaningfully analyze numerical implementations in terms of cost, accuracy and robustness, the use of simplified test cases is appropriate. We however agree that the test cases should not be too unrealistic if we want their results to be informative of how a numerical scheme might behave in a realistic settings. That it is why we have used realistic forcings and initial conditions.

We revised the manuscript to specify our intention more clearly. We explain that our simple test cases are meant to ease the comparison of the numerical implementations of the surface-internal energy budgets, but that our toy-model should not be viewed as proper a snowpack/glacier model as many important components are lacking.

P12 - L330
"Two simple examples, showcasing the differences between numerical treatments, are presented below. We note that these simulations cannot be considered as fully realistic simulations of a snowpack or glacier surface, as many processes, such as the deposition of atmospheric precipitation or mechanical settling, are lacking. The goal is rather to provide a simplified setting in which the impact of the numerical implementation of the SEB can be analyzed. In the same idea, we do not attempt to compare the simulation results to field observations. Indeed, it would not be possible to decipher errors due numerical discretization (the focus of this paper) from errors due to the assumed physics, parametrizations and atmospheric forcing. Nonetheless, in order for the results to still be informative of how a given numerical implementation might behave in a realistic setting, we use realistic atmospheric forcings, initial conditions, and physical parametrizations. The first simulation is meant to highlight the behavior of the numerical models when simulating the surface energy balance on a snow-free glacier. The second one focuses on the impact of the model implementations on the simulation of the energy budget of a seasonal snowpack, during the melting period."

Lastly, the finding that a coupled surface model can outperform other models at coarser grid sizes is implied here to be more computationally efficient due to the change in mesh size. However, this is not generally true when you are also changing the numerical scheme, so the assertion of computational cost savings which maintaining accuracy (as claimed here) should be backed up by either reports of the time taken for the computations and/or a clear statement that the numerical implementations are computationally identical by construction. This, if true, should also be mentioned in the conclusion as it is an important outcome! This is somewhat related to the discussion of numerical reduction (back to the same order of the original models) that you get from the Schur complement, but they are not discussed together and the data are not shown.
To answer this question we have computed the number of basic operations (addition/substraction and multiplication/division) required to perform the linear algebra

problem solvings of the three presented models, including the use of Schur-complements. The exact number are now presented in the new Appendix A and discussed in the article. We found that in terms of operations the standard skin-layer scheme requires about 40% less operations than the coupled-surface and no-surface schemes (which both require very similar number of operations). The last two schemes are more computationally expensive as they require the extra computation of the Schur-complement that is a bit more costly than the standard inversion used in the standard-skin layer formulation. Therefore, and based on the Figures 5 to 9, the introduction of a coupled degree of freedom at the surface (to transform a Class 1 into the coupled-surface scheme) is an interesting numerical trade-off, as it only marginally increase the numerical cost of the method while allowing coarser meshes. Concerning the standard skin-layer models, the trade-off of transforming into a coupled-surface scheme is not as evident as the numerical cost is multiplied by a bit less than 1.70. It allows the use of large time steps, without numerical instabilities, but at the expense of an increased number of steps.

We propose to discuss in more details the numerical cost of the methods in Section 4.1.1

P11 - L294
"An analysis of the numerical cost (in terms of number of basic operations) of this numerical scheme is given in Appendix A, alongside analyses of the numerical cost of Class 1 and 2 models. It shows that the proposed scheme and the Class 1 models have similar numerical costs, which a bit less than 1.7 times larger than the standard-skin layer."

in the conclusion:
P25 - L551
"Furthermore, a reduction technique, based on the computation of a Schur complement, is presented so that the numerical cost of the proposed framework remains of the same order as that of the standard implementations for the same mesh. In particular, for a given mesh, the numerical cost is similar to that of models not explicitly having a surface and about 1.7 larger than that of the standard-skin layer formulation."

P26 - L563
"Moreover, a tightly-coupled treatment of the SEB allows unconditional stability, while the standard skin-layer formulation can be unstable and displays large spurious oscillations with large time steps and small mesh sizes. Thus, while a bit more numerically costly, the formulation presented in this article can be used to overall reduce the numerical cost of a snowpack/glacier model through the use of larger time steps."

As well as in the new Appendix A:
"We see that whole system of Eqs. (A1) is a tri-diagonal system of dimension (N+1)x (N+1), with N the number of cells. Without a Schur-complement, the computation of $A^{-1}B$ can thus be solved with Thomas algorithm in 10N -1 base operations (addition, subtraction, multiplication, and division) per non-linear iteration (neglecting the time spent assembling the matrices). We also note that A_{diag} is a tri-diagonal matrix, and thus Thomas algorithm also applies. Moreover, we see that A_{up} and A_{low} are almost empty matrices, which simplifies the number of operations necessary to compute $A_{diag}^{-1} A_{up}$ and $A_{low} A_{diag}^{-1} A_{up}$. Specifically, the Schur-complement technique used in this paper can be employed with 7N-9 ($A_{diag}^{-1} A_{up}$, once per time step) + 10N-21 ($A_{diag}^{-1} B_{int}$, once per time step) + 15 (assembly and solving of Schur-complement, once per iteration) + 2N (re-injection to compute T_{int}, once per time step) steps, i.e. a total of 17N-6 + 15n_{it} steps, with n_{it} the number of non-linear iterations. We see, that the advantage of the Schur-complement technique is that the cost of performing non-linear iterations do not increase with the mesh

resolution, yielding a smaller numerically cost than inverting the while system for each non-linear iteration.

One may then wonder how the numerical cost of the scheme proposed in the article compares to the Class 1 and 2 models discussed in the paper. The Class 1 model (once a Schur-complement technique has been employed) as a similar numerical cost as the proposed coupled-surface scheme approach, namely 17N-23 + 15n_{it} steps. For a given mesh, it has one less degree of freedom as the coupled-surface scheme and is thus only marginally cheaper. The Class 2 model is the cheapest of all schemes discussed in the paper. Indeed, once the SEB and the surface temperature have been solved through scalar non-linear iterations, it relies on a single tri-diagonal inversion of dimension NxN, which can be done in 10N-11 steps. The ratio of the numerical cost of the scheme proposed in the article over that of the standard skin-layer is of about 1.7."

Finally, we note that we cannot analyze this numerical cost directly in terms of computation time in our implementations. Indeed, they were implemented using the (interpreted) python language with only some parts using pre-compiled (and thus much faster) libraries. Directly comparing computation time would unfairly favor the schemes using pre-compiled librairies.

Specific comments:

L3-4: "This surface energy budget is the sum of the various surface energy fluxes, that depend on the input meteorological variables and surface temperature, and to which heat conduction towards the interior of the snow/ice and potential melting need to be added." the comma between 'fluxes' and 'that' is incorrect, as are similarly positioned commas throughout, and 'that' should be 'which.'
This is now corrected. The same error is also corrected elsewhere in the text.

L2-4: 'and to which heat conduction towards the interior…" this sentence is unclear to me
We wanted to highlights that the conduction of heat towards the interior of the snowpack/glacier is an important factor that affects the SEB and hence the surface temperature. We clarified this in the revised manuscript:

P1 - L2
"This surface energy budget is the result of various surface energy fluxes, which depend on the input meteorological variables and surface temperature, of heat conduction towards the interior of the snow/ice, and potentially of surface melting if the melt temperature is reached."

L26: once the SEB acronym is introduced, it should be used consistently in the paper
We now systematically use SEB instead of "surface energy budget" once introduced.

L25-30: There is a large focus on the nonlinearity of SEB processes, which is important but not hugely challenging in the modeling field, as many of the nonlinearities are easily solved. It would be good to mention this and discuss sources of nonlinearity in a more mechanistic sense. For example, the "regime change" mentioned is due to thermal energy being used for processes with different reaction coefficients in warming frozen ice vs. phase change. This will help build intuition to support the truncation method discussed later. Perhaps mention another example.

We have reformulated the paragraph to lighten the references to non-linearity and clarified that the regime change between a melting and non-melting surface occurs at the fusion point (and not above as previously stated).
We have also precised how the SEB of melting and non-melting surface differs.

P2 - L29
"Mathematically, the SEB thus appears as a non-linear top boundary condition for snowpacks and glaciers. This non-linearity is even reinforced by the existence of a regime change between a melting and non-melting surface, with different thermodynamical behaviors below and at the melting point. Indeed, once the melting point is reached at the surface, the SEB becomes more akin to a Stefan-problem with a discontinuity in the energy fluxes and can no longer be simply described in terms of surface temperature. This leads to numerical challenges when solving the governing equations."

L42: which domain? The ice domain?
By domain we mean the physical space over which the equations are solved, that is to say in our case the snowpack or the glacier. This is now clearer in the text.

P2 - L40
"On the other hand, some FVM implementations do not define a specific temperature associated with the surface, but rather use the temperature of the top-most numerical layer of the domain (i.e. the top layer of the simulated snowpack/glacier) for solving the SEB (Anderson, 1976, Brun et al., 1989, Jordan, 1991, Vionnet et al., 2012, van Kampenhout et al., 2017)."

L63: specify Fourier's law of heat conduction
This is now specified.

L90-95: specify the sign convention used for fluxes
We now specify the sign convention for the fluxes.

Figure :1: clarify the meaning of the blue/orange colors of dots in the figures. Additional labels within the diagram would improve the clarity of the figure. It is also somewhat redundant to label Class 1 as a), class 2 as b) etc. since they are all in essentially the same panel. Consider just labeling the columns as class 1, class2, this paper.
We now specify that the nodes corresponds to variables to be solved (i.e. the cell temperatures and the surface state) and their position in space. This was also added to the caption. The color are meant to group the variables that are solved simultaneously and will be explained in the caption. We also revised the Figure to change the panels labeling to "Class1", "Class2", and "proposed scheme".

We propose for the new caption:
P6 - Fig 1
"Classification of FVM models with respect to their treatment of the SEB. Class 1: The surface energy and the internal temperatures are solved in a tightly-coupled manner but there is no explicit surface. Class 2: An explicit surface temperature (and surface melting) exists but it is solved in sequential manner with respect to the internal temperatures. Proposed scheme in this article: An explicit surface temperature is considered and is solved in a tightly-coupled manner with the internal temperatures. In the schematic, dots represent the prognostic variables of the schemes (with or without temperature at the surface) while the colors indicate which variables are solved simultaneously."

L115: “We therefore do not treat the finite elements method, which is for instance used in the SNOPACK model.” -> “We therefore exclude implementations of the the finite elements method, such as in the SNOWPACK model.”
Following the review of Michael Lehning, we now discuss the equivalent of our implementation in a FEM setting. We explain that by construction, the FEM posses a surface node which naturally allows one to computed a tightly-coupled SEB with the interior of the snowpack, but that the mix of node-wise (temperatures) and element-wise (energy content, liquid water content) variables in the FEM complexifies its use. The implementation of an equivalent FEM scheme is presented in the new Appendix C (attached at the end of this response) and discussed in the manuscript:

P4 - L112
“Moreover, we focus on numerical schemes based on FVM, as it is the method employed by most models (e.g. Anderson, 1976, Sauter et al., 2020, Westermann et al., 2023). We note that, contrary to the FVM, the use of the finite element method (FEM) naturally incorporates the presence of a surface temperature, which can be used for a fully-coupled treatment of the SEB, as done in SNOWPACK for instance (Bartelt and Lehning, 2002).”

P11 - L292
“Finally, a translation of this numerical strategy (including the fictitious variable and the Schur-complement technique) in a FEM framework is presented in Appendix C.”

P12 - L329
“Finally, note that we do not include the FEM in this comparison. As detailed in Appendix C, a specificity of FEM models is to rely on a temperature field that can be defined element-wise or node-wise. It is thus required to convert back and forth between these two representations. However, the relation between the two is not bijective. This prevents an unambiguous transformation from element-wise to node-wise temperatures, affecting the end-result of our simulations. Because of this problem, the FEM is not further explored in this article, as a direct comparison to the FVM models is not possible.”

L179: omit the word “let’s” or use “we” instead
We modified the manuscript accordingly.

L275: the introduction of new terminology in representing equations 5 and 9 as a block-matrix system with decomposed components (Adiag, etc.) requires additional explanatio of the correspondence between terms in Equations 5 and 9 and their placement in Equation 11.
We now clearly explain how Eqs (5) and (9) can be cast as the block-system of Equation (11). This is done in a new Appendix A, attached at the end of this response.

L350: the bottom boundary no heat flux assumption seems strong to me, or at least appropriate in a limited set of conditions. A citation or further discussion of this would help.
We think that in the glacier test case, the assumption of a no-flux boundary condition at the bottom is appropriate as the temperature is essentially isothermal in this region (as given by the initial conditions derived from a COSIPY run). Moreover, as this boundary condition is far away from the surface (~189m), it would take much more than a year for it to influence the surface where we perform our analysis. To quantify this point we have run a simulation of the glacier test case with a 64.7 mW/m2 geothermal heat flux (GHF; Davies, 2013, Talalay et al., 2020) instead of a no-flux conditions. This difference in surface temperature between the simulation with and without GHF is displayed in the Figure below. It barely exceeds 4mK over the simulation, with a standard deviation of 0.4mK.

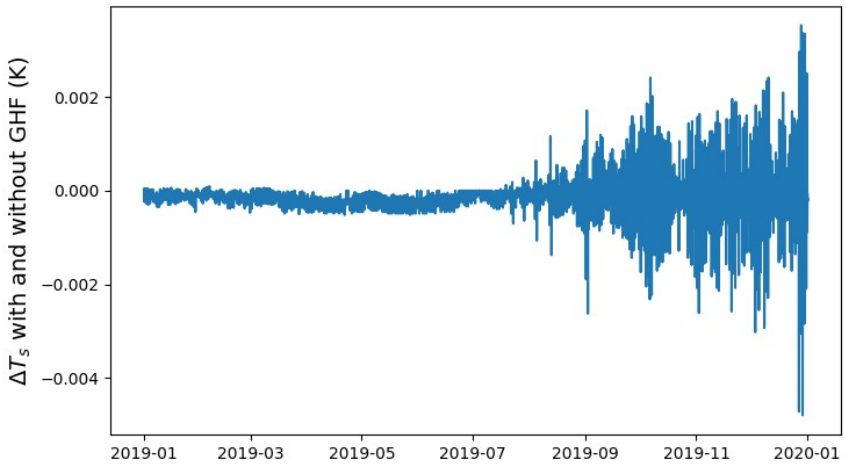

We added this number in the text:

P13 - L352

"For instance, we performed a simulation in which a 64.7 mW m^{-2} geothermal heat flux is applied instead (Davies, 2013). The impact on the surface temperature remains below 0.4 mK."

Finally, we also want to note that the goal of our simplified simulation set-up is to provide an easy framework for the comparison of numerical methods. While more realistic boundary conditions could be used, this will not change our conclusion that are confined to behavior of the numerical schemes.

L353-355: these constants are also introduced on L 66 and 72-75, use the same symbols here to connect them.
We now re-use the alredy introduced symbol to refer to the physical variables.

L354: thermal conductivity of ice is temperature sensitive! If making this assumption, please explain why it is warranted in this case (i.e., the temperature ranges reasonably experienced in this case are small enough that there is not meaningful variation?)
Indeed, the thermal conductivity of ice is expected to vary of about 10% over the range of temperature considered in this test case (from 2.5 W/K/m at 240K to about 2.22 W/K/m at 273K[1]).
We however chose not to introduce the temperature dependence of ice in our computation as (i) this is the assumption followed by the other models discussed in the paper (i.e. COSIPY or Crocus) and (ii) this added complexity would not influence the numerical benefit of tight-coupling the surface and internal energy budgets, and the properties we want to study (time step and mesh sensitivity, stability, etc). We also want to add that including a temperature-dependence for the thermal conductivity would render the system of equation globally non-linear (rather than just locally near the surface) and would thus obscure the advantage of variable elimination to speed up the resolution of system of equation where non-linearities only appears locally. We think this last point is important has it is relevant for simplified snowpack/glacier models, which do not necessarily include such temperature dependence, and that are part of larger climate and Earth system models and where speed up of the snowpack/glacier component would be beneficial.

1 https://www.engineeringtoolbox.com/ice-thermal-properties-d_576.html

Furthermore, we have run a simulation of the glacier test case with the temperature dependence on the thermal conductivity. The difference in surface temperature between the simulations with and without this temperature-dependence is visible in the Figure below. It shows that the difference remains below 0.06K, with a standard-deviation of 0.01K.

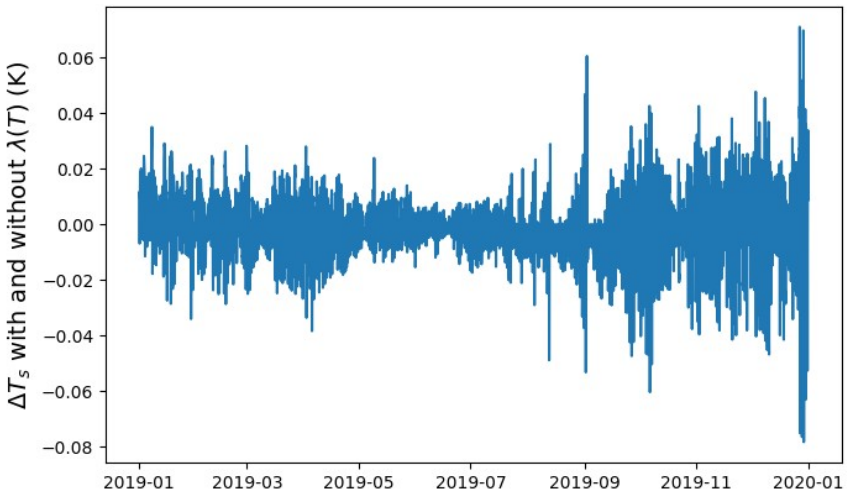

We now in the revised manuscript that considering the thermal conductivity (and specific thermal capacity) as temperature-independent is a simplifying assumption that is regularly made in models and that allows the internal heat budget equation to be linear (and hence more easily solvable). This assumption could be relaxed, but to the detriment of a more numerically costly system to be solved.

P3 - L82

"Finally, in this article we consider the thermal conductivity λ and capacity c_p not to depend on temperature. The motivation for this is twofold as it (i) corresponds to a simplifying assumption regularly made by snowpack and glacier surface models (e.g. van Pelt et al., 2012, Vionnet et al., 2012, Sauter et al., 2020, Covi et al., 2023) and (ii) it allows keeping the internal heat equation linear"

P11 - L294

"We also note that to apply this technique, the assumption of temperature-independent thermal capacity and conductivity is important, as otherwise the internal heat equation system would not be linear and thus the matrices A_{diag}, A_{up}, and A_{low} not constant."

L385: albedo over what wavelength range? In most of the visible spectrum, this would be a quite low value in clean snow. Further, the longwave emissivity of snow is more density dependent due to the presence of air. It seems reasonable to use 1 for this approach, as the emissivity is still usually quite high

The albedo used in this work refers to the broadband albedo (i.e. integrated over the while solar spectrum). This is now specified in the manuscript.

We chose a simple constant value of 0.6 as the simulation is meant to take place during the melting season, when the snow albedo is at its lowest. We agree that this value is on the lower-hand of snow albedo. Thus, we have changed this value to 0.7 in the article (Section 5.2), increased the duration of the snowpack simulations, re-ran them, and

updated the numbers in the manuscript (notably Figures 4, 7, 8, 11, 12, and 14). The conclusions of the article remain unchanged.

L435: the “lag” of one time step mentioned here is interesting and well explained. The impacts of this on interpreting a snow model output may be sensitive to the time step. If there is a long time step, this would be problematic as it may prevent modeling melt. A short time step may be more resilient to this lag.
We added to the text that this lag become less problematic with short time step.

P16 - L435
“The impact of this lagging problem can be mitigated by the use of small time steps, but with the drawback of numerical cost.”

L440: the observation that numerical instability is leading to differences between class 2 models and other models is interesting and seen clearly in Figure 4. The fact that this is not happening in the glacier model is only vaguely referenced. A direct comparison of the reasons for this – if there is an inherent numerical instability in class 2 models, why is there not an instability in the glacier model? Is all of the oscillation occurring in the meltwater percolation?
We do not think that the overall difference between models visible in Figure 4 can be readily explained by the presence of oscillations in the Class 2 model. For instance, at the beginning of the plot the Coupled surface and Class 2 appear quite in agreement on average, despite the occasional instabilities of Class 2. The two models then diverges (even not considering the presence of instabilities) before re-agreeing later in the graph. It is therefore not straight forward to link the overall agreement/disagreement of the two models with the presence/absence of instabilities, as there are periods with a good agreement despite instabilities, and periods a divergence despite the absence of instabilities.

While less visible, instabilities in the glacier test case are still possible, as for instance seen in Figure 13. As far as we understand, the presence or absence of oscillations is linked to the stiffness of the equations that relates the SEB and the internal temperature, and will depend on the specific thermal conductivity, thermal capacity, cell sizes, and on the time step at play.

To illustrate this point we performed a simple stability analysis of the standard skin-layer scheme (keeping in mind that this kind of stability analysis requires to linearize the system of equations, which departs from the actual scheme). The derivation is available at the end of this response and in the new Appendix E. It shows that the standard skin-layer scheme is not unconditionally stable, and that there is exist a maximum time step size. The presence of instabilities is favored in the case of large thermal conductivities or of a large derivative of the atmospheric fluxes with respect to the surface temperature in the SEB. On the contrary, these instabilities are hindered in the case of large cell sizes or large specific thermal capacity.

This is now discussed in the manuscript:

P21 - L503
“The unstable nature of class 2 models can be shown with a linear stability analysis, provided in Appendix E. Such analysis shows that class 2 models are only conditionally stable, and confirm that instabilities are favored in the case of large time steps and small mesh sizes. We stress that these oscillations can appear even if the time integration of the

internal energy budget relies on the Backward Euler method, known for its robustness against instabilities (Fazio, 2001, Butcher, 2008). Our understanding is that the sequential treatment of the standard skin-layer formulation breaks the implicit nature of the time integration by using "lagged" (in other words, explicit rather than implicit) terms. This, combined with the fact that the surface layer does not possess any thermal inertia and that its temperature can thus vary rapidly in time, permits large temperature swings if the time step is too large or the mesh size too small. On the other hand, it can be shown that the two schemes with a tightly-coupled SEB are unconditionally stable (Appendix E), in agreement with the absence of oscillations in their simulations. Notably, the unconditional stability of the coupled-surface scheme proposed in this article entails that the model does not need an adaptive time step size strategy depending on the mesh size. This ensures that it remains robust, regardless of the time step and mesh size.

P26 - L563
"Moreover, a tightly-coupled treatment of the SEB allows unconditional stability, while the standard skin-layer formulation can be unstable and displays large spurious oscillations with large time steps and small mesh sizes."

Figure 4: it is impossible to see the coupled surface line in panel b – consider adding markers or some other formatting choice which would allow us to see it clearly. Layering the coupled surface model on the front may help if markers are not working favorably.
Indeed, for some reason panel b of the Figure was done using a lighter shade of blue for the coupled-surface line. This was fixed and the Figure should be more readable now.

Figure 6: right panel y axis would benefit from additional labels
We added additional labels in Figures 6.

L490-495: as worded, the phrase "the class 2 model exhibits the largest phase change rate errors for an initial number of cells of 225" is ambiguous – is 225 the worst number of cells for C2 models or is C2 the worst option when working with 225 cells? From the graph, it is the second option, which is potentially less important than discussing the fact that for the other two model options, a larger number of cells generally confers better performance (within the parameter space explored here), but that is not the case for class 2 when moving from 90 to 225. Why might this be?
This deterioration is due to the development of numerical instabilities with small mesh size in the Class 2 model. This is now specified in the text.

P20 - L 490
"Finally, Fig. (10) reveals that in the glacier test case, the phase change rate errors of the class 2 tend to deteriorate with further mesh refinement past a certain point (here for an initial cell number above 90). We interpret this deterioration as a result of the appearance of numerical instabilities that develop with small mesh sizes."

L504: implicit backward Euler method?
There is one backward too much. It is now corrected.

L506: "explicit" ?
We modified the text to:

P21 - L506
"'(in other words, explicit rather than implicit)".

L509: “too”
We corrected the typo.

519: is the Dirichlet approach actually used? If not, it is not relevant to compare it here
The same comment was brought-up by Richard Essery. The potentiality of using the surface temperature as a Dirichlet condition rather than the subsurface conduction flux was made aware to us from reading the publicly available COSIPY code (cosipy/modules/heatEquation.py files, last accessed 08/11/2023) and EBFM codes. However, we stress that these codes use a Forward Euler time stepping, and in this case the using the sub-surface conduction flux or a Dirichlet condition are equivalent.

As mentioned in our response to the Richard Essery’s review, we think it is important to mention and show that using a Dirichlet condition will lead to greatly deteriorated simulations, since the use of a Dirichlet condition actually numerically stabilizes the system (which can be seen with the absence of instabilities in the orange curve of Fig. 14 and can be demonstrated with a stability analysis, provided at the end of this document and in the new Appendix E) and might be used in this attempt. However, this stabilization is at the detriment of accuracy and energy conservation.

We propose to better justify in the manuscript that the use of a Dirichlet condition might be tempting to obtain stability, but that it will produce large errors in response. We also propose to shorten the first part of the Section:

P23 - L511
“As explained in Section 2.2, the heat conduction flux from the surface to the interior of the domain (i.e. G in Equation 3) needs to have the same value in the computation of the SEB and in the computation of the energy budget of the first interior cell. Inconsistencies in G between these two budgets lead to the violation of energy conservation and create an artificial energy source/sink near the surface. Such inconsistencies could be created when implementing the standard skin-layer formulation (class 2 models) due to the sequential treatment of the surface and internal energy budgets. Indeed, after solving the SEB, one can either use the surface temperature or the subsurface heat flux G as a boundary condition for the computation of the internal temperatures. We note that the use the computed surface temperature as a boundary condition leads to an unconditionally stable numerical scheme (Appenddix E). However, using such Dirichlet condition in order to stabilize the standard-skin layer formulation comes at the expense of energy conservation and deteriorates of the simulated results.”

Figure 13: this is a time series of temperature, not a graph of numerical instabilities and should be labeled as such. It seems that the goal is to point out the larger variance in the higher number of cells-driven runs, so I would recommend either adding the time average standard deviation, or converting this plot to a time series of deviation from some sort of rolling mean in order to focus more on the instability-driven variance. Or, add a second column that contains histograms of that variance for each case.
We modified the caption to refer to the Figure as a temperature time series, and we will add the computation of a rolling standard deviation to quantify the instabilities and their presence.

P24 - Fig. 13
“Time series of surface temperatures (in blue, left y-axis) and of their 24hr-running standard deviations (in orange, right y-axis) highlighting the presence of numerical instabilities with the standard skin-layer scheme. The simulations correspond to the glacier

test case with a time step of 2 hr. Each panel corresponds to a level of mesh refinement. The lowest mesh refinement is at the top and displays the smallest level of instabilities, while the highest mesh refinement is at the bottom and displays numerous large instabilities in the first half of the simulation."

L560: the level of accuracy is similar but not identical
We are not sure to fully understand the comment of the referee. We have have modified the manuscript to explain that the tightly-coupled scheme results *overall* in a better accuracy, but not always.

P26 - L559
"Mesh and time step convergence analyses show that combining a coupled treatment of the SEB with the explicit introduction of a surface results in an overall better accuracy when compared to the classical implementations."

L613 "This approach is, for instance, used in the Crocus model" add commas
We added the commas.

We thank the referee for their constructive review. Please find below our point by point response to the review. The comment of the referee are shown in blue and our response in black below. Proposed modifications of the manuscript are shown in green with page and line numbering corresponding to the preprint version of the article.

The authors present an approach to numerical modeling of snowpack or glacier interface with atmosphere using a finite volume method discretization of thermodynamic relations. The novelty of the approach lies in coupled computation of heat transfer through the ice/snow and the thermodynamic balance at the surface. The authors provide sufficient numerical experiments to support the agreement of their implementation with previously published results.
The only critical comment I would like to make is the relatively vague mathematical description of their approach, or the problem at hand. The authors discus the Fourier's law for the heat transfer in ice (Equation 1) and the balance of energy fluxes at the ice surface (Equation 3). Then, they immediately follow on to numerical discretization, leaving the reader curious as to what assumptions and specific method choices they made. I would outline below a few of my concerns.

We revised the manuscript trying to be more precise on the mathematical framework and on the notations. We hope the following modifications clarified the text.

The authors start with the heat equation:

$\partial t h - \mathrm{div}(\lambda\, \mathrm{grad}(T)) = Q$
where
$h = c_p(T-T_0) + \rho_w L \theta$

which leads to

$c_p \partial_t T + \rho_w L \partial_t \theta - \mathrm{div}(\lambda\, \mathrm{grad}(T)) = Q. \qquad (1)$

In the subsequent paragraph they discuss issues with representing the effects of phase changes on the temperature, but I believe they mean that they neglect the $\rho_w L \partial_t \theta$ term in their model. Please state that clearly.

Yes, we meant that while solving the processes of heat conduction and shortwave absorption, we neglect the $\rho_w L \partial_t \theta$ term, and all accumulated energy is used to modify the temperature, even if the fusion point has been crossed. Note that this term is then used in a second step to re-establish thermal equilibrium between the ice and liquid water. In case of melt/refreeze, the sensible heat ($c_p \partial_t T$ term) and liquid water latent heat ($\rho_w L \partial_t \theta$ term) are both used to create/remove water while maintaining the energy conservation.

This is now rephrased more clearly in the revised manuscript:

P3 - L75
"Note that in Eq. (1) the time derivative of the internal energy content h cannot in principle be replaced by $c_p\, d_t T$, but should also include the term $\rho_w\, L_{fus}\, d_t\theta$. Indeed, once the temperature has reached the fusion point, a further increase in energy translates into an increase in the liquid water content ($d_t\theta$!= 0) and of the associated latent heat content, rather than a further increase in the temperature. Yet, as discussed below, snowpack and glacier models nonetheless usually consider that the temperature can increase past the fusion point when integrating Eq. (1) in time (Vionnet et al., 2012, Sauter et al., 2020). This

is equivalent to neglecting the effects of first-order phase changes (melting and refreezing) on the temperature field, and thus setting $\rho_w L_{fus} d_t\theta$ to zero while solving the heat equation."

Moving on, the authors jump to Equation 5, where they present the discretized version of (1) using finite volumes. It would be useful to state the implicit assumptions here, that the three dimensional equation (1) is now considered as one-dimensional equation

$cp\partial tT - \partial z (\lambda \partial zT) = Q,$

which is then integrated over each "volume", which in this case is segment of length Δzk. This integration, along with replacing the point variables with their volume averages (with abuse of notation: $Tk = 1/\Delta zk \int Tdz$), and using fundamental theorem of calculus (we are in one dimension now, no need for divergence theorem) gives
$\Delta zkcp\partial tT - (\lambda \partial zT)k+1/2 + (\lambda \partial zT)k-1/2 = \Delta zkQ$, where subscripts k+1/2 and k-1/2 refer to the (top and bottom) endpoints of the cell Δzk

We now state directly from Eq. (1) that we are working in a 1D setting.

P3 - L70
"In this article, we assume that the snowpack/glacier can be represented as 1D column, and therefore Eq. (1) should be understood as 1D equation."

For the introduction of Equation (5) we specify that the T_k in represent the average temperature of the k^{th} cell. Moreover, reading the reviewer comment we realized that a subscript k is missing for the temperature in Equation (5). This is now corrected.

At this point the authors introduce the approximation of the $(\lambda \partial zT)k+1/2$ term with Equation 6. I am curious, however, whether it is not better to leave the term $(\lambda \partial zT)z=surf$ at the top of the first layer as is, and replace it with the term G from the surface energy balance equation (3)? I am not sure whether this is the way the authors achieve coupling, or whether they still discretize the temperature gradient at the ice surface using the surface temperature and half of the top layer size?

We were indeed sloppy in the description of the fluxes at the cell boundaries. We believe that the issue arises from the fact the top (and bottom) cell is a special case, which was not reflected in our article. For the top cell, the top flux is not computed using Eq. (6), but rather with the subsurface conduction flux G.
We propose to modify the text to clearly state that Eqs (5) and (6) only applies to interior cells, and that cells touching the top and bottom boundaries needs to include the boundary fluxes (which is G for the top most-cell).

P7 - L183
"where Δz_k is the thickness of the k^{th} cell, c_{pk} its volumetric thermal capacity, Q_k the average volumetric energy source in the cell, and $F_{k+1/2}$ and $F_{k-1/2}$ are the heat conduction fluxes at the top and bottom interfaces of the cell. For internal cells, $F_{k+1/2}$ and $F_{k-1/2}$ correspond to the fluxes between the k^{th} and the $k+1^{th}$ cells and the $k-1^{th}$ and k^{th} cells, respectively. For the top cell $F_{k+1/2}$ corresponds the heat flux leaving towards the surface (i.e. -G) and for the bottom cell $F_{k-1/2}$ corresponds to the flux from the ground."

P7 - L189
"The heat conduction fluxes between cells need to be estimated from the temperatures and thermal conductivities of adjacent cells. The flux $F_{k+1/2}$ between cells k and k+1 is computed as:

Eq. (6)

where $\lambda^{harm}_{k+1/2}$ is the weighted harmonic average of the thermal conductivity of the two adjacent cells. The use of an harmonic average provides better results in the case of layered media such as snow (Kadioglu et al., 2008) and ensures that no heat conduction occurs in case one of the cells is a perfect thermal insulator.
Note that Eq. (6) only applies to fluxes between cells and must be replaced for the two boundary cells, at the top and bottom of the domain. For the bottom cell, a flux between the domain and the ground below must be used as a bottom boundary condition. For the top cell, the heat flux coming from the surface must be used. This flux corresponds to the discretized version of the term G in the SEB, provided in Eq. (10) below."

The authors discuss in lines 103-105 that term G depends on surface temperature and temperature within ice, which indicates that this term is indeed discretized.

This term is discretized using Eq(10), and used instead of F_{k+1/2} for the energy budget of the top-most cell. This is now clearly put in the text:

P7 - L195
"This flux corresponds to the discretized version of the term G in the SEB, provided in Eq. (10) below."

I would urge the authors to provide a more detailed and careful mathematical description of their work, as it would improve the reproducibility of their result, not only for the finite volume method community, but also researchers working with other numerical discretizations.

Following the review of Michael Lehning, we have also added an Appendix describing how to implement an equivalent model using FEM (attached at the end of this response). However, in the FEM framework appears the problem of converting element-wise temperatures into node-wise temperatures. This transformation has no straight-forward answer and requires some additional assumptions that affects the end-result of the simulations. As such, we were not able to integrate a FEM model in comparisons to the FVM ones.

This is now is explained in the new Appendix C, as well as in the main part of the revised manuscript:

P11 - L292
"Finally, a translation of this numerical strategy (including the fictitious variable and the Schur-complement technique) in a FEM framework is presented in Appendix C."

P12 - L329
"Finally, note that we do not include the FEM in this comparison. As detailed in Appendix C, a specificity of FEM models is to rely on a temperature field that can be defined element-wise or node-wise. It is thus required to convert back and forth between these two

representations. However, the relation between the two is not bijective. This prevents an unambiguous transformation from element-wise to node-wise temperatures, affecting the end-result of the simulations. Because of this problem, the FEM is not further explored in this article, as a direct comparison to the FVM models is not possible."

We are thankful the Micheal Lehning for its constructive review. Please find below our point by point response to the review. The comment of the referee are shown in blue and our response in black below. Proposed modifications of the manuscript are shown in green with page and line numbering corresponding to the preprint version of the article.

General:
The paper presents a review on how to numerically implement the surface energy budget into a certain class of snow and ice models. The paper is very well written and in general presents the material in a clear manner. It is overall considered to be a useful contribution to the scientific community dealing with snow and ice modelling despite its rather theoretical setting, in which conclusions on existing snow and ice models are only possible in a limited way.

In this context, it is mandatory that existing snow and ice models that have schemes that come close to the solution presented here are discussed in sufficient detail. In particular, since for example SNOWPACK uses a finite element method (FEM), for which the nodal temperature is explicitly solved at the surface, it already achieves both aspects of the paper, an explicit surface and a tight coupling with internal heat transfer merely by construction of the FEM. This is true for the original version of SNOWPACK, which is now more than 20 years old. Moreover, the statement in l.81 is not a fair representation of the current state of snow models, since also efforts have been made to implement a coupled solver in SNOWPACK that does not generate temperature overshoots. This was crucial for sea ice simulations, where an additional complexity is created by the fact that the melting point of the snow and ice is a function of salinity, and that salinity in turn is impacted by the phase changes. This means that a simple approach of allowing overshoots to occur and then setting back the temperature to fusion value is not suitable any longer. This has been presented in Wever et al. (2020) and should be discussed in the current paper. The proper acknowledgment of the state of art is necessary and as a consequence limits the novelty of the proposed approach here. It is not acceptable to say “we don’t discuss FEM models” as the authors do. This neglect is even more surprising since an overlapping group of authors proposes in another paper to use the FEM method for snow modelling (Brondex et al., 2023).

It is indeed true that FEM offers the advantage of naturally having a surface node, which facilitates the tightly-coupled modeling of the SEB, as done in SNOWPACK. This is now clearly mentioned in the article. We also specified that the choice of our article to focus on FVM is motivated by the fact that the FVM is broadly employed in snowpack/glacier 1D modelling. We also now include a short analysis of the FEM case (see Appendix C and modifications listed below).

P4 - L112
“Moreover, we focus on numerical schemes based on the FVM, as it is the method employed by most models (e.g. Anderson, 1976, Sauter et al., 2020, Westermann et al., 2023). We note that, contrary to the FVM, the use of the finite element method (FEM) naturally incorporates the presence of a surface temperature, which can be used for a fully-coupled treatment of the SEB, as done in SNOWPACK for instance (Bartelt and Lehning, 2002).”

We also clarified throughout the text that the classification that we propose is applies to FVM models only, for instance in the caption of Figure 1:

P6 - Fig 1
"Classification of FVM models with respect to their treatment of the SEB. Class 1: The surface energy and the internal temperatures are solved in a tightly-coupled manner but there is no explicit surface. Class 2: An explicit surface temperature (and surface melting) exists but it is solved in sequential manner with respect to the internal temperatures. Proposed scheme in this article: An explicit surface temperature is considered and is solved in a tightly-coupled manner with the internal temperatures. In the schematic, dots represent the prognostic variables of the schemes (with or without temperature at the surface) while the colors indicate which variables are solved simultaneously."

While the article is mainly focus on FVM, we wanted to include in the revised version a brief comparison with FEM, and explain how some of the points discussed in the paper (namely fictitious variable and linear elimination) can be directly translated in a FEM framework.
Doing so we stumble upon the issue of transforming element-wise energy and temperature (description required for the bucket-scheme for instance) into temperature-wise temperature (required for the FEM solving of the heat equation). This step is non-trivial as (i) it is non-unique and (ii) it can create oscillating node-wise temperature fields. While a solution to this problem has been proposed for SNOWPACK, it could not be directly translated into the sequential treatment adopted in our paper. Our different attempts to implement this elements to nodes transformation had an impact on the simulated surface temperature. Thus, the comparison between the FVM and FEM scheme in terms of accuracy and speed of convergence towards a common solution cannot be pursued in the article.

We propose to present the implementation of the FEM equivalent to the tightly-coupled scheme already discussed in the article. This is done in the new Appendix C (attached at the end of this response) and discussed in the manuscript:

P11 - L292
"Finally, a translation of this numerical strategy (including the fictitious variable and the Schur-complement technique) in a FEM framework is presented in Appendix C."

P12 - L329
"Finally, note that we do not include the FEM in this comparison. As detailed in Appendix C, a specificity of FEM models is to rely on a temperature field that can be defined element-wise or node-wise. It is thus required to convert back and forth between these two representations. However, the relation between the two is not bijective. This prevents an unambiguous transformation from element-wise to node-wise temperatures, which affects the end-result of our simulations. Because of this problem, the FEM is not further explored in this article, as a direct comparison to the FVM models is not possible."

A second major point to address is the inconsistency and incompleteness with respect to the phase change (fusion) implementation as suggested. If I understand the set-up correctly, you explicitly implement the fusion process at the surface and keep the temperature solution at the phase change temperature with your variable switching formulation supported by the truncation method. But you don't do so below the surface, which generates an inconsistency for the sub-surface heat flux. For example, for the case of shortwave penetration into snow and ice, you would generate temperatures above the melt temperature below the surface, which would lead to an upwards heat flux towards the surface, which is at the melt temperature. But heat would flow downwards in reality. This inconsistency is not even mentioned in section 6.4 and probably has consequences for

energy conservation. While the tight coupling and explicit surface are sufficiently investigated with sensitivity cases in the paper, the same needs to be done for this fusion treatment. The effect needs to be quantified and compared to the more classical “overshoot” solution.

While doing our study, we hesitated to include phase-change directly into the internal heat budget. As pointed out by the review, this treatment is closer to the actual physics at play (with phenomena such as the blocking of heat conduction fluxes in an isothermal snowpack). We nonetheless decided not to include this effect as (i) this strategy corresponds to a large portion of current snowpack and glacier models, and (ii) we foremost focus on the treatment of the SEB and a proper study/discussion on internal phase changes would be out the scope we aim for. We note that current models that do not take into the capping of internal temperatures still do include some capping of the surface temperature, since it has a large influence on the SEB (notably through the outgoing longwave radiation).
While neglecting internal phase change when solving the heat equation might lead to a deteriorated estimation of the heat conduction fluxes within the snowpack/glacier, this does not have consequences on the energy conservation of the models. As long as these heat fluxes are consistently distributed, the models remain strictly energy conservative.

To test the influence of including phase-change while solving the internal heat equation, we have implemented versions of the three FVM models used in the article that includes phase-changes directly in the heat equation, as suggested in the referee’s comment. Specifically, this was done using the enthalpy method (Meyer and Hewitt, 2017, Tubini et al., 2021). Comparison with the base versions of the models shows that this inclusion has no effect on the glacier test case (as melting occurs at the surface and not internally) and an effect of a couple of degrees on the surface temperature in the snowpack test-case. Nonetheless, the conclusions of the article on the accuracy and stability of the SEB strategies remain unchanged. This can be seen in the Figures below that compare the results of the convergence study with and without internal phase change. For each figure, the left panel corresponds to the convergence plot of the manuscript (no internal phase change in the heat equation), while the right panel corresponds to the convergence plot taking into account internal phase change in the heat equation.

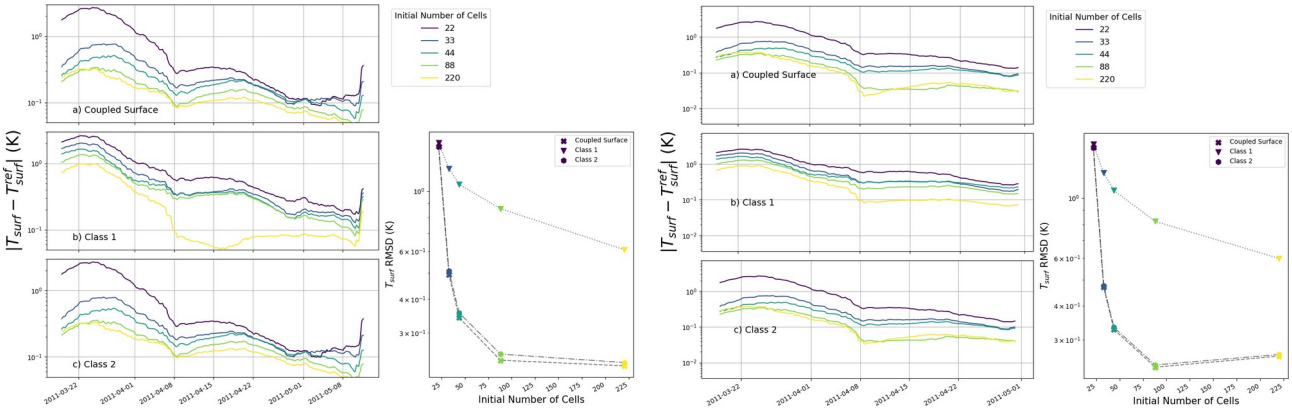

Fig. 1 – *Impact of internal phase-changes on the mesh converge analysis.*

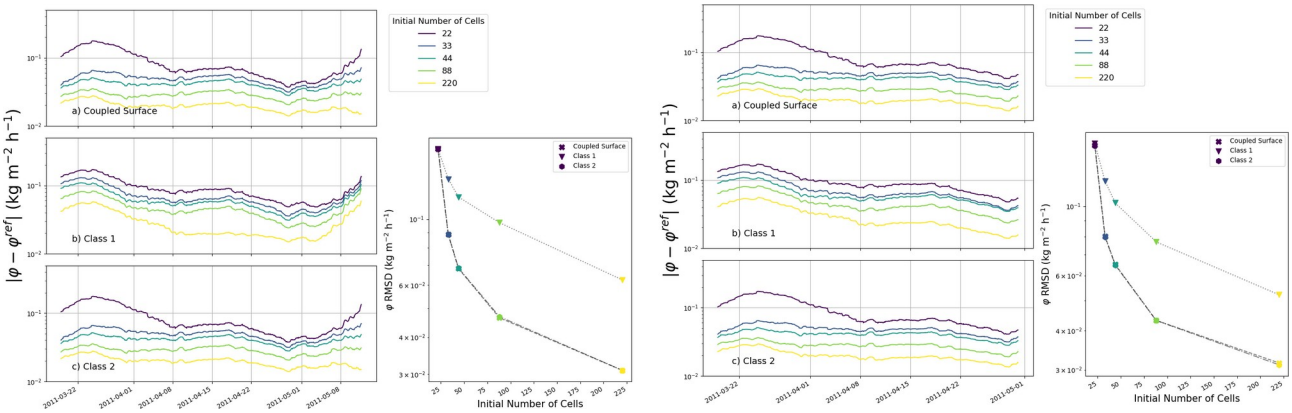

Fig. 2 – *Impact of internal phase-changes on the mesh converge analysis.*

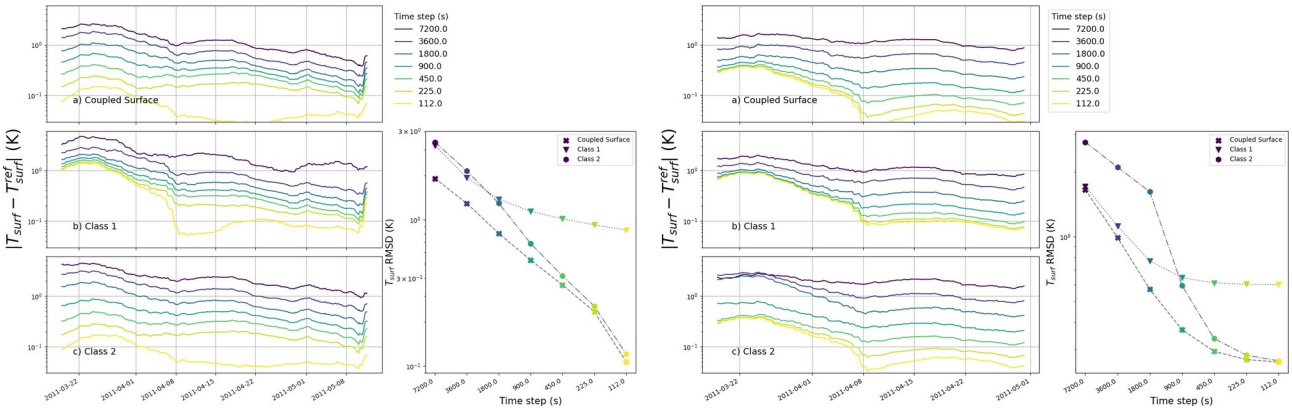

Fig. 3 – *Impact of internal phase-changes on the time step converge analysis.*

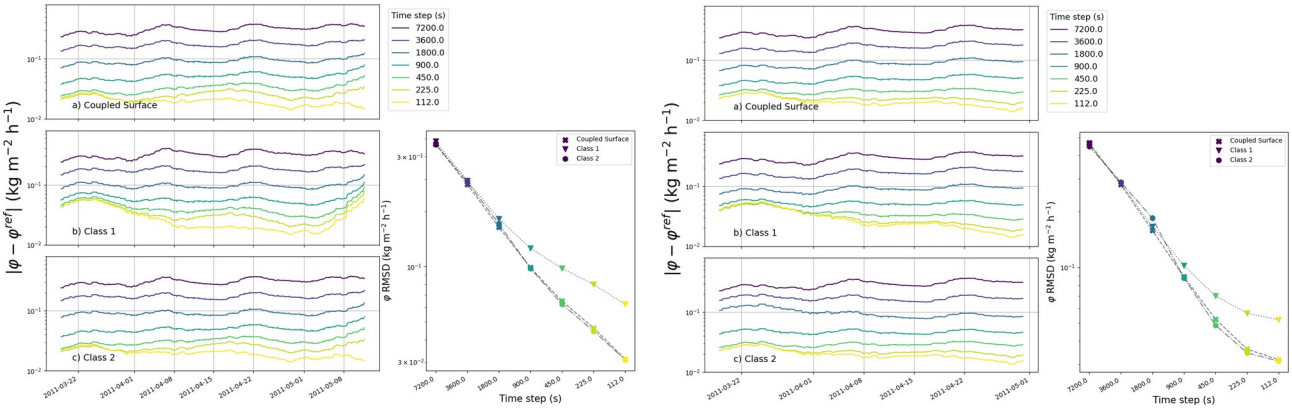

Fig. 4 – *Impact of internal phase-changes on the time step converge analysis.*

We now mention in the revised manuscript that other strategies have been proposed in the literature, and we have corrected our mistake on the strategy employed by SNOWPACK.

P3 - L81

"This results in temperature overshoots that are then corrected in a second step by creating melt and setting back the temperature to the melt value (e.g. Vionnet et al., 2012, Sauter et al., 2020). In this article, we follow this simple scheme as it is commonly employed in snowpack and glacier models. That being said, other, more complex,

strategies have been proposed in the literature. This notably includes the use of a finite temperature-range over which melt/freezing occurs (e.g. Albert, 1983, Dutra et al., 2010), including melt/refreeze as an additional energy source term (e.g. Bartelt and Lehning, 2002, Wever et al., 2020), or the use of enthalpy as the prognostic variable (e.g. Meyer and Hewitt, 2017, Tubini et al., 2021).”

We also now mention that we have tested the sensitivity of our results to the implementation of phase-changes and that the conclusions of the article remain unchanged.

P12 - L329
“Also, as some of the current snowpack and glacier models include the effect of internal phase-change while solving the internal heat equation (e.g. Bartelt and Lehning, 2002, Meyer and Hewitt, 2017), we quantified the sensitivity of our results to this specific treatment of melt/freeze. For that, we have also implemented versions of our three models that include such internal phase-changes in the heat equation.”

P16 - L441
“Finally, using the versions of the models including phase-changes in the heat equation, we quantified the sensitivity of these observations to the treatment of the melt/refreeze. While the simulated temperature sometimes differ from our basic implementations (especially in the snowpack test case where melt occurs internally), the general behavior of the models, including the potential presence of instabilities in the Class 2 models, remain unchanged.”

P20 - L493
“Finally, using the versions of the models including phase-changes in the heat equation, we verified that the conclusions of this convergence analysis remain valid in the case of a different treatment of the internal phase-changes”

Minor comments:

1) At least I am more used to the terms “melt” temperature and “heat” capacity instead of “fusion” and “thermal”.
We have reformulated “fusion” and “thermal capacity” into “melt” and “heat capacity”, except for *“enthalpy of fusion”* as the formulation *“enthalpy of melt(ing)”* appears less common.

2) Eq. (3) does not contain heat advection by precipitation.
We have added a rain precipitation term in the SEB throughout the article.

3) l. 108: Not true, SNOWPACK does not do a separate SEB, see above.
We now specify throughout the manuscript that the proposed classification only applies to FVM models.

4) l. 126: “result” not results.
We have corrected the typo.

5) l. 284: “equation” not equations.
We have replaced sentence with:

P11 - L284
"The system of Eqs.(13) is a 2x2 non-linear system where only A_s and B_s need to be re-assembled at each non-linear iteration and whose solution for U_s is the same as the large system of Eqs. (11)."

6) I don't understand the argument here: "Note that the method used to downscale the data does not guarantee physical consistency of the variables. This allows us to take into account shortwave, longwave and turbulent energy fluxes at the top of our domain".
We wanted to explain that we directly used the forcing data of Potocki et al. (2022), which provides all necessary inputs for the model. However, as briefly discussed in Brun et al. (2023) there are questions about the more appropriate method to downscale ERA5 data to South Col glacier.

As the goal of our article is solely focused on numerical methods and is not meant to address the quality of the forcings, we propose to simply rewrite the sentence to:

P13 - L341
"As such, our simulations are forced by the weather data provided by Potocki et al. (2022) that include all necessary information to take into account the shortwave, longwave and turbulent energy fluxes at the top of our domain."

7) Figures 3,4: These uncertainties should be discussed in light of typical snow/ice model errors.
We now compare the difference between the modeled snow surface temperature with bias observed during the inter-comparison exercise ESM-SnowMIP.

P15 - L432
"As with the glacier test case, the models exhibit surface temperature differences of about a couple of degrees. This is of the same order as the biases observed in the snow model inter-comparison exercise ESM-SnowMIP (Menard et al., 2021)."

Unfortunately, we are not aware of such an inter-comparison model exercise for glacier temperature surfaces. We therefore propose to include a mention of Sauter et al., (2020) which includes a comparison of COSIPY with measured glacier surface temperatures.

P15 - L421
"Concerning the glacier test-case, Fig. 3 shows that the class 1 model (no explicit surface) is systematically different compared to the two other models, with a slower decrease of the surface temperature at night, resulting in a surface temperature that is usually warmer of a couple of degrees for the represented period. For comparison, Sauter et al., (2020) report root mean square errors around 3K when comparing COSIPY simulations with observations of the Zhadang glacier surface temperature."

8) l. 438: why "model 2" now, not clear?
There was indeed a typo here, it the Class 1 model that produces less melt and thus that percolates less. This is now corrected in the text:

P16 - L 438
"This effect is due to the smaller melting predicted by the class 1 model."

9) l. 450 ff. should the reference not be a hundreds (900) of seconds consistent with typical time steps used?

The reference simulation is meant to replace the analytical solutions, that we cannot derive. It is meant to provide the reference toward which the numerical schemes should converge at high spatial and temporal resolutions, and should therefore be obtained with a quite small time step (30s here).

For the range of other tested time step, we decided to go above 900s as some models use larger time steps by default (3600s for COSIPY for instance) and we think it is interesting to analyze the behavior of models at large time step, as such a choice can be motivated to reduce the numerical cost of snowpack/glacier models in large simulation systems such as Earth system models.

P17 - L452

"The largest time step of 7200 s corresponds to twice the default value used for instance in COSIPY (Sauter et al., 2020) and is meant to represent the case of models used at quite large time steps for numerical cost considerations."

10) l. 460: should it be "worse" instead of better?

We wanted to state that sometimes the Class 2 yields smaller error than the scheme we proposed, but that in these cases the Class 2 is only slightly better. This was visibly not clearly enough stated in the manuscript as Richard Essery had the same comment. We revised the sentence to:

P17 - L458

"For almost all investigated time steps and in both test cases, the newly proposed scheme displays the lowest level of errors. Sometimes, the class 2 model yields the smallest error, but does so only by a small margin."

We have also re-formulated a similar sentence later in the manuscript.

P20 - L481

"Again, among the three implementations the tightly-coupled surface model yields the smaller errors for almost all investigated mesh refinements (as in the glacier test case, the class 2 model is however sometimes marginally better)."

11) l. 491: can you explain the deterioration?

This increase of error with smaller mesh size is a result of numerical instabilities, that develop with small mesh sizes. This is now mentioned in the text:

P20 – L 490

"Finally, Fig. (10) reveals that in the glacier test case, the phase change rate errors of the class 2 tend to deteriorate with further mesh refinement past a certain point (here for an initial cell number above 90). We interpret this deterioration as a result of the appearance of numerical instabilities that develop with small mesh sizes."

References:

Brondex, J., Fourteau, K., Dumont, M., Hagenmuller, P., Calonne, N., Tuzet, F., and Löwe, H.: A
finite-element framework to explore the numerical solution of the coupled problem of heat conduction, water vapor diffusion and settlement in dry snow (IvoriFEM v0.1.0), Geosci. Model Dev. Discuss., 2023, 1–50, https://doi.org/10.5194/gmd-2023-97, 2023.

Wever, N., Rossmann, L., Maaß, N., Leonard, K. C., Kaleschke, L., Nicolaus, M., and Lehning, M.: Version 1 of a sea ice module for the physics-based, detailed, multi-layer SNOWPACK model, Geosci. Model Dev., 13, 99–119, https://doi.org/10.5194/gmd-13-99-2020, 2020).

Appendix A: Matrix expressions and numerical cost of the coupled-surface scheme

A1 Matrix expressions

Combing Eqs. (5), (6), and (10), the Newton scheme of the coupled-surface model proposed in this article can be written under block matrix form

$$\left(\begin{array}{c|c} A_{\mathrm{diag}} & A_{\mathrm{up}} \\ \hline A_{\mathrm{low}} & A_{\mathrm{s}} \end{array}\right)\left(\begin{array}{c} T_{\mathrm{int}} \\ \hline U_{\mathrm{s}} \end{array}\right) = \left(\begin{array}{c} B_{\mathrm{int}} \\ \hline B_{\mathrm{s}} \end{array}\right) \tag{A1}$$

with non-zero terms being

$$A_{\mathrm{diag}}(k,k) = \Delta z_{\mathrm{k}} c_{\mathrm{p_k}} + \Delta t \left(\frac{\lambda^{\mathrm{harm}}_{\mathrm{k}+\frac{1}{2}}}{\frac{\Delta z_{\mathrm{k}}}{2} + \frac{\Delta z_{\mathrm{k}+1}}{2}} + \frac{\lambda^{\mathrm{harm}}_{\mathrm{k}-\frac{1}{2}}}{\frac{\Delta z_{\mathrm{k}}}{2} + \frac{\Delta z_{\mathrm{k}-1}}{2}} \right) \tag{A2}$$

$$A_{\mathrm{diag}}(k,k-1) = -\Delta t \frac{\lambda^{\mathrm{harm}}_{\mathrm{k}-\frac{1}{2}}}{\frac{\Delta z_{\mathrm{k}}}{2} + \frac{\Delta z_{\mathrm{k}-1}}{2}} \tag{A3}$$

$$A_{\mathrm{diag}}(k,k+1) = -\Delta t \frac{\lambda^{\mathrm{harm}}_{\mathrm{k}+\frac{1}{2}}}{\frac{\Delta z_{\mathrm{k}}}{2} + \frac{\Delta z_{\mathrm{k}+1}}{2}} \tag{A4}$$

$$A_{\mathrm{up}}(N-1,1) = A_{\mathrm{low}}(1,N-1) = -\Delta t \frac{\lambda^{\mathrm{harm}}_{\mathrm{N}-\frac{1}{2}}}{\frac{\Delta z_{\mathrm{N}-1}}{2} + \frac{\Delta z_{\mathrm{N}}}{2}} \tag{A5}$$

$$A_{\mathrm{s}}(1,1) = \Delta z_{\mathrm{N}} c_{\mathrm{p_N}} + \Delta t \left(\frac{\lambda^{\mathrm{harm}}_{\mathrm{N}-\frac{1}{2}}}{\frac{\Delta z_{\mathrm{N}}}{2} + \frac{\Delta z_{\mathrm{N}-1}}{2}} + \frac{\lambda_{\mathrm{N}}}{\frac{\Delta z_{\mathrm{N}}}{2}} \right) \tag{A6}$$

$$A_{\mathrm{s}}(2,2) = \Delta t \left(\frac{\lambda_{\mathrm{N}}}{\frac{\Delta z_{\mathrm{N}}}{2}} \mathrm{d}_\tau T_{\mathrm{surf}} + L_{\mathrm{fus}} \mathrm{d}_\tau \dot{m} - \mathrm{d}_\tau H - \mathrm{d}_\tau L - \mathrm{d}_\tau L W_{\mathrm{out}} - -\mathrm{d}_\tau R \right) \tag{A7}$$

$$A_{\mathrm{s}}(1,2) = -\Delta t \frac{\lambda_{\mathrm{N}}}{\frac{\Delta z_{\mathrm{N}}}{2}} \mathrm{d}_\tau T_{\mathrm{surf}} \tag{A8}$$

$$A_{\mathrm{s}}(2,1) = -\Delta t \frac{\lambda_{\mathrm{N}}}{\frac{\Delta z_{\mathrm{N}}}{2}} \tag{A9}$$

$$B_{\mathrm{int}}(k) = \Delta z_{\mathrm{k}} c_{\mathrm{p_k}} T_{\mathrm{k}}^{n-1} + \Delta t \mathrm{SW}_{\mathrm{int,k}} \tag{A10}$$

$$B_{\mathrm{s}}(1) = \Delta z_{\mathrm{N}} c_{\mathrm{p_N}} T_{\mathrm{N}}^{n-1} + \Delta t \left(\mathrm{SW}_{\mathrm{int,N}} - \frac{\lambda_{\mathrm{N}}}{\frac{\Delta z_{\mathrm{N}}}{2}} \left(\mathrm{d}_\tau T_{\mathrm{surf}} \tau^{\mathrm{i}} - T_{\mathrm{s}}(\tau^{\mathrm{i}}) \right) \right) \tag{A11}$$

$$\begin{aligned} B_{\mathrm{s}}(2) = \Delta t \Big(& SW_{\mathrm{net}}^{\mathrm{surf}} + LW_{\mathrm{in}} - \frac{\lambda_{\mathrm{N}}}{\frac{\Delta z_{\mathrm{N}}}{2}} \left(T_{\mathrm{s}}(\tau^{\mathrm{i}}) - \mathrm{d}_\tau T_{\mathrm{surf}} \tau^{\mathrm{i}} \right) - L_{\mathrm{fus}} \left(m(\tau^{\mathrm{i}}) - \mathrm{d}_\tau m \tau^{\mathrm{i}} \right) \\ & + \left(H(\tau^{\mathrm{i}}) - \mathrm{d}_\tau H \tau^{\mathrm{i}} \right) + \left(L(\tau^{\mathrm{i}}) - \mathrm{d}_\tau L \tau^{\mathrm{i}} \right) + \left(R(\tau^{\mathrm{i}}) - \mathrm{d}_\tau R \tau^{\mathrm{i}} \right) + \left(LW_{\mathrm{out}}(\tau^{\mathrm{i}}) - \mathrm{d}_\tau LW_{\mathrm{out}} \tau^{\mathrm{i}} \right) \Big) \end{aligned} \tag{A12}$$

In the above expressions, T_{k}^{n-1} is the temperature of cell k at the previous time step, $\mathrm{SW}_{\mathrm{int,k}}$ is the quantity of shortwave radiation absorbed in cell k, and τ^{i} is the value of the fictitious variable τ at the start of the current non-linear iteration. The terms $T_{\mathrm{s}}(\tau^{\mathrm{i}})$, $H(\tau^{\mathrm{i}})$, etc, and $\mathrm{d}_\tau T_{\mathrm{surf}}$, $\mathrm{d}_\tau H$, etc, are the values of the surface temperature, sensible heat flux, etc, and their derivatives at the current τ^{i} estimation.

Among the different partial derivatives, $\mathrm{d}_\tau H$ and $\mathrm{d}_\tau L$ can be difficult to analytically derive. For that, we first note that the chain rule yields $\mathrm{d}_\tau H = \mathrm{d}_{T_{\mathrm{s}}} H \mathrm{d}_\tau T_{\mathrm{s}}$, and $\mathrm{d}_\tau L = \mathrm{d}_{T_{\mathrm{s}}} L \mathrm{d}_\tau T_{\mathrm{s}}$. Then, for the expression of H given in Appendix D we have:

$$\mathrm{d}_{T_{\mathrm{s}}} H = \rho_{\mathrm{a}} c_{\mathrm{p,a}} u \left(\mathrm{d}_{T_{\mathrm{s}}} C_{\mathrm{H}} (T_{\mathrm{a}} - T_{\mathrm{s}}) - C_{\mathrm{H}} \right) \tag{A13}$$

Moreover, the chain rule yields $\mathrm{d}_{T_{\mathrm{s}}} C_{\mathrm{H}} = \mathrm{d}_{\mathrm{Ri_b}} C_{\mathrm{H}} \mathrm{d}_{T_{\mathrm{s}}} \mathrm{Ri_b}$. In our case:

$$\mathrm{d}_{\mathrm{Ri_b}} C_{\mathrm{H}} = \frac{\kappa^2}{\ln\left(\frac{z}{z_0}\right)\left(\frac{z}{z_{0t}}\right)} \begin{cases} 0 & \text{if } \mathrm{Ri_b} < 0 \\ 50\mathrm{Ri_b} - 10 & \text{if } 0 \leq \mathrm{Ri_b} < 0.2 \\ 0 & \text{if } 0.2 \leq \mathrm{Ri_b} \end{cases} \tag{A14}$$

and

$$\mathrm{d}_{T_{\mathrm{s}}} \mathrm{Ri_b} = -\frac{g z_{\mathrm{a}}}{T_{\mathrm{a}} u^2} \tag{A15}$$

Similarly, for L, we have:

$$\mathrm{d}_{T_{\mathrm{s}}} L = \rho_{\mathrm{a}} L_{\mathrm{s}} u \left(\mathrm{d}_{T_{\mathrm{s}}} C_{\mathrm{E}} (q_{\mathrm{a}} - q_{\mathrm{s}}) - C_{\mathrm{E}} \mathrm{d}_{T_{\mathrm{s}}} q_{\mathrm{s}} \right) \tag{A16}$$

The derivative $\mathrm{d}_{T_{\mathrm{s}}} C_{\mathrm{E}}$ can be computed as the one of C_{H} through the chain rule and its dependence to $\mathrm{Ri_b}$. The derivative of q_{s} with respect to T_{s} can be easily obtained using the derivative of the saturated water vapor pressure, which is given by the Clausius-Clapeyron relation.

Appendix C: Finite Element Method scheme

In this paper, we focus on the FVM for spatial discretization. However, the heat budget equation could also be spatially discretized with the FEM. Indeed, the FEM naturally includes a node at the surface, and thus possesses a surface temperature, which helps to tightly couple the SEB to the interior of the snowpack/glacier. This strategy is for instance employed in the SNOWPACK model (Bartelt and Lehning, 2002; Wever et al., 2020). Specifically, in SNOWPACK, the coupled SEB is introduced as a top Robin boundary condition.

The goal of this appendix is to briefly present how the techniques presented in the main part of the manuscript (namely the use of fictitious variable and of a Schur-complement) can be used to implement a tightly-coupled FEM model.

C1 Expression of the heat equation in FEM

We consider the mesh of the domain to be discretized into N 1D elements (the direct equivalent of the cells in FVM) and thus of $N+1$ nodes (the end-points of the elements). As classically done with FEM (Pepper and Heinrich, 2005), we assume the temperature field to be a linear combination of basis functions φ_j, i.e. $T(z,t) = \sum_{k=1}^{N} T_j(t)\varphi_j(z)$. Here, we use basic linear elements. In this framework, $T_j(t)$ corresponds to the nodal value of the temperature field (which evolves over time) and the basis functions $\varphi_j(z)$ are piece-wise linear functions, valued 1 at node j and 0 at all other nodes. The standard Galerkin form (Pepper and Heinrich, 2005) of the internal heat budget (Eq. (1)) is:

$$\forall i \quad \sum_j \mathrm{d}_t T_j \int_\Omega c_\mathrm{p}\varphi_j\varphi_i \mathrm{dL} + \sum_j T_j \int_\Omega \lambda \nabla\varphi_j \cdot \nabla\varphi_i \mathrm{dL} = \int_\Omega Q\varphi_i \mathrm{dL} + F_\mathrm{s}\varphi_i(\mathrm{s}) \tag{C1}$$

where Ω represents the domain of simulation, F_s is the energy fluxes entering at the top of the domain (i.e. G), and $\varphi_i(\mathrm{s})$ is the basis function φ_i evaluated at top of the domain. We note that similarly to the FVM case, the temperature at the top of the domain presents a regime change whether the surface is melting or not. To handle this, we rely on the fictitious variable τ, i.e. $T_\mathrm{s} = T_\mathrm{s}(\tau)$. The vector of unknowns, denoted U, is thus composed of the internal temperatures and of the surface fictitious variable. Finally, we have not included any bottom energy flux to lighten the notation, but it could be included easily. Once temporally discretized with a Backward Euler scheme and linearized, the problem can be expressed in matrix form $AU^n = B$, with $A = (M + \Delta t K + \Delta t L)J_T$ and $B = MT^{n-1} + \Delta t Q + \Delta t F$ (T^{n-1} being the vector of temperature from the previous time step), and

$$M(i,j) = \int_\Omega c_\mathrm{p}\varphi_j\varphi_i \mathrm{dL} \tag{C2}$$

$$K(i,j) = \int_\Omega \lambda \nabla\varphi_j \cdot \nabla\varphi_i \mathrm{dL} \tag{C3}$$

$$L(N+1,N+1) = -d_\tau SEB + L_{\text{fus}} d_\tau \dot{m} \tag{C4}$$

$$J_T(i,i) = \begin{cases} 1 & \text{if } i \leq N \\ d_\tau T_{\text{s}} & \text{else} \end{cases} \tag{C5}$$

$$Q(i) = \int_\Omega Q \varphi_i \mathrm{dL} \tag{C6}$$

and

$$F(N+1) = SEB(\tau^i) - d_\tau SEB \tau^i - \dot{m} + L_{\text{fus}} \left(d_\tau \dot{m} \tau^i \right) \tag{C7}$$

where SEB and $d_\tau SEB$ corresponds to the atmospheric fluxes in the SEB and their derivatives with respect to τ at the current iteration, and $\dot{m}$ and $d_\tau \dot{m}$ are the melting rate and its derivative at the current iteration. In the equations above, only the non-zero terms have been given.

As in the FVM case, this system is composed of a linear-part (the interior, corresponding to the first $N-1$ equations) and a non-linear part (the surface, corresponding to the last two equations). Its solving can thus be accelerated using a Schur-complement technique (Section 4.1.1) by breaking the matrix A into four blocks: a constant $(N-1) \times (N-1)$ diagonal A_{diag} block, a constant $(N-1) \times 2$ vertical A_{up} block, a constant $2 \times (N-1)$ horizontal A_{low} block, and a 2×2 diagonal block A_{s} to be re-computed at each non-linear iteration.

C2 The rest of the model

After solving the coupled heat budgets with FEM, we obtain a nodal temperature field. Since conserved quantities, such as energy or mass, are defined element-wise in snowpack/glacier FEM models (Bartelt and Lehning, 2002), the nodal temperature field needs to be converted into an element-wise energy field. We note that this also defines an element-wise temperature field, where the temperature of an element is simply the average of the nodal temperatures at its end. This element-wise energy field can then be used to simulate melt/refreeze, liquid water percolation, and to remesh the domain using the same routines as in FVM models.

Once all routines for a given time step have been performed, we are left with an element-wise temperature field that needs to be converted back to a nodal temperature field, as required for the FEM. However, this conversion is not straightforward.

First, as we have N element-wise temperatures to transform into $N+1$ nodal temperatures, the problem is not properly closed and an extra (arbitrary) constraint needs to be added. This could, for instance, be setting the surface temperature to the value computed in the SEB. Furthermore, even after choosing an extra constraint to close the problem, the element-wise to node-wise transformation can produce spurious oscillations in the nodal field even if the element-wise field is monotonous (in other words, the transformation does not respect a form of discrete maximum principle; Ciarlet and Raviart, 1973). It is therefore not possible to derive an optimal scheme for this transformation that would (i) not modify the element-wise temperature field and (ii) not create spurious oscillations in the node-wise temperature field.

As spurious oscillations in the temperature field would affect the estimation of the temperature gradients that are used in snowpack models to estimate metamorphism (e.g. Bartelt and Lehning, 2002; Vionnet et al., 2012), it seems preferable to rather allow the modification of the element-wise temperature field. That being said, such a strategy implies a spatial re-distribution of energy between elements that is not motivated by any underlying physical mechanism. We note that the SNOWPACK model handles this element to node transformation during a phase change step after the liquid percolation scheme, and does so without creating large spurious temperature oscillations.

Unfortunately, it is not possible to directly implement the SNOWPACK scheme in our toy-model, as the sequential treatment is not the same. Moreover, we did not manage to derive a scheme that performs this element to node transformation without affecting the surface temperature. Thus, in our numerical simulations, the FVM and FEM models yield different results. In the absence of an analytical solution, a direct comparison of the FEM and FVM implementations remains impossible.

Appendix E: Stability Analysis

Here, we present the derivation of the criteria for the numerical stability of the different numerical schemes presented in the paper. We follow the proof classically used to show the (un)conditional stability of the Forward and Backward Euler method (Butcher, 2008). Notably, the proof relies on a linearized version of the system of equations. As the system needs to be linearized, we cannot account for the potential melting of the surface. Under this consideration, the atmospheric fluxes in the SEB (long-wave radiations, turbulent fluxes, etc) are simply expressed as a linear function of the surface temperature T_s, i.e. as $fT_\mathrm{s} + b$, where f and b are constant scalars expressed in $\mathrm{J\,s^{-1}\,m^{-2}\,K^{-1}}$ and in $\mathrm{J\,s^{-1}\,m^{-2}}$, respectively.

Also, for simplicity, we consider a system composed of only one cell and its surface. The problem could be generalized to more cells, but it would make the computation more cumbersome and is not crucial as we are considering numerical instabilities that develop in the vicinity of the surface.

E1 Standard skin-layer formulation (Class 2)

To compute the surface temperature T_s^{n+1} at time step $n+1$, we use the discretized Surface Energy Balance (SEB):

$$fT_\mathrm{s}^{n+1} + b + \frac{2\lambda}{\Delta z}\left(T_\mathrm{s}^{n+1} - T_\mathrm{i}^{n}\right) = 0 \tag{E1}$$

where the first two terms corresponds to the sum of outgoing/incoming atmospheric fluxes, and the last term to the subsurface heat conduction flux. Here, λ is the thermal conductivity of the internal cell and Δz its thickness. Note that the internal temperature T_i^{n} is taken from the previous time step. To compute the internal temperature at time step $n+1$, we use the heat budget of the internal cell:

$$\Delta z c_p T_\mathrm{i}^{n+1} + \Delta t \frac{2\lambda}{\Delta z}\left(T_\mathrm{i}^{n} - T_\mathrm{s}^{n+1}\right) = \Delta z c_p T_\mathrm{i}^{n} \tag{E2}$$

where the second term of the LHS is the opposite of the subsurface conduction flux appearing in the SEB (for energy conservation), and c_p is the heat capacity of the internal cell. The two above equations can be expressed in matrix form $MU_{n+1} = NU_n + B$, with U_n the solution vector $[T_\mathrm{s}, T_\mathrm{i}]^T$ at the n^{th} time step and

$$M = \begin{bmatrix} 1 & 0 \\ -\frac{2\Delta t\lambda}{c_p \Delta z^2} & 1 \end{bmatrix} \tag{E3}$$

$$N = \begin{bmatrix} 0 & \frac{2\lambda}{2\lambda + \Delta z f} \\ 0 & 1 - \frac{2\Delta t\lambda}{c_p \Delta z^2} \end{bmatrix} \tag{E4}$$

and $B = [-\frac{\Delta z b}{\Delta z f + 2\lambda}, 0]^T$. We thus have, $U_{n+1} = QU_n + M^{-1}B$, with

$$Q = M^{-1}N = \begin{bmatrix} 0 & \frac{2\lambda}{2\lambda+\Delta z f} \\ 0 & 1 - \Delta t \frac{2\lambda}{c_p \Delta z^2} \frac{\Delta z f}{2\lambda+\Delta z f} \end{bmatrix} \tag{E5}$$

By recursion, it follows that $U_n = Q^n U_0 + M^{-n} B$. The numerical scheme is deemed stable if $\lim_{n\to\infty} Q^n = 0$. This is achieved if:

$$|1 - \Delta t \frac{2\lambda}{c_p \Delta z^2} \frac{\Delta z f}{2\lambda + \Delta z f}| < 1 \tag{E6}$$

which after some computation yields a criterion of the time step Δt:

$$\Delta t < \Delta t_{\mathrm{crit}} = \frac{c_p \Delta z}{\lambda} \frac{2\lambda + \Delta z f}{f} \tag{E7}$$

The (linearized) standard skin-layer is thus only conditionally stable. The stability criterion is relaxed with increasing heat capacity (c_p) and increasing cell size (Δz), and is made more restrictive with increasing thermal conductivity (λ) or if the SEB is more sensitive to changes in the surface temperature (f term).

E2 Coupled-surface formulation

Similarly, for a one cell system, the coupled-surface equations, after linearization, write:

$$f T_{\mathrm{s}}^{n+1} + b + \frac{2\lambda}{\Delta z} \left(T_{\mathrm{s}}^{n+1} - T_{\mathrm{i}}^{n+1} \right) = 0 \tag{E8}$$

for the SEB, and

$$\Delta z c_p T_{\mathrm{i}}^{n+1} + \Delta t \frac{2\lambda}{\Delta z} \left(T_{\mathrm{i}}^{n+1} - T_{\mathrm{s}}^{n+1} \right) = \Delta z c_p T_{\mathrm{i}}^{n} \tag{E9}$$

for the cell's heat budget. These two equations can be cast into the matrix form $MU_{n+1} = NU_n + B$, with $B = [-\frac{\Delta z b}{\Delta z f + 2\lambda}, 0]^T$,

$$M = \begin{bmatrix} 1 & \frac{-2\lambda}{2\lambda+\Delta z f} \\ -\frac{2\Delta t \lambda}{c_p \Delta z^2 + 2\lambda \Delta t} & 1 \end{bmatrix} \tag{E10}$$

and

$$N = \begin{bmatrix} 0 & 0 \\ 0 & \frac{c_p \Delta z^2}{c_p \Delta z^2 + 2\lambda \Delta t} \end{bmatrix} \tag{E11}$$

We thus have $U_n = Q^n U_0 + M^{-n} B$, with:

$$Q = \begin{bmatrix} 0 & \frac{2\lambda}{2\lambda+\Delta z f} \frac{c_p \Delta z^2}{c_p \Delta z^2 + 2\lambda \Delta t} \\ 0 & \frac{c_p \Delta z^2}{c_p \Delta z^2 + 2\lambda \Delta t} \end{bmatrix} \tag{E12}$$

The numerical scheme is deemed stable if $\lim_{n\to\infty} Q^n = 0$. This is always achieved, as $\frac{c_p \Delta z^2}{c_p \Delta z^2 + 2\lambda \Delta t} < 1$. Thus, the surface-coupled scheme is unconditionally stable.

E3 Non-conservative skin-layer formulation

For the non-conservative skin-layer formulation (see Section 6.4), we start with the linearized discrete SEB:

$$f T_{\mathrm{s}}^{n+1} + b + \frac{2\lambda}{\Delta z} \left(T_{\mathrm{s}}^{n+1} - T_{\mathrm{i}}^{n} \right) = 0 \tag{E13}$$

Using the surface temperature T_{s}^{n+1} as a Dirichlet condition for the internal energy budget, we thus have

$$\Delta z c_p T_{\mathrm{i}}^{n+1} + \Delta t \frac{2\lambda}{\Delta z} \left(T_{\mathrm{i}}^{n+1} - T_{\mathrm{s}}^{n+1} \right) = \Delta z c_p T_{\mathrm{i}}^{n} \tag{E14}$$

These two equations can be cast into the matrix form $M U_{n+1} = N U_n + B$, with $B = [-\frac{\Delta z b}{\Delta z f + 2\lambda}, 0]^T$,

$$M = \begin{bmatrix} 1 & 0 \\ -\frac{2\Delta t \lambda}{c_p \Delta z^2 + 2\lambda \Delta t} & 1 \end{bmatrix} \tag{E15}$$

and

$$N = \begin{bmatrix} 0 & \frac{2\lambda}{2\lambda+\Delta z f} \\ 0 & \frac{c_p \Delta z^2}{c_p \Delta z^2 + 2\lambda \Delta t} \end{bmatrix} \tag{E16}$$

We thus have $U_n = Q^n U_0 + M^{-n} B$, with:

$$Q = \begin{bmatrix} 0 & \frac{2\lambda}{2\lambda+\Delta z f} \\ 0 & X \end{bmatrix} \tag{E17}$$

where $X = \frac{2\lambda \Delta t \frac{2\lambda}{2\lambda+\Delta z f} + c_p \Delta z^2}{2\Delta t \lambda + c_p \Delta z^2}$. The scheme is deemed stable if $|X| < 1$.

As $\frac{2\lambda}{2\lambda+\Delta z f} < 1$, we always have that $2\lambda \Delta t \frac{2\lambda}{2\lambda+\Delta z f} + c_p \Delta z^2 < 2\Delta t \lambda + c_p \Delta z^2$, and thus that the scheme is unconditionally stable. That being said, we recall that this scheme is not energy conservative and can lead to large errors.

E4 No-surface formulation (Class 1)

Finally, we note that the linearized No-surface formulation corresponds to a classic heat equation with a Backward Euler time integration. As demonstrated elsewhere in the literature (e.g. Butcher, 2008), it is unconditionally stable.

A novel numerical implementation for the surface energy budget of melting snowpacks and glaciers

Kévin Fourteau[1], Julien Brondex[1], Fanny Brun[2], and Marie Dumont[1]

[1]Univ. Grenoble Alpes, Université de Toulouse, Météo-France, CNRS, CNRM, Centre d'Études de la Neige, Grenoble, France

[2]Univ. Grenoble Alpes, CNRS, IRD, Grenoble INP, IGE, Grenoble, France

Correspondence: Marie Dumont (marie.dumont@meteo.fr)

Abstract. The surface energy budget drives the melt of the snow cover and glacier ice and its computation is thus of crucial importance in numerical models. This surface energy budget is the ~~sum~~ result of various surface energy fluxes, ~~that~~ which depend on the input meteorological variables and surface temperature, ~~and to which~~ of heat conduction towards the interior of the snow/ice~~and potential melting need to be added~~, and potentially of surface melting if the melt temperature is reached. The surface temperature and melt rate of a snowpack or ice are thus driven by coupled processes. In addition, these energy fluxes are non-linear with respect to the surface temperature, making their numerical treatment challenging. To handle this complexity, some of the current numerical models tend to rely on a sequential treatment of the involved physical processes, in which surface fluxes, heat conduction, and melting are treated with some degree of decoupling. Similarly, some models do not explicitly define a surface temperature and rather use the temperature of the internal point closest to the surface instead. While these kinds of approaches simplify the implementation and increase the modularity of models, it can also introduce several problems, such as instabilities and mesh sensitivity. Here, we present a numerical methodology to treat the surface and internal energy budgets of snowpacks and glaciers in a tightly-coupled manner, including potential surface melting when the ~~fusion~~ melt temperature is reached. Specific care is provided to ensure that the proposed numerical scheme is as fast and robust as classical numerical treatment of the surface energy budget. Comparisons based on simple test cases show that the proposed methodology yields smaller errors for almost all time steps and mesh sizes considered and does not suffer from numerical instabilities, contrary to some classical treatments.

1 Introduction

Snowpacks and glaciers are crucial parts of the Earth system that have a profound impact, among others, on the water cycle (e.g. Barnett et al., 2005) and on the radiative budget of continental surfaces (e.g. Flanner et al., 2011). A key tool to understand the interaction between snowpacks/glaciers and the other components of the Earth system are numerical models ~~,~~that aim to quantitatively represent the evolution of snowpacks and glaciers under various atmospheric forcings. To reach this goal, the representation and evolution of the thermodynamical state (that is to say temperature profiles and phase changes) of snowpacks and glaciers are implemented in most ~~(if not all) numerical models (e.g. Jordan, 1991; Bartelt and Lehning, 2002; Liston and Elder, 2006; Vion~~ numerical snowpack/glacier models (e.g. Anderson, 1976; Brun et al., 1989; Jordan, 1991; Bartelt and Lehning, 2002; Liston and Elder, 2

.

Among the various processes driving the thermodynamical state of snowpacks and glaciers, the surface energy budget (SEB) has received detailed attention in the past, notably because of its central role (e.g. Etchevers et al., 2004; Miller et al., 2017; Schmidt et al., 2017, among many others). Indeed, the ~~surface energy budget~~ SEB governs most of the net energy input and output within the snowpack/glacier and thus has a fundamental role for its warming/cooling and for its melting. This SEB is the net result of various energy fluxes, including turbulent fluxes and long-wave radiative flux ~~, that directly and non-linearly~~ that directly depend on the surface temperature of the snowpack/glacier. Mathematically, the ~~surface energy budget~~ SEB thus appears as a ~~highly~~ non-linear top boundary condition for snowpacks and glaciers. This non-linearity is even reinforced by the existence of a regime change between a melting and non-melting surface, with different thermodynamical behaviors below and ~~above~~ at the melting point. ~~This profoundly non-linear nature~~ Indeed, once the melting point is reached at the surface, the SEB becomes more akin to a Stefan-problem with a discontinuity in the energy fluxes and can no longer be simply described in terms of surface temperature. This leads to numerical challenges when solving the governing equations.

As a consequence, there are currently no uniquely employed strategies to treat this problem, and various numerical schemes have been proposed and implemented for solving the SEB and its link with the thermodynamical state of a snowpack/glacier (Bartelt and Lehning, 2002; Vionnet et al., 2012; van Pelt et al., 2012; Sauter et al., 2020). Among the different published implementations, one can notably cite the so-called "skin-layer" formulation, usually employed in combination with a finite volume method (FVM) for the internal heat equation, in which the surface and internal temperatures are solved sequentially over a given time step (Oerlemans et al., 2009; Kuipers Munneke et al., 2012; van Pelt et al., 2012; Covi et al., 2023). While this approach naturally offers modularity and simplifies the treatment of the SEB (and of the associated surface temperature), a sequential treatment of tightly-coupled processes or variables is also known to display some instability (e.g. Ubbiali et al., 2021; Brondex et al., 2023) and large time step sensitivity (e.g. Barrett et al., 2019). On the other hand, some FVM implementations do not define a specific temperature associated with the surface, but rather use the temperature of the top-most numerical layer of the domain (i.e. the top layer of the simulated snowpack/glacier) for solving the SEB (Anderson, 1976; Brun et al., 1989; Jordan, 1991; Vionnet et al., 2012; van Kampenhout et al., 2017). While this enables to easily solve the SEB and the internal heat budget in a tightly-coupled way, this method requires to refine the numerical grid near the surface, in order to properly simulate the SEB. Thus, currently-employed FVM strategies in snowpack/glacier models present some limitations ~~,~~that can be detrimental for the obtained numerical solutions.

Here, we propose a FVM numerical scheme meant to combine the advantages of the previously published numerical strategies. Precisely, our goal is to offer a tightly-coupled treatment (as opposed to a sequential treatment) of the internal and surface temperatures of a snowpack or glacier. For this, the proposed implementation explicitly defines a temperature right at the surface (viewed as an infinitely ~~small~~ thin horizontal layer), which improves the simulated results in terms of accuracy and stability. As the snowpack and glacier models are sometimes used in distributed or long-time spanning simulations, specific care is taken to ensure that the proposed numerical scheme has a similar numerical cost as the already published ones.

The article is organized as follows: Section 2 presents the physical equations governing the energy budget of snowpacks and glaciers, Section 3 briefly recalls some of the existing numerical schemes to solve these governing equations, and Section 4

presents the proposed numerical scheme overcoming some of the limitations of existing strategies, while keeping their strong points. Finally, some simple examples are presented in Section 5, and a discussion comparing the different numerical schemes is provided in Section 6.

2 Governing equations

The goal of this Section is to briefly recall the general equations governing the thermal regime of snowpacks and glaciers, before presenting their numerical discretization in the next Section. As snowpack and glaciers share many similarities and processes, such as heat conduction or the presence of a phase transition when the melt temperature is reached, they can be represented by the same type of equations. These similarities enable simulations mixing snow and glacier ice within a single framework (e.g. Sauter et al., 2020). Hence, for the sake of generality, the equations discussed in the following sections apply to both snow and glacier ice. That being said, snow and glacier ice present some differences, notably concerning liquid water percolation. As addressed later, this might require a differential treatment of glacier ice and snow when implementing the liquid water percolation scheme.

2.1 Internal energy budget

The thermal regime of the inner part of a snowpack or glacier is governed by the principle of energy conservation. Assuming that Fourier's law of heat conduction applies in snow/ice with a well-defined macroscopic thermal conductivity (e.g. Calonne et al., 2011), this energy conservation writes:

$$\partial_t h - \nabla \cdot (\lambda \nabla T) = Q \tag{1}$$

where h is the internal energy content of snow/ice (expressed in $\mathrm{J\,m^{-3}}$), λ the thermal conductivity, T the temperature, and Q volumetric energy sources (such as the distributed absorption of shortwave radiations). Here, h is understood as the energy content, including latent heat associated with the presence of liquid water (Tubini et al., 2021). The volumetric energy sources Q (expressed in $\mathrm{W\,m^{-3}}$) therefore do not include the absorption or release of latent heat during solid/liquid water phase changes. In this article, we assume that the snowpack/glacier can be represented as 1D column, and therefore Eq. (1) should be understood as 1D equation.

Assuming thermodynamical equilibrium between the ice and liquid water, the temperature T and the energy content h are related through:

$$h = c_\mathrm{p}(T - T_0) + \rho_\mathrm{w} L_\mathrm{fus} \theta \tag{2}$$

where c_p is the volumetric ~~thermal~~ heat capacity of snow/ice (expressed in $\mathrm{J\,K^{-1}\,m^{-3}}$), T_0 an arbitrary reference temperature taken as the ~~fusion~~ melt temperature, ρ_w the density of liquid water, L_fus the specific enthalpy of fusion of water (expressed in

J kg^{-1}), and θ the liquid water content (expressed in m^3 of liquid water per m^3 of snow/ice) (Tubini et al., 2021).

Note that in Eq. (1) the time derivative of the internal energy content h cannot in principle be replaced by $c_\mathrm{p}\partial_t T$, but should also include the term $\rho_\mathrm{w} L_\mathrm{fus}\partial_t\theta$. Indeed, once the temperature has reached the ~~fusion~~ melting point, a further increase in energy translates into an increase in the liquid water content ($\partial_t\theta \neq 0$) and of the associated latent heat content, rather than a further increase in the temperature. Yet, as discussed below, snowpack and glacier models nonetheless usually consider that the temperature can increase past the ~~fusion~~ melting point when integrating Eq. (1) in time (Vionnet et al., 2012; Sauter et al., 2020). This is equivalent to neglecting the effects of first-order phase changes (melting and refreezing) on the temperature field, and thus setting $\rho_\mathrm{w} L_\mathrm{fus}\partial_t\theta$ to zero while solving the heat equation. This results in temperature overshoots that are then corrected in a second step by creating melt and setting back the temperature to the ~~fusion value (e.g., Bartelt and Lehning, 2002; Vionnet et al., 2012; Sauter e~~ melt value (e.g., Vionnet et al., 2012; Sauter et al., 2020). In this article, we follow this simple scheme as it is commonly employed in snowpack and glacier models. That being said, other, more complex, strategies have been proposed in the literature. This notably includes the use of a finite temperature-range over which melt/freezing occurs (e.g. Albert, 1983; Dutra et al., 2010), including melt/refreeze as an additional energy source term (e.g. Bartelt and Lehning, 2002; Wever et al., 2020), or the use of enthalpy as the prognostic variable (e.g. Meyer and Hewitt, 2017; Tubini et al., 2021). Finally, in this article we consider the thermal conductivity λ and capacity c_p not to depend on temperature. The motivation for this is twofold as it (i) corresponds to a simplifying assumption regularly made by snowpack and glacier surface models (e.g. van Pelt et al., 2012; Vionnet et al., 2012; Sauter et al and (ii) it allows keeping the internal heat equation linear.

2.2 Surface energy balance

To model an actual snowpack/glacier subjected to atmospheric forcings, it is necessary to complement the internal energy budget with an appropriate boundary condition. At the top of the snowpack/glacier, this boundary condition is given by the ~~surface energy balance~~SEB. This SEB states that the net sum of energy fluxes between the top of the snowpack/glacier and the atmosphere equals the energy thermally conducted from the surface to the interior of the snowpack plus a potential surface melting term if the ~~fusion~~ melt temperature is reached (Oerlemans et al., 2009; Sauter et al., 2020; Covi et al., 2023). We thus have:

$$SW_\mathrm{net}^\mathrm{surf} + LW_\mathrm{in} + LW_\mathrm{out} + H + L + R = G + \dot{m} L_\mathrm{fus} \tag{3}$$

where $SW_\mathrm{net}^\mathrm{surf}$ is the net shortwave radiation absorbed right at the surface (that is thus distinguished from the portion of shortwave radiation penetrating within the snow/ice), LW_in is the incoming longwave radiation flux, LW_out is the outgoing longwave radiation flux, H is the turbulent sensible heat flux, L is the turbulent latent heat flux, R the surface energy brought by precipitating rain, G is the conductive heat flux penetrating within the snowpack/glacier, and $\dot{m}$ is the rate of surface melting (expressed in kg m^{-2} s^{-1}). Fluxes are orientated towards the bottom, and thus towards the surface for $SW_\mathrm{net}^\mathrm{surf}$, LW_in, LW_out, H, L, and R and away from the surface for G. The surface melting rate $\dot{m}$ vanishes when the surface temperature T_s is be-

low the ~~fusion~~ melt temperature, and can take non-zero values when the surface temperature equals the ~~fusion~~ melt temperature.

Among the various terms of the ~~surface energy balance~~ SEB of Eq. (3), LW_{out}, H, L, and G depend non-linearly on the surface temperature T_{s}. Notably, the outgoing longwave radiation is given by Stefan-Boltzmann law, i.e. $LW_{\mathrm{out}} = -\sigma T_{\mathrm{s}}^4$ (with σ the Stefan-Boltzmann constant) and the turbulent heat fluxes H and L can be estimated through the use of a bulk approach (e.g. Foken, 2017). These three terms are therefore non-linear functions of the surface temperature. In addition, the conductive heat flux is given by

$$G = -\left(\lambda \partial_z T\right)|_{z=\mathrm{surf}} \tag{4}$$

and is therefore proportional to the temperature gradient within snow/ice right below the surface. This conductive flux depends on both the surface temperature T_{s} and the temperature within the snow/ice. This flux is responsible for the thermal coupling between the surface and the interior of the snowpack/glacier.

3 Numerical strategy of existing models

Since the computation of the heat budget with a SEB as a top boundary condition is at the core of all snow/glacier models, several numerical implementations have been proposed for solving the resulting system of equations. In order to provide a general overview of the numerical frameworks and strategies, we propose to separate them into two broad classes, to which most existing models can somehow be related. While classifying existing strategies into only two groups (and not more) remains arbitrary, we believe it is helpful to highlight differences in handling the numerical solving of the energy budget. Moreover, we ~~only consider~~ focus on numerical schemes based on ~~the finite volumes method (FVM)~~FVM, as it ~~matches the discretizations~~ is the method employed by most models ~~(e.g. Vionnet et al., 2012; Sauter et al., 2020; Westermann et al., 2023). We therefore do not treat the finite elements method , which is for instance used in the SNOWPACK model~~ (e.g. Anderson, 1976; Sauter et al., 2020; Westerman . We note that, contrary to the FVM, the use of the finite element method (FEM) naturally incorporates the presence of a surface temperature, which can be used for a fully-coupled treatment of the SEB, as done in SNOWPACK for instance (Bartelt and Lehning, 2002).

3.1 Class 1: Finite volumes without explicit surface

A first class of models relies on FVM for discretization of the internal heat budget, without the inclusion of an extra degree of freedom to model the surface temperature (schematically depicted ~~in panel a of~~ as Class 1 in Fig. 1). To this end, the domain to be modeled (snowpack or glacier) is first decomposed into a finite number of cells with non-zero thicknesses (that are also sometimes referred to as layers, but should not be confused with the strata forming a snowpack). Then, the equations governing the temporal evolution of the average heat content of each cell is determined by integrating Eq. (1) over each cell. The energy

fluxes between cells are finally estimated based on cell-to-cell temperature differences and on the thermal conductivities of the cells. As discussed above, the effects of the first-order phase transition during melting/refreezing are usually not taken into account when solving the internal heat budget. Rather, it is considered that snow/ice temperature can exceed the ~~fusion~~ melt temperature without modification of its physical behavior (i.e., of its ~~thermal~~ heat capacity). When integrating the equations in time, this can ~~results~~ result in temperature overshooting the ~~fusion~~ melt point. These overshoots are later used to determine where the ~~fusion~~ melting point has been crossed, and the excess energy is then used to estimate melting (e.g. Vionnet et al., 2012).

This FVM framework thus amounts to determining the average temperature in each cell, which is usually considered to correspond to the temperature at the center of the cell. Without further modification, the surface temperature, which corresponds to the temperature on the upper edge of the top cell, is not present in the system of equations. In order to apply the ~~surface energy balance~~ SEB as a boundary condition, this first class of models considers the surface temperature to be equal to the temperature of the top-most cell. The energy fluxes between the surface and the atmosphere are then directly integrated into the heat budget of the top cell. The internal heat budget and the integrated surface fluxes can then be solved at the same time, i.e. in a tightly-coupled fashion. The advantage of this approach is that it naturally allows one to take into account the SEB within a standard FVM framework, without the necessity to handle extra degrees of freedom. This numerical strategy roughly corresponds to the one adopted in ~~Crocus~~ SNTHERM (Jordan, 1991), Crocus (Vionnet et al., 2012), CLM (van Kampenhout et al., 2017), or CryoGrid (Westermann et al., 2023).

3.2 Class 2: Finite volumes with an explicit but decoupled surface

The second class of models also relies on FVM for the spatial discretization of the internal heat budget. Similarly to the models of class 1, the first-order phase transition of snow/ice is usually neglected for the resolution of the equations, resulting in temperature overshoots that are later corrected by creating melting.

However, this class of models explicitly takes into account the presence of a surface temperature ~~,~~ that differs from the temperature of the cell just below (schematically depicted ~~in panel b of~~ as Class 2 in Fig. 1). This surface temperature is computed by searching for the temperature that equilibrates the ~~surface energy budget~~ SEB of Eq. (3), assuming no melting. If the equilibrium temperature is larger than the ~~fusion~~ melting point, it is then capped to the ~~fusion~~ melt temperature and the excess surface energy converted into surface melting.

Because of the numerical complexity of this task, it is usually performed separately from the computation of the internal heat budget. Typically, the surface temperature is first resolved, using the internal temperatures of the previous time-step for the heat conduction term of the ~~surface energy balance~~SEB, and then the internal temperatures are solved using the newly computed surface temperature and ~~surface energy budget~~SEB.

This class of models encompasses the models using a so-called skin-layer formulation for the ~~surface energy budget~~SEB. Its advantage is that it allows to explicitly define a surface temperature without complexifying the solving of the internal heat budget and keeping a low numerical cost. It roughly corresponds to the models SnowModel (Liston and Elder, 2006), EBFM

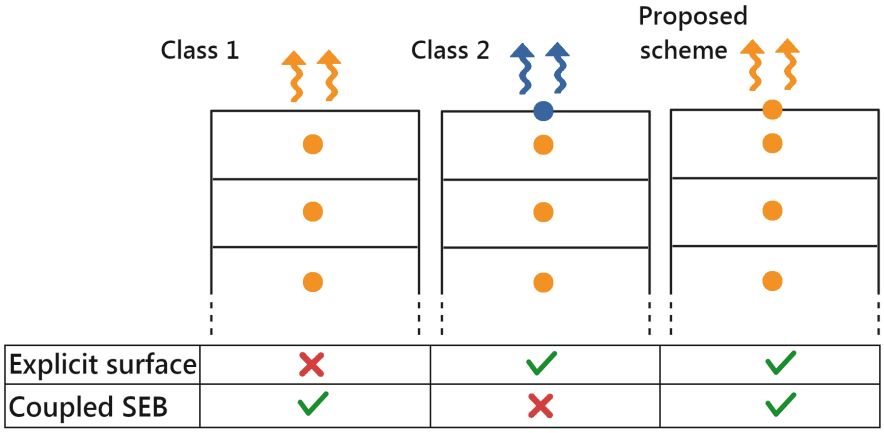

Figure 1. Classification of FVM models with respect to their treatment of the ~~surface energy budget~~SEB. ~~a)~~ Class 1: The surface energy and the internal temperatures are solved in a tightly-coupled manner, but there is no explicit surface. ~~b)~~ Class 2: An explicit surface temperature (and surface melting) exists, but it is solved in sequential manner with respect to the internal temperatures. ~~c)~~ Proposed scheme in this article: An explicit surface temperature is considered and is solved in a tightly-coupled manner with the internal temperatures. In the schematic, dots represent the prognostic variables of the schemes (with or without temperature at the surface) while the colors indicate which variables are solved simultaneously.

(van Pelt et al., 2012), or COSIPY (Sauter et al., 2020).

Finally, we want to stress that the actual implementations of the aforementioned models (e.g. Crocus, SNTHERM, COSIPY, EBFM, etc) cannot be perfectly captured by our simple classification. Particular choices regarding the spatial and temporal discretizations, the treatment of melting and refreezing, and the coupling between individual processes make each model unique and more complex than the above presentation. Also, models can in principle display the characteristics of both classes (i.e. no explicit surface and a ~~surface energy budget~~ SEB solved with a decoupling from the rest of the domain), although we did not find any concrete example. This diversity of models offers an actual illustration of how the numerical implementation of the same processes (internal heat budget with a complex ~~surface energy balance~~SEB) has been handled by different authors.

4 A tightly-coupled solution for the surface and internal heat budget

As seen above, each class of models comes with advantages but also limitations. While class 1 models solve the internal and ~~surface energy budgets~~ SEB in a tightly-coupled manner, they do not take into account the fact that the surface temperature is in general different from the temperature in the cell below. On the contrary, while class 2 models explicitly consider a surface temperature, the internal and ~~surface energy budgets~~ SEB are treated in a sequential, and therefore loosely-coupled fashion,

which can be detrimental to stability (Ubbiali et al., 2021).

Based on these observations, the goal of this section is to present a FVM methodology that allows one (i) to explicitly work with a surface temperature, (ii) to treat the surface and internal heat budgets in a tightly-coupled fashion. ~~As explained above, we restrain ourselves to a FVM discretization.~~ Moreover, as the goal of this paper is to focus on the treatment of the ~~surface energy budget~~ SEB and its coupling with the internal thermal state, we also follow the standard approach to handle melting in the interior of the domain. Namely, first-order phase transition effects are neglected while solving for the internal energy budgets. This means that interior temperatures will overshoot in case of melting, and this excess temperatures will be used to generate melt afterward.

4.1 Governing system of discretized equations

In this section, we derive the discretized equations governing the coupled surface and internal heat budgets, based on the FVM. For this, ~~let's~~ we consider a domain divided into N cells. The temporal evolution of the average heat content of each cell is given by integrating Eq. (1) over the cell and making use of the ~~divergence theorem~~ fundamental theorem of calculus. Neglecting phase change during the resolution of the internal heat budget, the time derivative of the ~~temperature~~ (average) temperature T_k of the k^{th} cell is given by:

$$\Delta z_\mathrm{k} c_{\mathrm{p_k}} \partial_t T_\mathrm{k} + F_{\mathrm{k}+\frac{1}{2}} - F_{\mathrm{k}-\frac{1}{2}} - \Delta z_\mathrm{k} Q_\mathrm{k} = 0 \tag{5}$$

where Δz_k is the thickness of the k^{th} cell, $c_{\mathrm{p_k}}$ its volumetric ~~thermal~~ heat capacity, Q_k the average volumetric energy source in the cell, and $F_{\mathrm{k}+\frac{1}{2}}$ and $F_{\mathrm{k}-\frac{1}{2}}$ are the heat conduction fluxes at the top and bottom interfaces of the cell. For internal cells, $F_{\mathrm{k}+\frac{1}{2}}$ and $F_{\mathrm{k}-\frac{1}{2}}$ correspond to the fluxes between the k^{th} and the $k+1^{\mathrm{th}}$ cells and the $k-1^{\mathrm{th}}$ and k^{th} cells, respectively. For the top cell $F_{\mathrm{k}+\frac{1}{2}}$ corresponds the heat flux leaving towards the surface (i.e. $-G$) and for the bottom cell $F_{\mathrm{k}-\frac{1}{2}}$ corresponds to the flux from the ground. By convention, we take $F_{\mathrm{k}+\frac{1}{2}}$ as positive if the heat flux is oriented from the k^{th} cell to the $k+1^{\mathrm{th}}$. Note that in this paper we consider the ~~0^{th}~~ 1^{st} cell to be at the bottom of the snowpack, and the cells to be counted positively upwards. Other numbering choices could be made and would lead to the same end-result.

~~These~~ The heat conduction fluxes between cells need to be estimated from the temperatures and thermal conductivities of adjacent cells. The flux $F_{\mathrm{k}+\frac{1}{2}}$ between cells k and $k+1$ is computed as:

$$F_{\mathrm{k}+\frac{1}{2}} = \lambda^{\mathrm{harm}}_{\mathrm{k}+\frac{1}{2}} \frac{T_\mathrm{k} - T_{\mathrm{k}+1}}{\frac{\Delta z_\mathrm{k}}{2} + \frac{\Delta z_{\mathrm{k}+1}}{2}} \tag{6}$$

where $\lambda^{\mathrm{harm}}_{\mathrm{k}+\frac{1}{2}}$ is the weighted harmonic average of the thermal conductivity of the two adjacent cells. The use of ~~an~~ a harmonic average provides better results in the case of layered media such as snow (Kadioglu et al., 2008) and ensures that no heat conduction occurs in case one of the cells is a perfect thermal insulator.

Note that ~~slightly modified version of~~ Eq. ~~(6) applies~~ 6 only applies to fluxes between cells and must be replaced for the two boundary cells, at the top and bottom of the domain. For the bottom cell, a flux between the domain and the ground below must be used as a bottom boundary condition. For the top cell, the heat flux coming from the surface must be used. This flux ~~corresponds to~~ is given by the discretized version of the term G ~~of the SEB~~in the SEB, provided in Eq. (~~3)~~ 10) below.

This FVM discretization results in N equations governing the evolution of the N internal temperatures. The surface temperature can be added to this system of equations by introducing an additional degree of freedom, localized at the top of the domain. This surface temperature can be deduced from the ~~surface energy balance~~ SEB of Eq. (3) and its coupling to the interior of the domain through the subsurface heat flux G of Eq. (4). However, the ~~surface energy balance~~ SEB cannot be fully characterized using the surface temperature only. Indeed, in case of melting, the surface temperature is blocked at the ~~fusion~~ melt temperature T_0 and can no longer be used as a prognostic variable to characterize the surface. In this case, it is necessary to introduce a non-zero melting rate $\dot{m}$ to close the energy budget. We thus have two regimes for the surface: below the ~~fusion~~ melting point the surface is fully characterized by its temperature and the melting rate term vanishes; at the ~~fusion~~ melting point, the surface temperature becomes constant and the melting rate term $\dot{m}$ becomes the quantity that characterizes the state of the surface. At any time, the surface is fully characterized by only one independent variable, but neither the temperature nor the melt rate can be used in the general case.

To circumvent this problem, we rely on a variable switching technique (Bassetto et al., 2020). Concretely, we introduce a fictitious variable, denoted τ, whose goal is to behave as T_s below the ~~fusion~~ melting point and as $\dot{m}$ during melting. In other words, we parametrize the $\{T_\mathrm{s}(\tau), \dot{m}(\tau)\}$ graph, such that every possible state of the surface can be appropriately described by a well-defined τ value. A possibility is to take τ such as:

$$T_\mathrm{s} = \begin{cases} \tau & \text{if} \quad \tau < T_0 \\ T_0 & \text{otherwise} \end{cases} \tag{7}$$

and

$$\dot{m} = \begin{cases} 0 & \text{if} \quad \tau < T_0 \\ \frac{\tau - T_0}{\beta} & \text{otherwise} \end{cases} \tag{8}$$

where β is an arbitrary constant, necessary to ensure dimensional homogeneity (concretely taken as $1\,\mathrm{kg\,m^{-2}\,s^{-1}\,K^{-1}}$ in our implementation).

Then, the ~~surface energy budget~~ SEB can be expressed as:

$$SW_\mathrm{net}^\mathrm{surf} + LW_\mathrm{in} + LW_\mathrm{out}(\tau) + H(\tau) + L(\tau) + R(\tau) - G(\tau) - \dot{m}(\tau) L_\mathrm{fus} = 0 \tag{9}$$

where the dependence of LW_{out}, H, L, R, and G to τ through T_{s} has been made explicit. The subsurface conduction heat flux can thus be approximated by spatially discretizing Eq. (4):

$$G = \lambda_{\mathrm{k}} \frac{T_s(\tau) - T_k}{\Delta z_{\mathrm{k}}/2} \tag{10}$$

where the index k is taken to correspond to the top-most cell. As explained above, this flux must also be taken into account in the equation governing the heat content of the top-most cell.

We thus have a system of $N+1$ equations (one for each cell plus the ~~surface energy balance~~SEB), which governs the evolution of $N+1$ prognostic variables (the temperature of each cell plus the surface temperature/melt-rate encapsulated into τ). To be numerically solved, this system also requires a temporal discretization. In this article, we choose an implicit backward Euler's method for its simplicity and stability (Fazio, 2001; Butcher, 2008). Nonetheless, the method proposed here could also be applied with other temporal integration schemes (e.g. Crank-Nicolson).

This system of equations presents several non-linearities, coming from the non-linearity of some terms in the ~~surface energy budget~~ SEB with respect to the surface temperature (~~e.g.~~ LW_{out} ~~or~~ , H, and L) and from the regime change of the surface (between melting and non-melting conditions). In order to deal with these non-linearities, we rely on the use of a specific Newton's method, described below. We also note that some models made the choice of performing only a single iteration to solve this linear system of equations (with sometimes an extra iteration to handle specific cases, such as surface melting). However, we chose here to perform multiple iterations, in order to obtain the actual Backward Euler solution.

4.1.1 A dedicated Newton's method

One of the main benefits of the skin-layer formulation used by models of class 2 is its low numerical cost. Indeed, all the non-linearity of the problem only appears in the ~~surface energy budget~~SEB, i.e. in a single scalar equation that can be solved iteratively. While iterations are costly in numerical models, this cost is here tempered by the fact that this only needs to be performed on a scalar equation, with a limited number of terms to be re-estimated at each iteration. Once the surface temperature has been determined, the internal temperatures can be solved through a N×N linear system of equations ~~,~~that does not require multiple iterations. On the contrary, solving the (N+1)×(N+1) non-linear system of equations derived in Section 4 can be much more numerically expensive if the whole system is to be re-assembled and re-inverted at each iteration.

Keeping this issue of numerical cost in mind, we propose a numerical strategy to solve the system of equations describing the coupled internal and surface energy budgets. It is based on a modified Newton scheme, with two modifications proposed to make the iteration process both more robust and faster.

Truncation method for regime changes:

A first modification made to this standard Newton's method is the use of the truncation method when crossing discontinuities

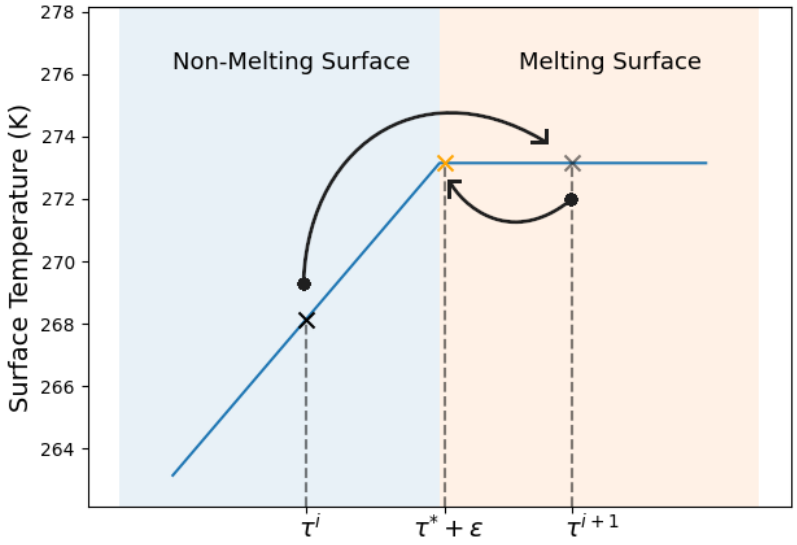

Figure 2. Example of the truncation method made to handle derivative discontinuities during Newton's iterations (schematic inspired by Fig. 2.3 of Bassetto, 2021). Starting from an estimate τ^i, a new estimate τ^{i+1} is computed based on the Jacobian estimated at τ^i. As a derivative discontinuity is crossed, the fictitious variable τ is set back near the discontinuity τ^* but in the "melting surface" regime.

during the iteration process (Wang and Tchelepi, 2013; Bassetto et al., 2020). The idea behind truncation is that the Jacobian (i.e. the ~~derivatives of the discretized~~ derivative of the equations with respect to the unknowns to be solved for) computed on one side of a derivative discontinuity does not apply on the other side, and can therefore perturb the convergence towards the solution, typically leading to an endless iteration loop. In our model, this problem notably arises from the ~~surface energy budget~~ SEB that shows discontinuity with respect to τ when crossing the melting point. A similar problem can also appear in the turbulence terms of the ~~surface energy budget~~SEB. For instance, some formulations of the turbulent fluxes can include derivative discontinuities for the stability correction of the latent and sensible fluxes with respect to the bulk Richardson number (as in e.g. Martin and Lejeune, 1998; Sauter et al., 2020). Thus, during the iteration process each time the surface changes regime (between non-melting/melting or stable/unstable conditions), the value of τ is brought back in the vicinity of the regime change by setting $\tau = \tau^* \pm \epsilon$, where τ^* is the value for which a derivative discontinuity occurs. This truncation procedure is schematized in Fig. 2, depicting a switch between a non-melting and melting surface. The numerical parameter ϵ is made to ensure that the next iteration starts from the good regime and needs to be taken small (typically 10^{-5}).

Variable elimination to reduce the size of the non-linear problem:

A second improvement can be made by realizing that most of the equations governing the internal heat budgets are actually linear equations, and thus only need to be assembled and inverted once per time step. Indeed, the (N-1) first equations, cor-

responding to the time evolution of the temperature of the internal cells not in contact with the surface, express simple linear relationships between the N internal cell temperatures. This can be used to reduce the size of the non-linear system to be iteratively solved.

For this, we eliminate the $N-1$ linearly-dependent variables using a Schur complement technique (Zhang, 2006). Concretely, writing the system of Eqs. (5) and (9) in block-matrix form, one has:

$$\left(\begin{array}{c|c} A_{\mathrm{diag}} & A_{\mathrm{up}} \\ \hline A_{\mathrm{low}} & A_{\mathrm{s}} \end{array}\right) \left(\begin{array}{c} T_{\mathrm{int}} \\ \hline U_{\mathrm{s}} \end{array}\right) = \left(\begin{array}{c} B_{\mathrm{int}} \\ \hline B_{\mathrm{s}} \end{array}\right) \tag{11}$$

where ~~A^{diag}, A^{up}, A^{low}, and A^{s}~~ A_{diag}, A_{up}, A_{low}, and A_{s} are $(N-1)\times(N-1)$, $(N-1)\times 2$, $2\times(N-1)$, and 2×2 matrices, respectively. Note that we refer to the vector composed of the two last unknowns, thus composed of $[T_N, \tau]$, as U_{s} in order not to have it mistaken with the surface temperature. The expressions of the matrices forming the block system are given in Appendix A, including the derivatives necessary for Newton's method.

Under this form, the matrices ~~A^{diag}, A^{up}, A^{low}~~ A_{diag}, A_{up}, A_{low} and the vector B_{int} are constant during the non-linear iterations and do not need to be re-estimated at each non-linear iteration. Thus, the ~~(N-1)~~ $(N-1)$ internal temperatures can be expressed as:

$$T_{\mathrm{int}} = A_{\mathrm{diag}}^{-1}\left(B_{\mathrm{int}} - A_{\mathrm{up}}U_{\mathrm{s}}\right) \tag{12}$$

and thus

$$(A_{\mathrm{s}} - A_{\mathrm{low}}A_{\mathrm{diag}}^{-1}A_{\mathrm{up}})U_{\mathrm{s}} = B_{\mathrm{s}} - A_{\mathrm{low}}A_{\mathrm{diag}}^{-1}B_{\mathrm{int}} \tag{13}$$

where $A_{\mathrm{s}} - A_{\mathrm{low}}A_{\mathrm{diag}}^{-1}A_{\mathrm{up}}$ corresponds to the Schur complement of A_{diag} in the system of Eqs. (11) (Zhang, 2006).

The ~~above equation~~ system of Eqs. (13) is a 2×2 non-linear ~~equations~~ system where only A_{s} and B_{s} need to be re-assembled at each non-linear iteration and whose solution for U_{s} is the same as the large system of Eqs.(11). Therefore, an efficient numerical scheme to solve the whole system of Eqs. (11) is to (i) first assemble A_{low}, A_{diag}, A_{up}, and B_{int}, (ii) ~~inverse~~ compute the products $A_{\mathrm{diag}}^{-1}B_{\mathrm{int}}$ and $A_{\mathrm{diag}}^{-1}A_{\mathrm{up}}$ (which is cheaper than directly inverting A_{diag}), (iii) iteratively solve the 2×2 non-linear system of Eqs. (13) yielding U_{s} (only reassembling A_{s} and B_{s} at each iteration), and (iv) retrieve the remaining internal temperatures by applying Eq. (12).~~The numerical cost of this scheme is composed of one $(N-1)\times(N-1)$ matrix inversion and of the iterative solving of a non-linear 2×2 system. This is of the same order as the standard skin-layer formulation, which is composed of one $N\times N$ matrix inversion and the iterative solving of a non-linear scalar equation.~~

This technique, namely eliminating linearly-dependent variables using a Schur complement to reduce the size of non-linear systems to be solved for, can also be applied to speed up the solving of class 1 models. This is presented in Appendix B. We also note that to apply this technique, the assumption of temperature-independent heat capacity and conductivity is important, as otherwise the internal heat equation system would not be linear and thus the matrices A_{diag}, A_{up}, and A_{low} not constant. Finally, a translation of this numerical strategy (including the fictitious variable and the Schur-complement technique) in a FEM framework is presented in Appendix C.

An analysis of the numerical cost (in terms of number of basic operations) of this numerical scheme is given in Appendix A, alongside analyses of the numerical cost of Class 1 and 2 models. It shows that the proposed scheme and the Class 1 models have similar numerical costs, which a bit less than 1.7 times larger than the standard-skin layer.

5 Simulation setup

The system of equations 11 and its resolution scheme presented in Section 4 enable the computation of the tightly-coupled evolution of the surface and of the internal energy budget. The goal of this section is to compare this approach to more classical implementations, falling either in class 1 (all temperatures solved at once but without an explicit surface) or class 2 (presence of an explicit surface, but sequential treatment for the computation of the surface and internal temperatures).

For this purpose, we thus implemented a class 1 and a class 2 model alongside the scheme presented in Section 4. For the implementation of a class 1 model, a specific treatment of the first cell is adopted. Indeed, in order to have results comparable with the other model implementations, the temperature of the first cell is computed taking into account the effect of first-order phase transition in order to cap the surface temperature at T_0. The resulting non-linear system is solved with the modified Newton method presented in Section 4.1.1, including the truncation and Schur-complement techniques. Not taking into account first-order phase transitions in the first cell would result in surface temperature overshoots (not present in the other implementations), which would be detrimental to the ~~surface energy budget~~SEB. We stress that our specific implementation has differences with already published models (for instance the Crocus model does not perform non-linear iterations and treats surface melting differently; Vionnet et al., 2012), and thus that the results obtained with our implementation might deviate from that of the aforementioned models (Crocus, SNTHERM, Cryogrid, or CLM).

For the implementation of a class 2 model, we adopt the following sequential treatment for each time step: (i) first the surface temperature that equilibrates the SEB is computed using the internal temperatures of the previous time step and ignoring potential melting, (ii) if the surface temperature exceeds ~~fusion~~ melt it is capped at T_0 and the excess energy used for surface melting, (iii) the internal temperatures are then computed using the value of the sub-surface heat flux G computed from the SEB as the top boundary condition. Again, our specific implementation of a class 2 model might differ from some of the

already existing "skin-layer" models (~~COIPY~~COSIPY, EBFM, or SnowModel).

In order to obtain physically sound results, note that we have included a treatment of water percolation through a simple bucket scheme (Bartelt and Lehning, 2002; Vionnet et al., 2012; Sauter et al., 2020) as well as the representation of the motion of the surface in response to surface melting and vapor sublimation/deposition. In our bucket-scheme, cells whose density is close to that of ice are considered as impermeable and water cannot percolate through them. Instead, excess water present in cells above an impermeable horizon is sent to runoff. This choice is meant to avoid liquid water percolation through an entire glacier. Our models also include a remeshing algorithm that merges adjacent cells when ~~then~~ they become smaller than a given threshold (defined here as ~~half the size~~ 75% of the smallest cell size at the start of a simulation). This remeshing step is also used to ensure that the melt of a layer cannot exceed its ice content. If such a case is encountered, the layer is merged with one of its neighbors before attempting melting. If the total melt exceeds the total mass, the simulations should be stopped. However, this last case did not arise in the simulations presented here. These processes (melting, percolation, and remeshing) are treated after the resolution of the heat budget and are handled in a sequential (and thus partially decoupled) fashion, as usually done in current snowpack/glacier modeling (e.g. Bartelt and Lehning, 2002; Vionnet et al., 2012; Sauter et al., 2020). To ease comparison between the various implementations, the melting, percolation, and remeshing routines are common to all of them. ~~Finally, the~~ The temporal integration scheme is also the same for all models in order to facilitate the comparison between them, namely an implicit backward Euler method. Also, as some of the current snowpack and glacier models include the effect of internal phase-change while solving the internal heat equation (e.g. Bartelt and Lehning, 2002; Meyer and Hewitt, 2017), we quantified the sensitivity of our results to this specific treatment of melt/freeze. For that, we have also implemented versions of our three models that include such internal phase-changes in the heat equation.

Finally, note that we do not include the FEM in this comparison. As detailed in Appendix C, a specificity of FEM models is to rely on a temperature field that can be defined element-wise or node-wise. It is thus required to convert back and forth between these two representations. However, the relation between the two is not bijective. This prevents an unambiguous transformation from element-wise to node-wise temperatures, which affects the end-result of our simulations. Because of this problem, the FEM is not further explored in this article, as a direct comparison to the FVM models is not possible.

Two simple examples, showcasing the differences between numerical treatments, are presented below. ~~While they are not meant to model the actual evolution~~ We note that these simulations cannot be considered as fully realistic simulations of a snowpack or ~~a glacier~~ glacier surface, as many processes, such as the deposition of atmospheric precipitation (rain or snow) or mechanical settling~~are lacking, they exemplify how different numerical implementations of the same physical equations yield different end-results. Two specific examples were set up~~, are lacking. The goal is rather to provide a simplified setting in which the impact of the numerical implementation of the SEB can be analyzed. In the same idea, we do not attempt to compare the simulation results to field observations. Indeed, it would not be possible to decipher errors due to the numerical discretization (the focus of this paper) from errors due to the assumed physics, parametrizations and atmospheric forcings. Nonetheless, in order for the results to still be informative of how a given numerical implementation might behave in a more realistic setting,

we use realistic atmospheric forcing, initial conditions, and physical parametrizations. The first ~~one~~ simulation is meant to highlight the behavior of the numerical models when simulating the ~~surface energy balance of~~ SEB on a snow-free glacier. The second one focuses on the impact of the model implementations on the simulation of the energy budget of a seasonal snowpack, during the melting period.

5.1 Test case 1: Snow-free glacier

We start by considering the case of a snow-free and firn-free glacier, neglecting the accumulation of mass through precipitation. This test case is motivated by the recent studies of Potocki et al. (2022) and Brun et al. (2022), which discuss current models capability of modeling the surface mass balance of such a snow and firn-free glacier in a cold environment.

As such, our simulations are forced by the weather data provided by Potocki et al. (2022) ~~for the South Col Glacier. Note that the method used to downscale the data does not guarantee physical consistency of the variables. This allows us~~ that include all necessary information to take into account the shortwave, longwave and turbulent energy fluxes at the top of our domain. To compute the shortwave absorption, we assume that the surface has a constant ~~0.4 albedo~~ broadband albedo of 0.4 and that $80\,\%$ of the flux is absorbed right at the surface (Bintanja and Broeke, 1995; Sauter et al., 2020), without penetrating deeper. The remaining shortwave radiation penetrates in the ice following an exponential decay profile with a $0.4\,\mathrm{m}$ e-folding depth (Bintanja and Broeke, 1995; Sauter et al., 2020). The longwave emissivity of the ice is assumed to be unity. Finally, the turbulent fluxes are computed based on a slightly modified version of Eqs. (17-21) of Sauter et al. (2020) and are described in the Appendix D. The roughness length over the ice surface is taken constant and set to $z_0 = 1.7\,\mathrm{mm}$ (Sauter et al., 2020). For the bottom boundary condition, we apply a simple no-heat-flux condition. As the simulated domain is large (about $189\,\mathrm{m}$) and the simulation only run for a single year, this choice of bottom boundary condition has little effect on the simulated surface temperature and energy budget. For instance, we performed a simulation in which a $64.7\,\mathrm{mW\,m^{-2}}$ geothermal heat flux is applied instead (Davies, 2013). The impact on the surface temperature remains below $0.4\,\mathrm{mK}$.
For the internal material properties, we assumed the ice ~~thermal capacity~~ heat capacity c_p to equal $2000\,\mathrm{J\,K^{-1}\,kg^{-1}}$ and not to depend on temperature (Lide, 2006). Similarly, the ice thermal conductivity λ is set to $2.24\,\mathrm{W\,K^{-1}\,m^{-1}}$, independently of temperature (Lide, 2006; Sauter et al., 2020). Finally, we want to stress that in such a case of a snow and firn-free glacier, the numerical implementation of our bucket-scheme results in the runoff of all melted water, without percolation into the glacier and thus without warming the ice below it.

For the initial conditions, we used a spin-up simulation presented in Brun et al. (2022) and generated with the COSIPY model (Sauter et al., 2020). It corresponds to an initially $189\,\mathrm{m}$ thick glacier. The output of the spin-up notably includes a non-uniform mesh for the glacier, from which we build the meshes for our simulations. In order to study the influence of spatial resolution on the simulation, the original spin-up mesh was refined/downgraded by increasing/decreasing the number of cells. This was done by keeping the same relative cell sizes in the domain, such that the smallest cells remained near the surface and

the largest ones deep in the glacier, as in the original spin-up mesh.

Finally, we want to stress that the aforementioned simplifying assumptions (such as constant albedo, constant surface roughness length, absence of precipitation, simplistic treatment of percolation, etc) imply that the results of our simulations should not be quantitatively interpreted. Rather, the choice of simplified physics is meant to ease the comparison of the numerical treatments of the ~~surface energy budget~~SEB.

For each numerical scheme, we perform simulations with initial numbers of cells varying between 22 and 450 and with time steps ranging from 30 to 7200 s. This range includes the time steps typically used in models (e.g. 900 s in Crocus or 3600 s in COSIPY). In the absence of an analytical solution, the simulations performed at a high spatial and temporal resolution (i.e. 30 s and 450 cells) are meant to provide a reference to study the convergence of the other simulations with the gradual increase of the spatial and temporal resolutions. These high-resolution simulations reveal that the class 1 model implementation (no explicit surface) remains different from the two other implementations even for this level of time step and mesh refinement. Therefore, as the reference solution for the glacier test-case, we take the average of the two implementations with an explicit surface, as they both converged to similar solutions (and similar results will thus be obtained if only the solution of the proposed tightly-coupled surface scheme were taken). Specifically, to quantify the difference between a given simulation and the reference, we focus on the surface temperature and on the phase change rate (understood in this article as the net melt and refreeze over the entire domain after solving the heat equation). For this purpose, we compute the time series of absolute differences between the simulations and the reference, as well as the corresponding Root-Mean-Square-Deviation (RMSD). Note that in this specific test case, no refreezing was observed (as melt occurs at the surface and is sent to runoff), meaning that the phase change rate directly corresponds to the melt rate.

5.2 Test case 2: Melting snowpack

Our second test case corresponds to the case of a melting snowpack. For simplicity, we assume that the snowpack surface has a constant ~~albedo of 0.6~~ broadband albedo of 0.7 and that all shortwave radiation penetrates in the snow following an exponential decay profile with a 0.058 m e-folding depth (Bintanja and Broeke, 1995; Sauter et al., 2020). Similarly to that of ice, the longwave emissivity of snow is assumed to be unity. The turbulent fluxes are computed with the same law as in the glacier test case but with a constant roughness length of $z_0 = 0.24$ mm (Sauter et al., 2020). As in the glacier case, the bottom boundary condition for the heat equation is taken as no-flux condition. The use of a more realistic boundary condition could be achieved by coupling the snowpack model to a soil model (e.g. Decharme et al., 2011). It however remains beyond the scope of this article, which is focused on the impact of the implementation of the ~~surface energy budget~~ SEB on simulations.

Regarding internal material properties, we assume snow to have the specific ~~thermal~~ heat capacity of ice, i.e. $2000\,\mathrm{J\,K^{-1}\,kg^{-1}}$, independent of temperature (Lide, 2006; Morin et al., 2010). The thermal conductivity of snow is taken as a function of density, following the Calonne et al. (2011) parametrization. For the percolation scheme, we assume that a snow cell is able to retain up to 5 % of its porosity as liquid water (Vionnet et al., 2012). Liquid water percolating from the last cell of the snowpack is

simply sent to runoff. The initial conditions of the simulation are taken from a Crocus simulation of the snowpack at Col de Porte (Lejeune et al., 2019) during the 2010/2011 season. As we are interested in the case of melting, we start our simulation from the 14/03/2011, corresponding to the peak of snow height in the Crocus simulation (1.49 m), run it for ~~49~~63 days, and stop it before reaching the total disappearance of the snowpack in our simulations. The original Crocus mesh is refined/downgraded by increasing/decreasing the number of cells in order to study the impact of mesh resolution of the numerical solutions. The atmospheric forcings, for both the spin-up and the simulation, are based on the reanalysis of Vernay et al. (2022). Finally, as in the glacier case, the results of the simulations should not be quantitatively interpreted (for instance in terms of days for snowpack disappearance) but are only meant to provide an easy way of comparison between numerical treatments of the internal and surface energy budgets.

The simulations are performed with initial cell numbers varying between 22 and 440 and with time steps ranging from 30 to 7200 s. As in the glacier test case, the high-resolution simulations (30 s time step and 440 cells) are meant to provide a reference solution. In this case, all three models converge to similar solutions with the considered levels of mesh and time step refinement. Thus, the reference solution was taken as the average of the three implementations. The comparison between a given simulation and the reference was done focusing on the surface temperature and the phase change rate, as in the glacier test-case.

6 Results and Discussion

6.1 General behavior of the models

An example of simulated surface temperature, phase change rate, and temperature profiles obtained in the glacier test case for a time step of 3600 s and an initial cell number of 44 (corresponding to a minimum cell size of 10 mm at the top) is displayed in Fig. 3. Similarly, for the snowpack test case, simulated surface temperatures, phase change rates, and temperature profiles obtained for a time step of 3600 s and a starting cell number of 44 (corresponding to minimum of cell size of 9.1 mm at the top) are visible in Fig. 4.

While the three models tend to generally agree in terms of simulated surface temperatures and phase change rates, they nonetheless present some notable differences. Concerning the glacier test-case, ~~the~~ Fig. 3 shows that the class 1 model (no explicit surface) is systematically different compared to the two other models, with a slower decrease of the surface temperature at night, resulting in a surface temperature that is ~~on average warmer~~ usually warmer of a couple of degrees for the represented period. For comparison, Sauter et al. (2020) report root-mean-square-errors around 3 K when comparing COSIPY simulations with observations of the Zhadang glacier surface temperature. Besides the surface temperature, the class 1 model also displays internal temperatures (starting from about 10 cm below the surface) that are colder (~~of~~ by about 0.50 K) than the two other implementations. This internal temperature difference is consistent with the fact that the surface temperature in the class 1 model is on average warmer than the two others, favoring the loss of energy through turbulent and radiative fluxes.

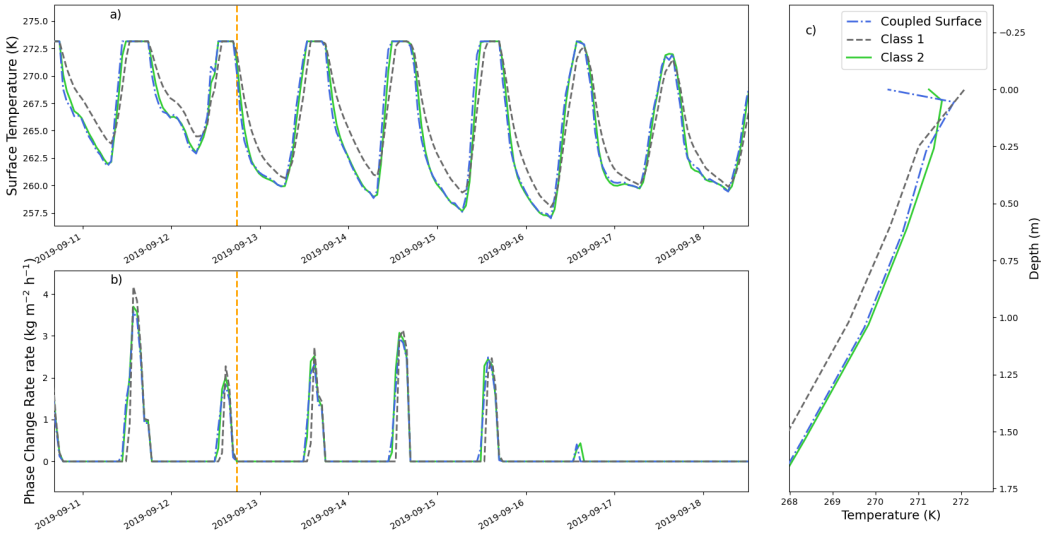

Figure 3. Overview of the simulation of a snow and firn-free glacier using three different numerical schemes. The simulations were performed with a time step of 3600 s and ~~a~~ an initial number of cells of 44 (minimum cell size of 10 mm). a) and b): Surface temperature and total phase change rate (including surface and subsurface melt/refreeze) around mid-September. c): Upper part of the temperature profiles on the 12/09/2019 at 15:45 local time. The dashed orange line in panels a) and b) corresponds to the selected date of panel c).

As in the glacier test case, models tend to generally agree in the snowpack case, with nonetheless some differences as displayed in Fig. 4. In particular, all predict that most of the melt occurs internally and without the surface temperature necessarily reaching the ~~fusion~~ melting point. As previously, the class 2 model and the new tightly-coupled approach exhibit the best agreement (even though the agreement is not as clear as with the glacier case), while the class 1 model displays surface temperatures that reach higher peaks during the day. As with the glacier test case, the models exhibit surface temperature differences of about a couple of degrees. This is of the same order as the biases observed in the snow model inter-comparison exercise ESM-SnowMIP (Menard et al., 2021). Despite their relative agreement, the class 2 model appears to "lag" by about one time step behind the tightly-coupled implementation. This lag can be explained by the fact that, in this case, shortwave radiations are not directly affected to the surface (as they penetrate). A large variation in shortwave radiations is therefore not directly visible by the surface, which only reacts to it at the next time step, once the shortwave radiations have impacted the cell below the surface. The impact of this lagging problem can be mitigated by the use of small time steps, but with the drawback of numerical cost. Beside surface temperature, the class 1 model also shows differences compared to the two other models in terms of internal temperatures, being colder in the deepest part of the snowpack. This effect is due to the smaller melting predicted by the class ~~2~~ 1 model. There is therefore less melt water percolating down the snowpack, which carries latent heat to warm the snowpack. Finally, we note that the class 2 model exhibits some time step to time step oscillations, characteristic

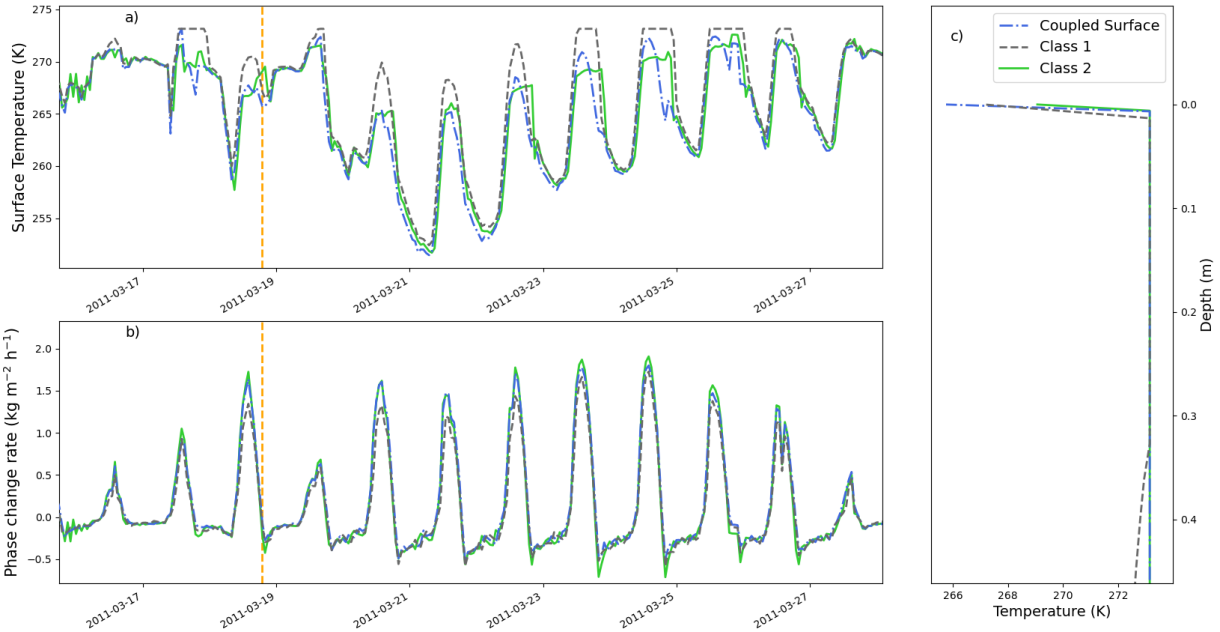

Figure 4. Overview of the simulation of a snowpack using three different numerical schemes. The simulations were performed with a time step of 3600 s and ~~a~~ an initial number of cells of 44 (minimum cell size of 9.1 mm). a) and b): Surface temperature and total phase change rate (including surface and subsurface melt/refreeze) near the end of March. Note that negative phase change rate values imply refreezing within the snowpack. c): Upper part of the temperature profiles on the ~~17~~18/03/2011 at ~~22~~19:00 local time. The dashed orange line in panels a) and b) corresponds to the selected date of panel c).

of numerical instability. Such oscillations are visible both in the surface temperature and the phase change rate ~~,~~that display over and undershoots compared to the other models.

Finally, using the versions of the models including phase-changes in the heat equation, we quantified the sensitivity of these observations to the treatment of the melt/refreeze. While the simulated temperature sometimes differ from our basic implementations (especially in the snowpack test case where melt occurs internally), the general behavior of the models, including the potential presence of instabilities in the Class 2 models, remain unchanged.

6.2 Convergence with time step and mesh refinement

As they solve the same physical equations, all numerical implementations of the heat budget are expected to converge to the same results when the time step size and mesh size tend to zero. However, in general different numerical implementations do not show the same levels of error and convergence rates toward this solution, as the time step and mesh size are progressively reduced. The goal of this section is to analyze the convergence of the three SEB implementations discussed in this article with

time step and mesh size refinement. In other words, we quantify their respective time step and mesh size sensitivities.

We start here by analyzing the sensitivity of the three numerical implementations to the time step. For this purpose, we analyze the differences between the reference solutions and the three implementations using about 220 cells (i.e. about 5 times the usual number of cells used in detailed models) and time steps between 112 and 7200 s. Figures 5 to 8 compare the simulations performed with various time steps to the reference (time step of 30 s) for the glacier and snowpack test cases, respectively. The largest time step of 7200 s corresponds to twice the default value used for instance in COSIPY (Sauter et al., 2020) and is meant to represent the case of models used at quite large time steps for numerical cost considerations. Note that for the left panels showing time series of absolute differences, a 10 days running average was used to remove daily and weekly variability from the data. Also, while the right panels display RMSDs over the entire simulation, we also computed biases. These were in general about an order of magnitude smaller than the RMSD values, except for the surface temperature of the snowpack test case, where the bias was about half of the RMSD.

As seen in the four Figures, all models show a general decrease in errors with smaller time steps. For almost all investigated time steps and in both test cases, the newly proposed scheme displays the lowest level of errors~~, with~~. Sometimes, the class 2 model ~~sometimes only marginally better~~yields the smallest error, but does so only by a small margin. Figure 5 reveals that for the glacier test case and at large time steps (between 30 min and 2 h), the decoupled skin-layer formulation (class 2 model) shows the largest errors in terms of surface temperature, with a marked increase of the error with increasing time steps. However, we do not observe such a sharp increase at large time steps for the phase change rate errors with the class 2 model, even though Fig. 6 highlights that for such large time steps, the class 2 model wrongly predicts melting early in the season (notably during the month of February). Figures 5 and 7 show that for smaller time steps and in both test cases, it is on the contrary the class 1 model that yields the largest errors in terms of surface temperature, with a limited decrease in the error level with decreasing time steps compared to the two other implementations. Concerning the phase change rate errors for small time steps, it depends on the investigated test case: for the glacier it is the class 2 model that shows the largest errors (Fig. 6), while it is the class 1 model for the snowpack test case (Fig. 8). The results of the glacier test case displayed in Figs. 5 and 6 thus highlight that depending on the considered metric (surface temperature or phase change rate), the ranking of models might differ.

Similarly, while the numerical results are expected to converge to the same solution when the grid is refined, they do not show the same errors and convergence rates with decreasing mesh size. Notably, integrating the top boundary conditions directly in the first cell (as in class 1 models) instead of adding an extra independent variable at the surface is known to slow the convergence of FVM with mesh refinement, as it requires a very small top-cell to properly approximate the surface temperature. As with time step sensitivity, we quantify the impact of mesh refinement by comparing simulations performed with different spatial resolutions to reference simulations. We used the same reference simulations as with the time step analysis. The results are displayed in Figs. 9 to 12 and show the errors in terms of surface temperature and phase change rate for both investigated

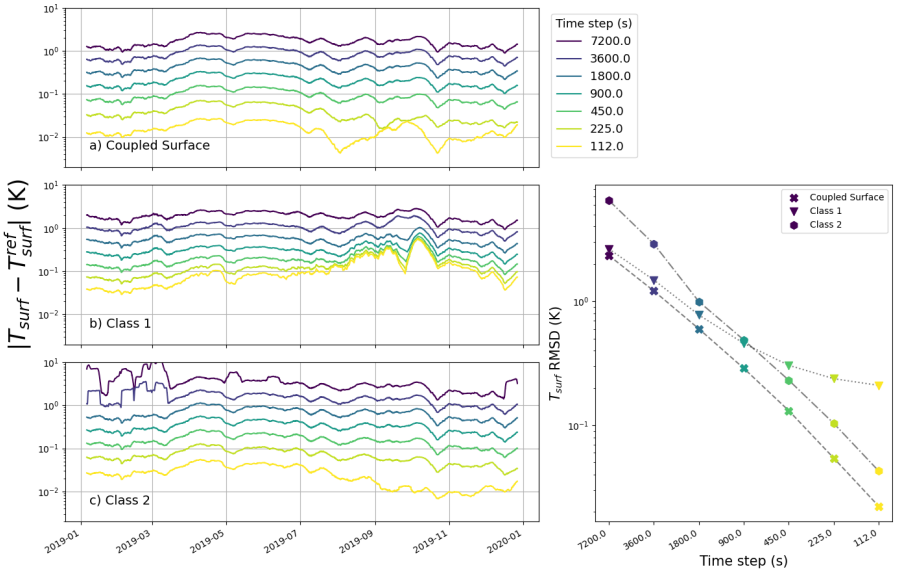

Figure 5. Impact of time step size on the simulated surface temperature for the glacier test case and for the three numerical schemes. Left panels a), b), and c): Errors in surface temperature for the different implementations (panels) and for different time step sizes (colors) during the simulated period. Right panel: RMSD of the surface temperature over the whole simulated period for each implementation (marker) and time step (color). The same time step color scheme applies to all panels.

test cases. As with the time step convergence, bias values over the simulations were found to be an order of magnitude smaller than the RMSD values.

As with time step refinement, all models display a general decrease of errors with finer meshes. Again, among the three implementations the tightly-coupled surface model yields the smaller errors for almost all investigated mesh refinements ~~, with~~ (as in the glacier test case, the class 2 model ~~sometimes only marginally better~~is however sometimes marginally better). On the other hand, the class 1 model displays comparatively large errors for almost all mesh refinements and for both test cases. As seen in Fig. 11, this is particularly marked in the snowpack simulation, where the ~~the~~ class 1 simulation with the finest mesh refinement (about 220 initial cells) has the same level of surface temperature error as the two other models with a coarser mesh (44 initial cells). In other words, in this case, the class 1 model needs about five times more cells (and thus five times thinner cells) to achieve the same precision as the two other implementations. The addition of an extra degree of freedom to represent the surface is thus highly beneficial and offers the possibility to use coarser (and thus computationally cheaper) meshes. Finally, Fig. 10 reveals that in the glacier test case, the phase change rate errors of the class 2 tend to deteriorate with further mesh refinement past a certain point (here for an initial cell number above 90). We interpret this deterioration as a result of the appearance of numerical instabilities that develop with small mesh sizes. Due to this effect, the class 2 model exhibits the largest phase change rate errors for an initial number of cells of 225. Finally, using the versions of the models including

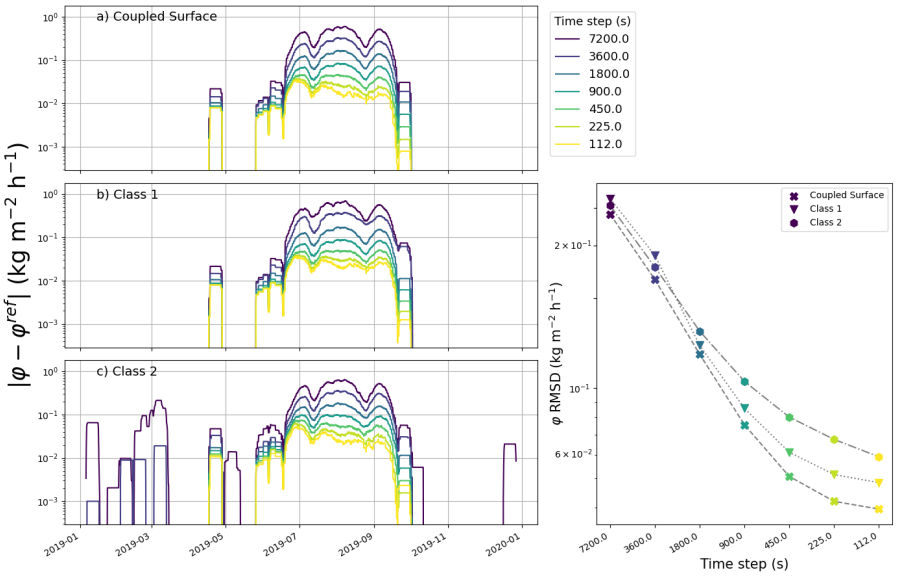

Figure 6. Impact of time step size on the simulated phase change rate (here denoted φ to lighten the plot) for the glacier test case and for the three numerical schemes. Left panels a), b), and c): Errors in phase change rate for the different implementations (panels) and for different time step sizes (colors) during the simulated period. Right panel: RMSD of the phase change rate over the whole simulated period for each implementation (marker) and time step (color). The same time step color scheme applies to all panels.

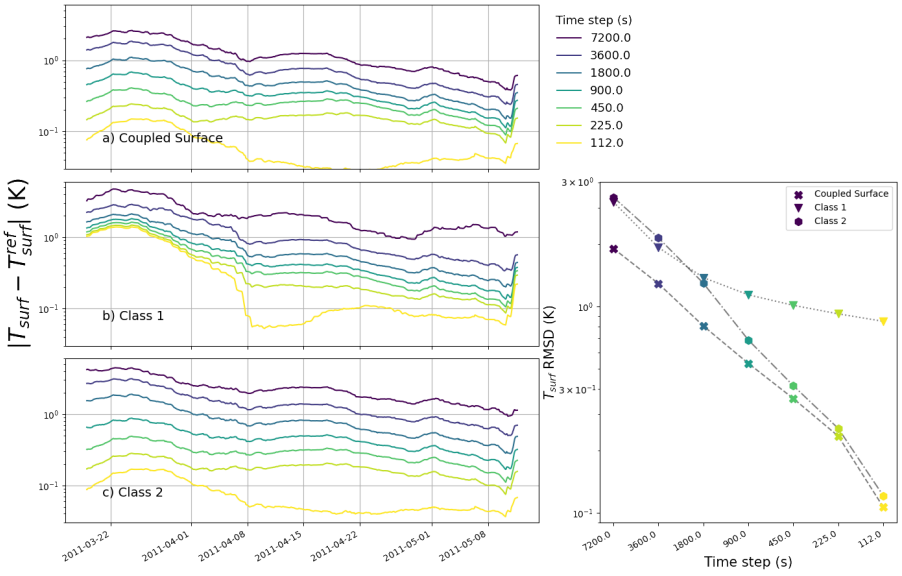

Figure 7. Same as ~~Figure~~Fig. 5, but for the snowpack test case.

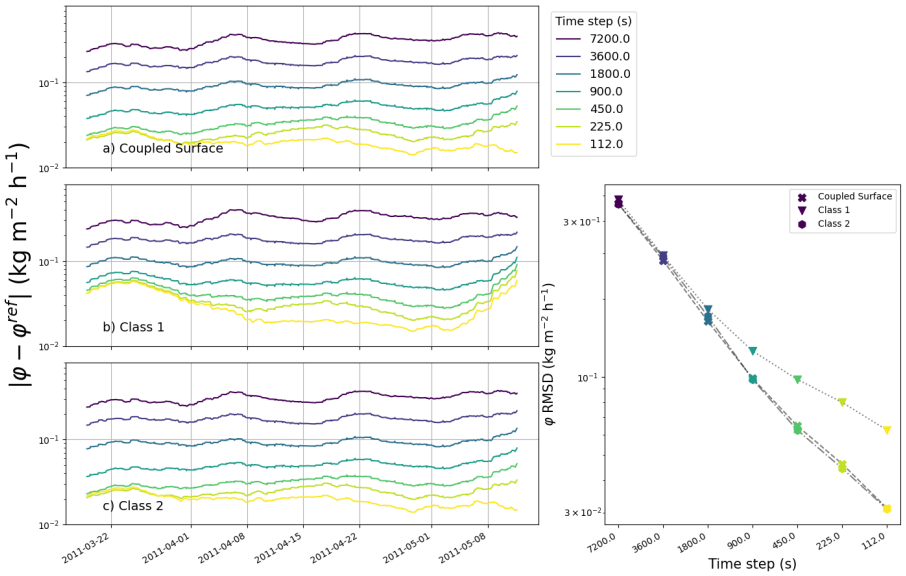

Figure 8. Same as ~~Figure~~Fig. 6, but for the snowpack test case.

phase-changes in the heat equation, we verified that the conclusions of this convergence analysis remain valid in the case of a different treatment of the internal phase-changes.

6.3 Tight-coupling as a way to reduce instabilities

As discussed above, the decoupled nature of the standard skin-layer formulation (class 2 models) leads to greater errors for large time steps compared to the two coupled formulations, with or without an explicit surface. Moreover, the class 2 model can show some deterioration in the case of highly-refined meshes (Fig. 10). Both these phenomena can be explained by the fact that the skin-layer formulation displays instabilities. We observe especially large instabilities for time steps of 2 hours, visible as oscillations in the temperatures of the surface and of the cell below, with peak-to-peak amplitudes sometimes reaching 100 K and with a daily running standard deviation up-to about 50 K. Such oscillations then lead to an abnormally cold and warm surface and a deteriorated ~~surface energy budget~~SEB. As displayed in Fig. 13, these instabilities are even worsened in the case of mesh refinement. On the contrary, no such instabilities have been observed for the tightly-coupled schemes (with or without an explicit surface).

The unstable nature of class 2 models can be shown with a linear stability analysis, provided in Appendix E. Such analysis shows that class 2 models are only conditionally stable, and confirm that instabilities are favored in the case of large time steps and small mesh sizes. We stress that these oscillations can appear ~~with the skin-layer schemes~~ even if the time integration of the internal energy budget relies on the ~~backward~~ Backward Euler method, known for its robustness against instabilities (Fazio, 2001; Butcher, 2008). Our understanding is that the sequential treatment of the standard skin-layer formulation breaks the implicit nature of the time integration by using "lagged" (in other words, ~~"explicited"~~explicit rather than implicit) terms. This,

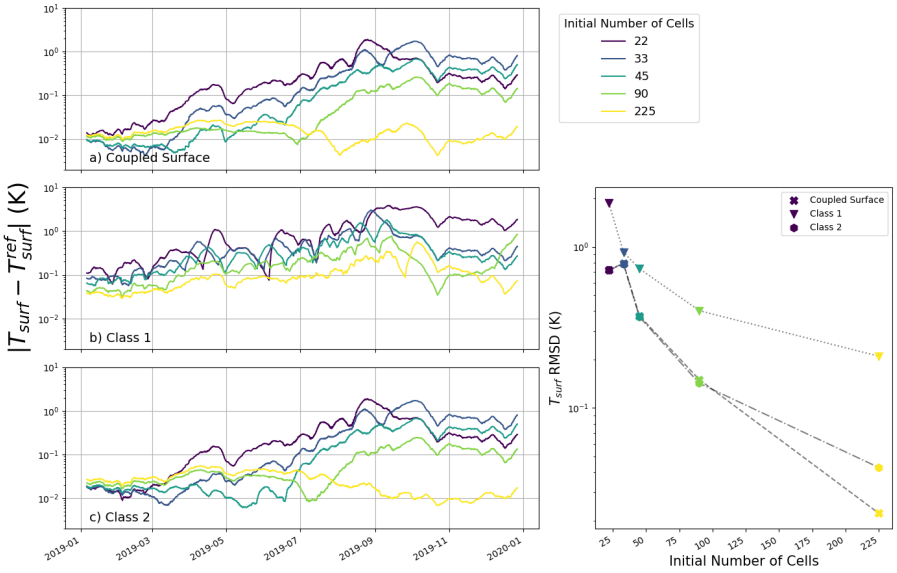

Figure 9. Impact of mesh size on the simulated surface temperature for the glacier test case and for the three numerical schemes. Left panels a), b), and c): Errors in surface temperature for the different implementations (panels) and for different mesh sizes (colors) during the simulated period. Right panel: RMSD of the surface temperature over the whole simulated period for each implementation (marker) and mesh size (color). The same mesh size color scheme applies to all panels.

combined with the fact that the surface layer does not possess any thermal inertia and that its temperature can thus vary rapidly in time, permits large temperature swings if the time step is too large or the mesh size ~~to small.~~ too small. On the other hand, it can be shown that the two schemes with a tightly-coupled SEB are unconditionally stable (Appendix E), in agreement with the absence of oscillations in their simulations. Notably, the unconditional stability of the coupled-surface scheme proposed in this article entails that the model does not need an adaptive time step size strategy depending on the mesh size. This ensures that it remains robust, regardless of the time step and mesh size.

6.4 Energy conservation in the standard skin-layer formulation

As explained in Section 2.2, the heat conduction flux from the surface to the interior of the domain (i.e. G in Equation 3) needs to have the same value in the computation of the ~~surface energy budget~~ SEB and in the computation of the energy budget of the first interior cell. Inconsistencies in G between these two budgets lead to the violation of energy conservation and create an artificial energy source/sink near the surface. Such inconsistencies ~~can easily~~ could be created when implementing the standard skin-layer formulation (class 2 models) due to the sequential treatment of the surface and internal energy budgets. Indeed, after solving the ~~surface energy budget~~SEB, one can either use the surface temperature or the subsurface heat flux G as a boundary condition for the computation of the internal temperatures. ~~In general, these two strategies will lead to different results and only the direct injection of G computed from the SEB will ensure the conservation of energy. Indeed, if~~

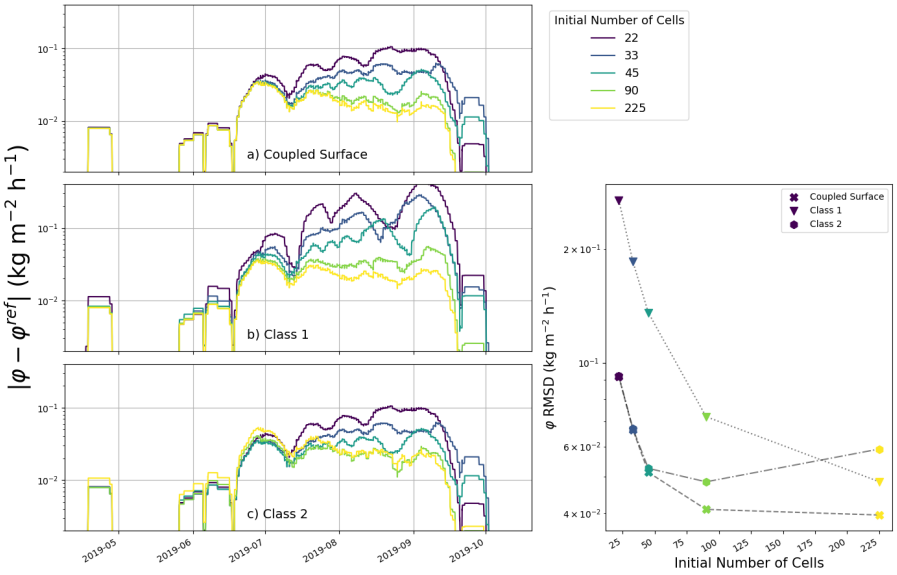

Figure 10. Impact of mesh size on the simulated phase change rate (denoted here φ to lighten the plot) for the glacier test case and for the three numerical schemes. Left panels a), b), and c): Errors in the phase change rate for the different implementations (panels) and for different mesh sizes (colors) during the simulated period. Right panel: RMSD of the phase change rate over the whole simulated period for each implementation (marker) and mesh size (color). The same mesh size color scheme applies to all panels.

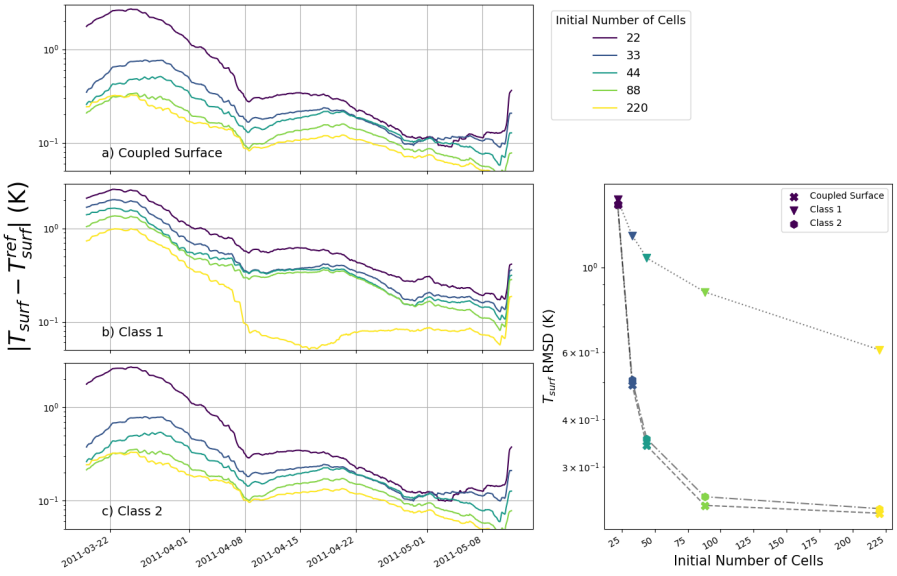

Figure 11. Same as ~~Figure~~Fig. 9, but for the snowpack test case.

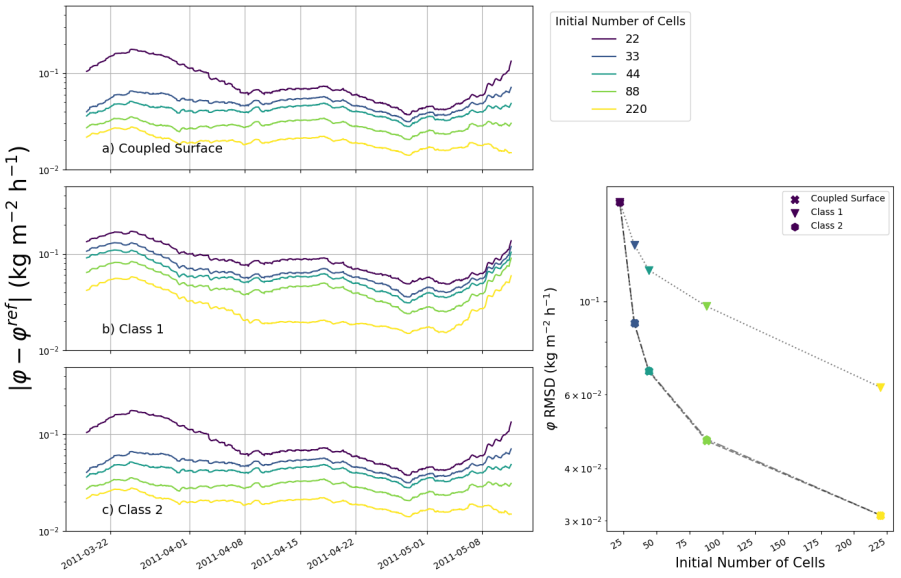

Figure 12. Same as ~~Figure~~Fig. 10, but for the snowpack test case.

~~the internal temperatures are driven using the~~ We note that the use of the computed surface temperature as a ~~Dirichlet boundary condition , the temperature gradient on which the computation of G during the second step is based would be impacted by the modification of the internal temperatures and the subsurface flux G would thus not be consistent with the value previously computed during the SEB. To avoid such an issue, the internal temperatures should be computed directly using the subsurface flux G given by the SEB. For our implementation of the standard skin-layer formulation, this consistency was concretely achieved by (i)closing the surface energy budget using~~ boundary condition leads to an unconditionally stable numerical scheme (Appendix E). However, using such Dirichlet condition in order to stabilize the standard-skin layer formulation comes at the expense of energy conservation and deteriorates of the ~~temperature of the first internal cell from the previous time step, (ii) saving the value of G necessary to close this surface energy budget, and (iii) using this value of G as a top boundary condition for the internal energy budget~~simulated results.

As an illustration, we have also run skin-layer simulations (class 2) ~~in which the flux G is re-computed~~ using the surface temperature as the boundary condition~~(i.e. using the surface temperature as a Dirichlet boundary condition)~~, rather than directly used as a flux boundary condition. A comparison of the energy-conserving and non-energy-conserving simulations is shown in Fig. 14. The surface temperatures show RMSDs of ~~4.00 and 2.97~~3.96 and 2.16 K and the phase change rates RMSDs of 3.6×10^{-1} and ~~4.2×10^{-1}~~3.0×10^{-1} kg m^{-2} h^{-1} for the glacier and snowpack test cases, respectively. In general, the non-conservative scheme displays smaller daily variations of the surface temperature, with a less pronounced warming during the day (sometimes impending surface melt) and a less pronounced cooling at night.

For the non-conservative implementation, the inconsistency in G can be expressed as an equivalent, and artificial, surface en-

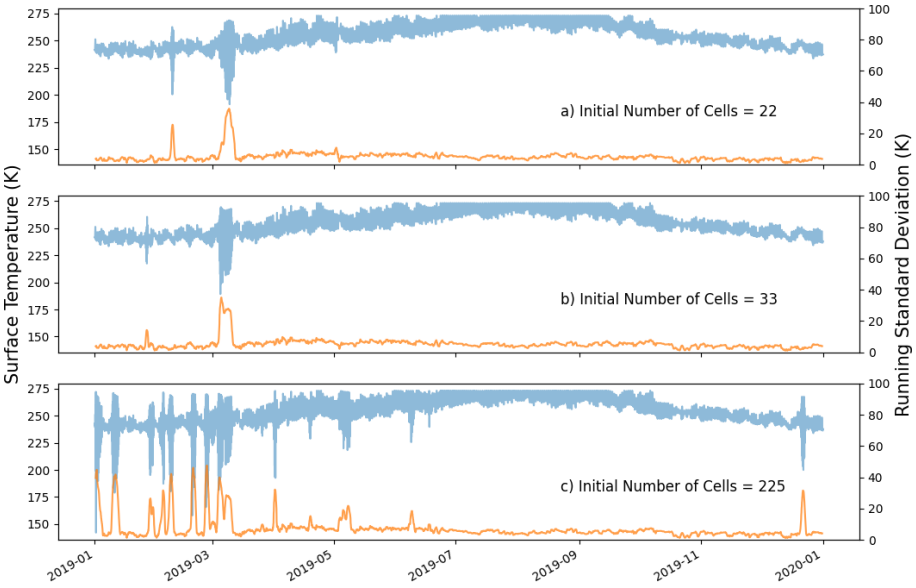

Figure 13. ~~Presence~~ Time series of surface temperatures (in blue, left y-axis) and of their 24hr-running standard deviations (in orange, right y-axis) highlighting the presence of numerical instabilities with the ~~decoupled surface~~ standard skin-layer scheme~~and~~. The simulations correspond to the glacier test case with a time step of 2 hr~~for the glacier test case~~. Each panel corresponds to a level of mesh refinement. The lowest mesh refinement is at the top and displays the smallest level of instabilities, while the highest mesh refinement is at the bottom and displays numerous large instabilities in the first half of the simulation.

ergy sink/source. For the glacier test case, this non-conservation of energy is equivalent to an additional energy flux with an average of $-14.5\,\mathrm{W\,m^{-2}}$ (thus cooling the domain) and a standard-deviation of $123.5\,\mathrm{W\,m^{-2}}$. In the snowpack test case, this corresponds to an additional energy flux with an average of ~~−2.3~~0.34 $\mathrm{W\,m^{-2}}$ (~~cooling~~ warming the domain) and a standard deviation of ~~52~~39 $\mathrm{W\,m^{-2}}$. In both cases, the large value of the standard deviation compared to the average indicates that this "artificial" energy term displays large fluctuations, strongly affecting the simulations. Notably, in both cases the ablation of the glacier and the snowpack is reduced, with a decrease of respectively 40 and ~~11 %~~ 8 % compared to the energy-conserving implementation.

7 Conclusions

Current implementations of the ~~surface energy balance~~ SEB in a finite volume framework can present one of the two limitations: (i) with the standard skin-layer formulation the ~~surface energy balance~~ SEB is solved sequentially with the internal heat budget, therefore creating a form of decoupling between the surface and the interior of the domain, or (ii) the ~~surface energy balance~~ SEB is integrated in the first cell, and there is no difference between this first cell temperature and the surface temperature. To circumvent these limitations, we derive a mathematical framework that includes both (i) an explicit surface, with a temperature

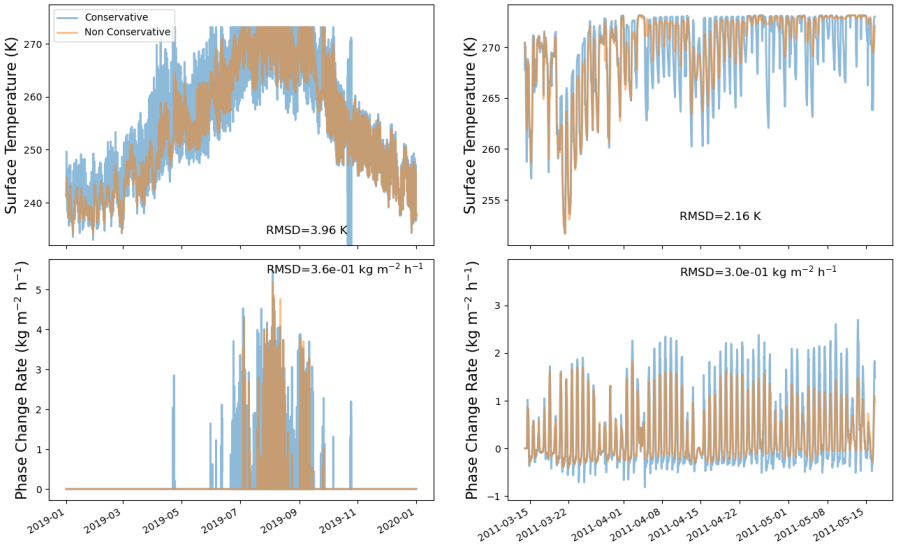

Figure 14. Comparison between the energy conservative and non-energy conservative skin layer numerical schemes. The left column corresponds to the glacier test case and the right column to the snowpack test case. Upper panels display the surface temperatures and the lower panels display the phase change rates.

different from that of the first cell below, and (ii) the tightly-coupled resolution of the surface and internal heat budgets including a potential surface melting. Notably, a unified treatment of melting and non-melting surface is proposed via the use of a fictitious variable playing the role of a switch between melting and non-melting conditions.

A specific Newton's method is also presented to robustly and efficiently solve the resulting non-linear system of equations. The robustness of the standard Newton's method is increased by using a truncation method, made to handle discontinuities in the equations. Furthermore, a reduction technique, based on the computation of a Schur complement, is presented so that the numerical cost of the proposed framework ~~is~~ remains of the same order as that of the standard implementations ~~, in particular~~for the same mesh. In particular, for a given mesh, the numerical cost is similar to that of models not explicitly having a surface and about 1.7 larger than that of the ~~skin-layer~~standard-skin layer formulation. It can therefore be implemented in existing snowpack and glacier models, while preserving their current numerical efficiency. Moreover, the reduction technique presented in this article can also be employed for other non-linear systems of equations (besides the energy budget treated here), by eliminating linearly-dependent variables and reducing the size of the non-linear system to be iteratively solved, providing substantial gain when only a small portion of the discretized equations contains non-linearities.

Numerical test cases, corresponding to a snow-free glacier and a snowpack, have been performed in order to compare the results obtained with the different numerical treatments of the ~~surface energy balance~~SEB. Mesh and time step convergence analyses show that combining a coupled treatment of the ~~surface energy balance~~ SEB with the explicit introduction of a surface results in ~~a~~ an overall better accuracy when compared to the classical implementations. Notably, defining an explicit surface temperature enables the use of about 5 times coarser meshes, compared to models using the temperature of the first cell as the

surface temperature, for the same level of accuracy on temperature and phase change. Moreover, a ~~coupled treatment appears more stable than~~ tightly-coupled treatment of the SEB allows unconditional stability, while the standard skin-layer formulation ~~, which can display~~ can be unstable and displays large spurious oscillations with ~~increasing~~ large time steps and small mesh sizes. Thus, while a bit more numerically costly, the formulation presented in this article can be used to overall reduce the numerical cost of a snowpack/glacier model through the use of larger time steps. Finally, we show that the conservation of energy could easily be broken when implementing a standard (loosely-coupled) skin-layer model~~, leading~~. While this could be used as a technique to numerically stabilize the model, it leads to greatly deteriorated simulations.

Appendix A: Matrix expressions and numerical cost of the coupled-surface scheme

A1 Matrix expressions

Combing Eqs. (5), (6), and (10), the Newton scheme of the coupled-surface model proposed in this article can be written under block matrix form

$$\left(\begin{array}{c|c} A_{\mathrm{diag}} & A_{\mathrm{up}} \\ \hline A_{\mathrm{low}} & A_{\mathrm{s}} \end{array}\right) \left(\begin{array}{c} T_{\mathrm{int}} \\ \hline U_{\mathrm{s}} \end{array}\right) = \left(\begin{array}{c} B_{\mathrm{int}} \\ \hline B_{\mathrm{s}} \end{array}\right) \tag{A1}$$

with non-zero terms being

$$A_{\mathrm{diag}}(k,k) = \Delta z_{\mathrm{k}} c_{\mathrm{pk}} + \Delta t \left(\frac{\lambda^{\mathrm{harm}}_{\mathrm{k}+\frac{1}{2}}}{\frac{\Delta z_{\mathrm{k}}}{2} + \frac{\Delta z_{\mathrm{k}+1}}{2}} + \frac{\lambda^{\mathrm{harm}}_{\mathrm{k}-\frac{1}{2}}}{\frac{\Delta z_{\mathrm{k}}}{2} + \frac{\Delta z_{\mathrm{k}-1}}{2}} \right) \tag{A2}$$

$$A_{\mathrm{diag}}(k,k-1) = -\Delta t \frac{\lambda^{\mathrm{harm}}_{\mathrm{k}-\frac{1}{2}}}{\frac{\Delta z_{\mathrm{k}}}{2} + \frac{\Delta z_{\mathrm{k}-1}}{2}} \tag{A3}$$

$$A_{\mathrm{diag}}(k,k+1) = -\Delta t \frac{\lambda^{\mathrm{harm}}_{\mathrm{k}+\frac{1}{2}}}{\frac{\Delta z_{\mathrm{k}}}{2} + \frac{\Delta z_{\mathrm{k}+1}}{2}} \tag{A4}$$

$$A_{\mathrm{up}}(N-1,1) = A_{\mathrm{low}}(1,N-1) = -\Delta t \frac{\lambda^{\mathrm{harm}}_{\mathrm{N}-\frac{1}{2}}}{\frac{\Delta z_{\mathrm{N}-1}}{2} + \frac{\Delta z_{\mathrm{N}}}{2}} \tag{A5}$$

$$A_{\mathrm{s}}(1,1) = \Delta z_{\mathrm{N}} c_{\mathrm{pN}} + \Delta t \left(\frac{\lambda^{\mathrm{harm}}_{\mathrm{N}-\frac{1}{2}}}{\frac{\Delta z_{\mathrm{N}}}{2} + \frac{\Delta z_{\mathrm{N}-1}}{2}} + \frac{\lambda_{\mathrm{N}}}{\frac{\Delta z_{\mathrm{N}}}{2}} \right) \tag{A6}$$

$$A_{\mathrm{s}}(2,2) = \Delta t \left(\frac{\lambda_{\mathrm{N}}}{\frac{\Delta z_{\mathrm{N}}}{2}} \mathrm{d}_\tau T_{\mathrm{surf}} + L_{\mathrm{fus}} \mathrm{d}_\tau \dot{m} - \mathrm{d}_\tau H - \mathrm{d}_\tau L - \mathrm{d}_\tau LW_{\mathrm{out}} - -\mathrm{d}_\tau R \right) \tag{A7}$$

$$A_{\mathrm{s}}(1,2) = -\Delta t \frac{\lambda_{\mathrm{N}}}{\frac{\Delta z_{\mathrm{N}}}{2}} \mathrm{d}_\tau T_{\mathrm{surf}} \tag{A8}$$

$$A_{\mathrm{s}}(2,1) = -\Delta t \frac{\lambda_{\mathrm{N}}}{\frac{\Delta z_{\mathrm{N}}}{2}} \tag{A9}$$

$$B_{\mathrm{int}}(k) = \Delta z_{\mathrm{k}} c_{\mathrm{pk}} T_{\mathrm{k}}^{n-1} + \Delta t \mathrm{SW}_{\mathrm{int,k}} \tag{A10}$$

$$B_{\mathrm{s}}(1) = \Delta z_{\mathrm{N}} c_{\mathrm{pN}} T_{\mathrm{N}}^{n-1} + \Delta t \left(\mathrm{SW}_{\mathrm{int,N}} - \frac{\lambda_{\mathrm{N}}}{\frac{\Delta z_{\mathrm{N}}}{2}} \left(\mathrm{d}_\tau T_{\mathrm{surf}} \tau^{\mathrm{i}} - T_{\mathrm{s}}(\tau^{\mathrm{i}}) \right) \right) \tag{A11}$$

$$B_{\mathrm{s}}(2) = \Delta t \Big(SW_{\mathrm{net}}^{\mathrm{surf}} + LW_{\mathrm{in}} - \frac{\lambda_{\mathrm{N}}}{\frac{\Delta z_{\mathrm{N}}}{2}} \left(T_{\mathrm{s}}(\tau^{\mathrm{i}}) - \mathrm{d}_\tau T_{\mathrm{surf}} \tau^{\mathrm{i}} \right) - L_{\mathrm{fus}} \left(m(\tau^{\mathrm{i}}) - \mathrm{d}_\tau m \tau^{\mathrm{i}} \right) + \left(H(\tau^{\mathrm{i}}) - \mathrm{d}_\tau H \tau^{\mathrm{i}} \right) + \left(L(\tau^{\mathrm{i}}) - \mathrm{d}_\tau L \tau^{\mathrm{i}} \right) + \left(R(\tau^{\mathrm{i}}) - \mathrm{d}_\tau R \tau^{\mathrm{i}} \right) + \left(LW_{\mathrm{out}}(\tau^{\mathrm{i}}) - \mathrm{d}_\tau LW_{\mathrm{out}} \tau^{\mathrm{i}} \right) \Big) \tag{A12}$$

In the above expressions, T_{k}^{n-1} is the temperature of cell k at the previous time step, $\mathrm{SW}_{\mathrm{int,k}}$ is the quantity of shortwave radiation absorbed in cell k, and τ^{i} is the value of the fictitious variable τ at the start of the current non-linear iteration. The terms $T_{\mathrm{s}}(\tau^{\mathrm{i}})$, $H(\tau^{\mathrm{i}})$, etc, and $\mathrm{d}_\tau T_{\mathrm{surf}}$, $\mathrm{d}_\tau H$, etc, are the values of the surface temperature, sensible heat flux, etc, and their derivatives at the current τ^{i} estimation.

Among the different partial derivatives, $\mathrm{d}_\tau H$ and $\mathrm{d}_\tau L$ can be difficult to analytically derive. For that, we first note that the chain rule yields $\mathrm{d}_\tau H = \mathrm{d}_{T_{\mathrm{s}}} H \mathrm{d}_\tau T_{\mathrm{s}}$, and $\mathrm{d}_\tau L = \mathrm{d}_{T_{\mathrm{s}}} L \mathrm{d}_\tau T_{\mathrm{s}}$. Then, for the expression of H given in Appendix D we have:

$$\mathrm{d}_{T_{\mathrm{s}}} H = \rho_{\mathrm{a}} c_{\mathrm{p,a}} u \left(\mathrm{d}_{T_{\mathrm{s}}} C_{\mathrm{H}} (T_{\mathrm{a}} - T_{\mathrm{s}}) - C_{\mathrm{H}} \right) \tag{A13}$$

Moreover, the chain rule yields $\mathrm{d}_{T_{\mathrm{s}}} C_{\mathrm{H}} = \mathrm{d}_{\mathrm{Ri_b}} C_{\mathrm{H}} \mathrm{d}_{T_{\mathrm{s}}} \mathrm{Ri_b}$. In our case:

$$\mathrm{d}_{\mathrm{Ri_b}} C_\mathrm{H} = \frac{\kappa^2}{\ln\left(\frac{z}{z_0}\right)\left(\frac{z}{z_{0t}}\right)} \begin{cases} 0 & \text{if } \mathrm{Ri_b} < 0 \\ 50\mathrm{Ri_b} - 10 & \text{if } 0 \leq \mathrm{Ri_b} < 0.2 \\ 0 & \text{if } 0.2 \leq \mathrm{Ri_b} \end{cases} \tag{A14}$$

and

$$\mathrm{d}_{T_\mathrm{s}} \mathrm{Ri_b} = -\frac{g z_\mathrm{a}}{T_\mathrm{a} u^2} \tag{A15}$$

Similarly, for L, we have:

$$\mathrm{d}_{T_\mathrm{s}} L = \rho_\mathrm{a} L_\mathrm{s} u \left(\mathrm{d}_{T_\mathrm{s}} C_\mathrm{E} (q_\mathrm{a} - q_\mathrm{s}) - C_\mathrm{E} \mathrm{d}_{T_\mathrm{s}} q_\mathrm{s}\right) \tag{A16}$$

The derivative $\mathrm{d}_{T_\mathrm{s}} C_\mathrm{E}$ can be computed as the one of C_H through the chain rule and its dependence to $\mathrm{Ri_b}$. The derivative of q_s with respect to T_s can be easily obtained using the derivative of the saturated water vapor pressure, which is given by the Clausius-Clapeyron relation.

A2 Numerical cost

We see that the whole system of Eqs. (A1) is a tri-diagonal system of dimension $(N+1) \times (N+1)$, with N the number of cells. Without a Schur-complement, the computation of $A^{-1}B$ can thus be solved with Thomas algorithm (Versteeg and Malalasekera, 2007) in $10N - 1$ base operations (addition, subtraction, multiplication, and division) per non-linear iteration (neglecting the time spent assembling the matrices). We also note that A_diag is a tri-diagonal matrix, and thus Thomas algorithm also applies. Moreover, we see that A_up and A_low are almost empty matrices, which simplifies the number of operations necessary to compute $A_\mathrm{diag}^{-1} A_\mathrm{up}$ and $A_\mathrm{low} A_\mathrm{diag}^{-1} A_\mathrm{up}$. Specifically, the Schur-complement technique used in this paper can be employed with $7N - 9$ ($A_\mathrm{diag}^{-1} A_\mathrm{up}$, once per time step) + $10N - 21$ ($A_\mathrm{diag}^{-1} B_\mathrm{int}$, once per time step) + 15 (assembly and solving of Schur-complement, once per iteration) + $2N$ (re-injection to compute T_int, once per time step) steps, i.e. a total of $17N - 6 + 15 n_\mathrm{it}$ steps, with n_it the number of non-linear iterations. We see, that the advantage of the Schur-complement technique is that the cost of performing non-linear iterations do not increase with the mesh resolution, yielding a smaller numerically cost than inverting the whole system for each non-linear iteration.

One may then wonder how the numerical cost of the scheme proposed in the article compares to the Class 1 and 2 models discussed in the paper. The Class 1 model (once a Schur-complement technique has been employed) as a similar numerical cost as the proposed coupled-surface scheme approach, namely $17N - 23 + 15 n_\mathrm{it}$ steps. For a given mesh, it has one less degree of freedom as the coupled-surface scheme and is thus only marginally less costly. The Class 2 model is the least costly of all

schemes discussed in the paper. Indeed, once the SEB and the surface temperature have been solved through scalar non-linear iterations, it relies on a single tri-diagonal inversion of dimension $N \times N$, which can be done in $10N - 11$ steps. The ratio of the numerical cost of the scheme proposed in the article over that of the standard skin-layer is of about 1.7.

Appendix B: System size reduction for class 1 models

The size-reduction technique presented in Section 4.1.1 can also be employed for class 1 models, i.e. models where the ~~surface energy budget~~ SEB is integrated directly within the first cell and where the temperature of this first cell plays the role of the surface temperature. Such an implementation is used for our comparison in Section 5 as a way to speed up our implementation of a class 1 model.

As explained in Section 5, we made sure that for our resolution of class 1 model, the top-most cell does not overshoot the ~~fusion~~ melt temperature, as it would bias the ~~surface energy budget~~SEB. This is done by including the effect of first-order phase change in the top-most cell. For that, we use the energy content h of the top cell as the prognostic variable, instead of its temperature. The discrete energy budget of the top cell thus writes:

$$\Delta_z h^{n+1} + \Delta t F_{\mathrm{SEB}} + \Delta t F = \Delta t Q + \Delta_z h^n \tag{B1}$$

where h^{n+1} and h^n are the energy content at the end and start of the time step, F_{SEB} the net energy sum of the surface energy fluxes (taken positive if oriented towards the domain), F the heat conduction flux exchanged with the cell below, Q the volumetric internal heat source, and Δt the time step size. The conduction flux F is computed as the other conduction fluxes (Eq. ~~6~~(6)), simply noting that the temperature of the top cell is a non-linear function of its energy content h.
Combining all budget equations over the domain leads to a matrix system of the type:

$$\left(\begin{array}{c|c} A_{\mathrm{diag}} & A_{\mathrm{up}} \\ \hline A_{\mathrm{low}} & A_{\mathrm{s}} \end{array}\right) \left(\begin{array}{c} T_{\mathrm{int}} \\ \hline U_{\mathrm{s}} \end{array}\right) = \left(\begin{array}{c} B_{\mathrm{int}} \\ \hline B_{\mathrm{s}} \end{array}\right) \tag{B2}$$

where $U_s = [T_{N-1}, h]$, and ~~A^{diag}, A^{up}, A^{low}~~ A_{diag}, A_{up}, A_{low} and the vector B_{int} are constant during the non-linear iterations. Therefore, the reduction technique presented in Section 4.1.1 applies and the unknown U_s can be solved through the 2×2 non-linear system:

$$(A_{\mathrm{s}} - A_{\mathrm{low}} A_{\mathrm{diag}}^{-1} A_{\mathrm{up}}) U_{\mathrm{s}} = B_{\mathrm{s}} - A_{\mathrm{low}} A_{\mathrm{diag}}^{-1} B_{\mathrm{int}} \tag{B3}$$

with only A_{s} and B_{s} to be re-assembled at each iteration.

Appendix C: Finite Element Method scheme

In this paper, we focus on the FVM for spatial discretization. However, the heat budget equation could also be spatially discretized with the FEM. Indeed, the FEM naturally includes a node at the surface, and thus possesses a surface temperature, which helps to tightly couple the SEB to the interior of the snowpack/glacier. This strategy is for instance employed in the SNOWPACK model (Bartelt and Lehning, 2002; Wever et al., 2020). Specifically, in SNOWPACK, the coupled SEB is introduced as a top Robin boundary condition.

The goal of this appendix is to briefly present how the techniques presented in the main part of the manuscript (namely the use of fictitious variable and of a Schur-complement) can be used to implement a tightly-coupled FEM model.

C1 Expression of the heat equation in FEM

We consider the mesh of the domain to be discretized into N 1D elements (the direct equivalent of the cells in FVM) and thus of $N+1$ nodes (the end-points of the elements). As classically done with FEM (Pepper and Heinrich, 2005), we assume the temperature field to be a linear combination of basis functions φ_j, i.e. $T(z,t) = \sum_{k=1}^{N} T_j(t)\varphi_j(z)$. Here, we use basic linear elements. In this framework, $T_j(t)$ corresponds to the nodal value of the temperature field (which evolves over time) and the basis functions $\varphi_j(z)$ are piece-wise linear functions, valued 1 at node j and 0 at all other nodes. The standard Galerkin form (Pepper and Heinrich, 2005) of the internal heat budget (Eq. (1)) is:

$$\forall i \quad \sum_j \mathrm{d}_t T_j \int_\Omega c_\mathrm{p}\varphi_j\varphi_i \mathrm{dL} + \sum_j T_j \int_\Omega \lambda \nabla\varphi_j \cdot \nabla\varphi_i \mathrm{dL} = \int_\Omega Q\varphi_i \mathrm{dL} + F_\mathrm{s}\varphi_i(\mathrm{s}) \tag{C1}$$

where Ω represents the domain of simulation, F_s is the energy fluxes entering at the top of the domain (i.e. G), and $\varphi_i(\mathrm{s})$ is the basis function φ_i evaluated at top of the domain. We note that similarly to the FVM case, the temperature at the top of the domain presents a regime change whether the surface is melting or not. To handle this, we rely on the fictitious variable τ, i.e. $T_\mathrm{s} = T_\mathrm{s}(\tau)$. The vector of unknowns, denoted U, is thus composed of the internal temperatures and of the surface fictitious variable. Finally, we have not included any bottom energy flux to lighten the notation, but it could be included easily. Once temporally discretized with a Backward Euler scheme and linearized, the problem can be expressed in matrix form $AU^n = B$, with $A = (M + \Delta t K + \Delta t L)J_T$ and $B = MT^{n-1} + \Delta t Q + \Delta t F$ (T^{n-1} being the vector of temperature from the previous time step), and

$$M(i,j) = \int_\Omega c_\mathrm{p}\varphi_j\varphi_i \mathrm{dL} \tag{C2}$$

$$K(i,j) = \int_{\Omega} \lambda \nabla \varphi_j \cdot \nabla \varphi_i \mathrm{dL} \tag{C3}$$

$$L(N+1, N+1) = -d_\tau SEB + L_{\mathrm{fus}} d_\tau \dot{m} \tag{C4}$$

$$J_T(i,i) = \begin{cases} 1 & \text{if } i \leq N \\ d_\tau T_{\mathrm{s}} & \text{else} \end{cases} \tag{C5}$$

$$Q(i) = \int_{\Omega} Q \varphi_i \mathrm{dL} \tag{C6}$$

and

$$F(N+1) = SEB(\tau^i) - d_\tau SEB \tau^i - \dot{m} + L_{\mathrm{fus}} \left(d_\tau \dot{m} \tau^i \right) \tag{C7}$$

where SEB and $d_\tau SEB$ corresponds to the atmospheric fluxes in the SEB and their derivatives with respect to τ at the current iteration, and $\dot{m}$ and $d_\tau \dot{m}$ are the melting rate and its derivative at the current iteration. In the equations above, only the non-zero terms have been given.

As in the FVM case, this system is composed of a linear-part (the interior, corresponding to the first $N-1$ equations) and a non-linear part (the surface, corresponding to the last two equations). Its solving can thus be accelerated using a Schur-complement technique (Section 4.1.1) by breaking the matrix A into four blocks: a constant $(N-1) \times (N-1)$ diagonal A_{diag} block, a constant $(N-1) \times 2$ vertical A_{up} block, a constant $2 \times (N-1)$ horizontal A_{low} block, and a 2×2 diagonal block A_{s} to be re-computed at each non-linear iteration.

C2 The rest of the model

After solving the coupled heat budgets with FEM, we obtain a nodal temperature field. Since conserved quantities, such as energy or mass, are defined element-wise in snowpack/glacier FEM models (Bartelt and Lehning, 2002), the nodal temperature field needs to be converted into an element-wise energy field. We note that this also defines an element-wise temperature field, where the temperature of an element is simply the average of the nodal temperatures at its end. This element-wise energy field

can then be used to simulate melt/refreeze, liquid water percolation, and to remesh the domain using the same routines as in FVM models.

Once all routines for a given time step have been performed, we are left with an element-wise temperature field that needs to be converted back to a nodal temperature field, as required for the FEM. However, this conversion is not straightforward. First, as we have N element-wise temperatures to transform into $N+1$ nodal temperatures, the problem is not properly closed and an extra (arbitrary) constraint needs to be added. This could, for instance, be setting the surface temperature to the value computed in the SEB. Furthermore, even after choosing an extra constraint to close the problem, the element-wise to node-wise transformation can produce spurious oscillations in the nodal field even if the element-wise field is monotonous (in other words, the transformation does not respect a form of discrete maximum principle; Ciarlet and Raviart, 1973). It is therefore not possible to derive an optimal scheme for this transformation that would (i) not modify the element-wise temperature field and (ii) not create spurious oscillations in the node-wise temperature field.
As spurious oscillations in the temperature field would affect the estimation of the temperature gradients that are used in snowpack models to estimate metamorphism (e.g. Bartelt and Lehning, 2002; Vionnet et al., 2012), it seems preferable to rather allow the modification of the element-wise temperature field. That being said, such a strategy implies a spatial re-distribution of energy between elements that is not motivated by any underlying physical mechanism. We note that the SNOWPACK model handles this element to node transformation during a phase change step after the liquid percolation scheme, and does so without creating large spurious temperature oscillations.

Unfortunately, it is not possible to directly implement the SNOWPACK scheme in our toy-model, as the sequential treatment is not the same. Moreover, we did not manage to derive a scheme that performs this element to node transformation without affecting the surface temperature. Thus, in our numerical simulations, the FVM and FEM models yield different results. In the absence of an analytical solution, a direct comparison of the FEM and FVM implementations remains impossible.

Appendix D: Expression of turbulent fluxes used in this work

The computations of the turbulent fluxes used in this work are based on those provided by Sauter et al. (2020), with slight modifications. The sensible and latent heat fluxes, H and L, are taken as:

$$H = \rho_{\mathrm{a}} c_{\mathrm{p,a}} C_{\mathrm{H}} u (T_{\mathrm{a}} - T_{\mathrm{s}}) \tag{D1}$$

and

$$L = \rho_{\mathrm{a}} L_{\mathrm{s}} C_{\mathrm{E}} u (q_{\mathrm{a}} - q_{\mathrm{s}}) \tag{D2}$$

with ρ_a the density of air, $c_{p,a}$ the ~~thermal~~ heat capacity of air at constant pressure, u the wind velocity (at a given height), L_v the latent heat of sublimation of water, T_a and q_a the temperature and specific humidity of the air, T_s and q_s the temperature and specific humidity of the surface, assuming the saturation of vapor, and C_H and C_E two coefficients given by:

$$C_H = \frac{\kappa^2}{\ln\left(\frac{z}{z_0}\right)\left(\frac{z}{z_{0t}}\right)}\psi(\mathrm{Ri}_b) \tag{D3}$$

and

$$C_E = \frac{\kappa^2}{\ln\left(\frac{z}{z_0}\right)\left(\frac{z}{z_{0q}}\right)}\psi(\mathrm{Ri}_b) \tag{D4}$$

with $\kappa = 0.41$ the von Kármán constant, z_0 the aerodynamic roughness length, z_{0q} and z_{0t} taken 1 and 2 orders of magnitude smaller than z_0, respectively (Sauter et al., 2020), and ψ a stability correction factor. Specifically, we take ψ as:

$$\psi(\mathrm{Ri}_b) = \begin{cases} 1 & \text{if } \mathrm{Ri}_b < 0 \\ (1 - 5\mathrm{Ri}_b)^2 & \text{if } 0 \leq \mathrm{Ri}_b < 0.2 \\ 0 & \text{if } 0.2 \leq \mathrm{Ri}_b \end{cases} \tag{D5}$$

with Ri_b the bulk Richardson number:

$$\mathrm{Ri}_b = \frac{g}{T_a}\frac{(T_a - T_s)\, z_a}{u^2} \tag{D6}$$

with z_a the height at which the air temperature measurement is performed.

There are two main differences compared to the expression of the turbulent fluxes given in (Sauter et al., 2020). First, in Sauter et al. (2020), the transition between the unstable and stable correction factor ψ is taken for $\mathrm{Ri}_b = 0.01$, while we take it for $\mathrm{Ri}_b = 0$. This choice is made to ensure the continuity of the stability factor, and thus of the turbulent fluxes, as a function of T_s. In the presence of a discontinuity, it can indeed happen that the SEB does not have a solution in terms of T_s, and the surface temperature is no longer defined in this case. Secondly, for the expression of the latent heat flux, we simply keep the latent heat of sublimation L_s and do not replace it with the latent heat of vaporization L_v. Again, the goal is to avoid discontinuities in the SEB as a function of T_s so that the problem remains mathematically well-posed. This approach is~~for instance~~, for instance, used in the Crocus model (personal communication; M. Lafaysse). Another strategy could be to fix the latent heat to either its sublimation or vaporization value, depending on the initial state of the surface.

Appendix E: Stability Analysis

Here, we present the derivation of the criteria for the numerical stability of the different numerical schemes presented in the paper. We follow the proof classically used to show the (un)conditional stability of the Forward and Backward Euler method (Butcher, 2008). Notably, the proof relies on a linearized version of the system of equations. As the system needs to be linearized, we cannot account for the potential melting of the surface. Under this consideration, the atmospheric fluxes in the SEB (long-wave radiations, turbulent fluxes, etc) are simply expressed as a linear function of the surface temperature T_s, i.e. as $fT_\mathrm{s}+b$, where f and b are constant scalars expressed in $\mathrm{J\,s^{-1}\,m^{-2}\,K^{-1}}$ and in $\mathrm{J\,s^{-1}\,m^{-2}}$, respectively.

Also, for simplicity, we consider a system composed of only one cell and its surface. The problem could be generalized to more cells, but it would make the computation more cumbersome and is not crucial as we are considering numerical instabilities that develop in the vicinity of the surface.

E1 Standard skin-layer formulation (Class 2)

To compute the surface temperature T_s^{n+1} at time step $n+1$, we use the discretized Surface Energy Balance (SEB):

$$fT_\mathrm{s}^{n+1}+b+\frac{2\lambda}{\Delta z}\left(T_\mathrm{s}^{n+1}-T_\mathrm{i}^{n}\right)=0 \tag{E1}$$

where the first two terms corresponds to the sum of outgoing/incoming atmospheric fluxes, and the last term to the subsurface heat conduction flux. Here, λ is the thermal conductivity of the internal cell and Δz its thickness. Note that the internal temperature T_i^{n} is taken from the previous time step. To compute the internal temperature at time step $n+1$, we use the heat budget of the internal cell:

$$\Delta z c_p T_\mathrm{i}^{n+1}+\Delta t\frac{2\lambda}{\Delta z}\left(T_\mathrm{i}^{n}-T_\mathrm{s}^{n+1}\right)=\Delta z c_p T_\mathrm{i}^{n} \tag{E2}$$

where the second term of the LHS is the opposite of the subsurface conduction flux appearing in the SEB (for energy conservation), and c_p is the heat capacity of the internal cell. The two above equations can be expressed in matrix form $MU_{n+1}=NU_n+B$, with U_n the solution vector $[T_\mathrm{s},T_\mathrm{i}]^T$ at the n^{th} time step and

$$M=\begin{bmatrix}1 & 0\\ -\frac{2\Delta t\lambda}{c_p\Delta z^2} & 1\end{bmatrix} \tag{E3}$$

$$N=\begin{bmatrix}0 & \frac{2\lambda}{2\lambda+\Delta z f}\\ 0 & 1-\frac{2\Delta t\lambda}{c_p\Delta z^2}\end{bmatrix} \tag{E4}$$

and $B=[-\frac{\Delta z b}{\Delta z f+2\lambda},0]^T$. We thus have, $U_{n+1}=QU_n+M^{-1}B$, with

$$Q = M^{-1}N = \begin{bmatrix} 0 & \frac{2\lambda}{2\lambda+\Delta z f} \\ 0 & 1 - \Delta t \frac{2\lambda}{c_p \Delta z^2} \frac{\Delta z f}{2\lambda+\Delta z f} \end{bmatrix} \tag{E5}$$

By recursion, it follows that $U_n = Q^n U_0 + M^{-n} B$. The numerical scheme is deemed stable if $\lim_{n\to\infty} Q^n = 0$. This is achieved if:

$$|1 - \Delta t \frac{2\lambda}{c_p \Delta z^2} \frac{\Delta z f}{2\lambda + \Delta z f}| < 1 \tag{E6}$$

which after some computation yields a criterion of the time step Δt:

$$\Delta t < \Delta t_{\mathrm{crit}} = \frac{c_p \Delta z}{\lambda} \frac{2\lambda + \Delta z f}{f} \tag{E7}$$

The (linearized) standard skin-layer is thus only conditionally stable. The stability criterion is relaxed with increasing heat capacity (c_p) and increasing cell size (Δz), and is made more restrictive with increasing thermal conductivity (λ) or if the SEB is more sensitive to changes in the surface temperature (f term).

E2 Coupled-surface formulation

Similarly, for a one cell system, the coupled-surface equations, after linearization, write:

$$f T_{\mathrm{s}}^{n+1} + b + \frac{2\lambda}{\Delta z} \left(T_{\mathrm{s}}^{n+1} - T_{\mathrm{i}}^{n+1} \right) = 0 \tag{E8}$$

for the SEB, and

$$\Delta z c_p T_{\mathrm{i}}^{n+1} + \Delta t \frac{2\lambda}{\Delta z} \left(T_{\mathrm{i}}^{n+1} - T_{\mathrm{s}}^{n+1} \right) = \Delta z c_p T_{\mathrm{i}}^{n} \tag{E9}$$

for the cell's heat budget. These two equations can be cast into the matrix form $M U_{n+1} = N U_n + B$, with $B = [-\frac{\Delta z b}{\Delta z f + 2\lambda}, 0]^T$,

$$M = \begin{bmatrix} 1 & \frac{-2\lambda}{2\lambda+\Delta z f} \\ -\frac{2\Delta t \lambda}{c_p \Delta z^2 + 2\lambda \Delta t} & 1 \end{bmatrix} \tag{E10}$$

and

$$N = \begin{bmatrix} 0 & 0 \\ 0 & \frac{c_p \Delta z^2}{c_p \Delta z^2 + 2\lambda \Delta t} \end{bmatrix} \tag{E11}$$

We thus have $U_n = Q^n U_0 + M^{-n} B$, with:

$$Q = \begin{bmatrix} 0 & \frac{2\lambda}{2\lambda + \Delta z f} \frac{c_p \Delta z^2}{c_p \Delta z^2 + 2\lambda \Delta t} \\ 0 & \frac{c_p \Delta z^2}{c_p \Delta z^2 + 2\lambda \Delta t} \end{bmatrix} \tag{E12}$$

The numerical scheme is deemed stable if $\lim_{n \to \infty} Q^n = 0$. This is always achieved, as $\frac{c_p \Delta z^2}{c_p \Delta z^2 + 2\lambda \Delta t} < 1$. Thus, the surface-coupled scheme is unconditionally stable.

E3 Non-conservative skin-layer formulation

For the non-conservative skin-layer formulation (see Section 6.4), we start with the linearized discrete SEB:

$$f T_{\mathrm{s}}^{n+1} + b + \frac{2\lambda}{\Delta z} \left(T_{\mathrm{s}}^{n+1} - T_{\mathrm{i}}^{n} \right) = 0 \tag{E13}$$

Using the surface temperature T_{s}^{n+1} as a Dirichlet condition for the internal energy budget, we thus have

$$\Delta z c_p T_{\mathrm{i}}^{n+1} + \Delta t \frac{2\lambda}{\Delta z} \left(T_{\mathrm{i}}^{n+1} - T_{\mathrm{s}}^{n+1} \right) = \Delta z c_p T_{\mathrm{i}}^{n} \tag{E14}$$

These two equations can be cast into the matrix form $M U_{n+1} = N U_n + B$, with $B = [-\frac{\Delta z b}{\Delta z f + 2\lambda}, 0]^T$,

$$M = \begin{bmatrix} 1 & 0 \\ -\frac{2\Delta t \lambda}{c_p \Delta z^2 + 2\lambda \Delta t} & 1 \end{bmatrix} \tag{E15}$$

and

$$N = \begin{bmatrix} 0 & \frac{2\lambda}{2\lambda + \Delta z f} \\ 0 & \frac{c_p \Delta z^2}{c_p \Delta z^2 + 2\lambda \Delta t} \end{bmatrix} \tag{E16}$$

We thus have $U_n = Q^n U_0 + M^{-n} B$, with:

$$Q = \begin{bmatrix} 0 & \frac{2\lambda}{2\lambda+\Delta z f} \\ 0 & X \end{bmatrix} \tag{E17}$$

where $X = \frac{2\lambda\Delta t \frac{2\lambda}{2\lambda+\Delta z f} + c_p \Delta z^2}{2\Delta t\lambda + c_p \Delta z^2}$. The scheme is deemed stable if $|X| < 1$.

As $\frac{2\lambda}{2\lambda+\Delta z f} < 1$, we always have that $2\lambda\Delta t \frac{2\lambda}{2\lambda+\Delta z f} + c_p \Delta z^2 < 2\Delta t\lambda + c_p \Delta z^2$, and thus that the scheme is unconditionally stable. That being said, we recall that this scheme is not energy conservative and can lead to large errors.

E4 No-surface formulation (Class 1)

Finally, we note that the linearized No-surface formulation corresponds to a classic heat equation with a Backward Euler time integration. As demonstrated elsewhere in the literature (e.g. Butcher, 2008), it is unconditionally stable.

Code and data availability. The source files of the code and the forcing data are provided at https://doi.org/10.5281/zenodo.10426228.

Author contributions. The research was designed by KF, JB and MD. MD acquired funding. The numerical models were developed by KF with the help of JB. The numerical simulations were performed by KF with the help of FB. FB and MD provided data for the simulations. The manuscript was written by KF with the help of all co-authors.

Competing interests. The authors declare having no competing interests.

Acknowledgements. We are thankful to the authors of Potocki et al., (2022) for making the meteorological forcings used in their study available. We acknowledge Marion Réveillet, Matthieu Lafaysse, Isabelle Gouttevin for the fruitful discussions on surface energy balance modeling and we acknowledge Clément Cancès for those on FVM modeling and fictitious variables. KF, JB and MD have received funding from the European Research Council (ERC) under the European Union's Horizon 2020 research and innovation program (IVORI, grant no. 949516). CNRM/CEN is part of Labex OSUG (ANR10 LABX56). We thank Richard Essery, Michael Lehning, and the two anonymous referees for their helpful reviews of the article, as well as Danilo Mello for editing it.

References

Albert, M. R.: Computer models for two-dimensional transient heat conduction, https://apps.dtic.mil/sti/pdfs/ADA134893.pdf, last accessed: 30/11/2023, 1983.

Anderson, E. A.: A point energy and mass balance model of a snow cover, https://repository.library.noaa.gov/view/noaa/6392, last accessed: 30/11/2023, 1976.

Barnett, T. P., Adam, J. C., and Lettenmaier, D. P.: Potential impacts of a warming climate on water availability in snow-dominated regions, Nature, 438, 303–309, https://doi.org/10.1038/nature04141, 2005.

Barrett, A. I., Wellmann, C., Seifert, A., Hoose, C., Vogel, B., and Kunz, M.: One Step at a Time: How Model Time Step Significantly Affects Convection-Permitting Simulations, J. Adv. Model. Earth Syst., 11, 641–658, https://doi.org/10.1029/2018MS001418, 2019.

Bartelt, P. and Lehning, M.: A physical SNOWPACK model for the Swiss avalanche warning: Part I: numerical model, Cold Regions Sci. Tech., 35, 123–145, https://doi.org/10.1016/S0165-232X(02)00074-5, 2002.

Bassetto, S.: Vers une prise en compte plus robuste et précise des effets capillaires lors de simulations d'écoulements multiphasiques en milieux poreux, Ph.D. thesis, Université de Lille, https://pepite-depot.univ-lille.fr/LIBRE/EDMADIS/2021/2021LILUB022.pdf, last accessed: 01/09/2023, 2021.

Bassetto, S., Cancès, C., and Tran, Q. H.: Robust Newton Solver Based on Variable Switch for a Finite Volume Discretization of Richards Equation, in: Finite Volumes for Complex Applications IX - Methods, Theoretical Aspects, Examples, edited by Klöfkorn, R., Keilegavlen, E., Radu, F. A., and Fuhrmann, J., vol. 253, pp. 385–393, Springer International Publishing, https://doi.org/10.1016/j.jcp.2013.06.041, 2020.

Bintanja, R. and Broeke, M. R. V. D.: The Surface Energy Balance of Antarctic Snow and Blue Ice, J. Appl. Meteorol. Climatol., 34, 902 – 926, https://doi.org/10.1175/1520-0450(1995)034<0902:TSEBOA>2.0.CO;2, 1995.

Brondex, J., Fourteau, K., Dumont, M., Hagenmuller, P., Calonne, N., Tuzet, F., and Löwe, H.: A finite-element framework to explore the numerical solution of the coupled problem of heat conduction, water vapor diffusion and settlement in dry snow (IvoriFEM v0.1.0), Geosci. Model Dev. Discuss., 2023, 1–50, https://doi.org/10.5194/gmd-2023-97, 2023.

Brun, E., Martin, , Simon, V., Gendre, C., and Coleou, C.: An Energy and Mass Model of Snow Cover Suitable for Operational Avalanche Forecasting, J. Glaciol., 35, 333–342, https://doi.org/10.3189/S0022143000009254, 1989.

Brun, F., King, O., Réveillet, M., Amory, C., Planchot, A., Berthier, E., Dehecq, A., Bolch, T., Fourteau, K., Brondex, J., Dumont, M., Mayer, C., and Wagnon, P.: Brief communication: Everest South Col Glacier did not thin during the last three decades, The Cryosphere Discussions, 2022, 1–27, https://doi.org/10.5194/tc-2022-166, 2022.

Butcher, J.: Numerical methods for ordinary differential equations, "John Wiley & Sons, Ltd, The Atrium, Southern Gate, Chichester, West Sussex PO19 8SQ, England", 2008.

Calonne, N., Flin, F., Morin, S., Lesaffre, B., du Roscoat, S. R., and Geindreau, C.: Numerical and experimental investigations of the effective thermal conductivity of snow, Geophy. Res. Lett., 38, https://doi.org/10.1029/2011GL049234, 2011.

Ciarlet, P. and Raviart, P.-A.: Maximum principle and uniform convergence for the finite element method, Comput. Methods Appl. Mech. Eng., 2, 17–31, https://doi.org/10.1016/0045-7825(73)90019-4, 1973.

Covi, F., Hock, R., and Reijmer, C. H.: Challenges in modeling the energy balance and melt in the percolation zone of the Greenland ice sheet, J. Glaciol., 69, 164–178, https://doi.org/10.1017/jog.2022.54, 2023.

Davies, J. H.: Global map of solid Earth surface heat flow, Geochem., Geophys., Geosys., 14, 4608–4622, https://doi.org/10.1002/ggge.20271, 2013.

Decharme, B., Boone, A., Delire, C., and Noilhan, J.: Local evaluation of the Interaction between Soil Biosphere Atmosphere soil multilayer diffusion scheme using four pedotransfer functions, J. Geophys. Res.: Atmos., 116, https://doi.org/10.1029/2011JD016002, 2011.

Dutra, E., Balsamo, G., Viterbo, P., Miranda, P. M. A., Beljaars, A., Schär, C., and Elder, K.: An Improved Snow Scheme for the ECMWF Land Surface Model: Description and Offline Validation, J. Hydrometeo., 11, 899 – 916, https://doi.org/10.1175/2010JHM1249.1, 2010.

Etchevers, P., Martin, E., Brown, R., Fierz, C., Lejeune, Y., Bazile, E., Boone, A., Dai, Y.-J., Essery, R., Fernandez, A., and et al.: Validation of the energy budget of an alpine snowpack simulated by several snow models (Snow MIP project), Ann. Glaciol., 38, 150–158, https://doi.org/10.3189/172756404781814825, 2004.

Fazio, R.: Stiffness in numerical initial-value problems: A and L-stability of numerical methods, Int. J. Math. Educ. Sci. Tech., 32, 752–760, https://doi.org/10.1080/0020739011753124619, 2001.

Flanner, M. G., Shell, K. M., Barlage, M., Perovich, D. K., and Tschudi, M.: Radiative forcing and albedo feedback from the Northern Hemisphere cryosphere between 1979 and 2008, Nature Geoscience, 4, 151–155, https://doi.org/10.1038/ngeo1062, 2011.

Foken, T.: Micrometeorology, 2, Springer Berlin, Heidelberg, https://doi.org/10.1007/978-3-642-25440-6, 2017.

Jordan, R. E.: A one-dimensional temperature model for a snow cover: Technical documentation for SNTHERM. 89, http://hdl.handle.net/11681/11677, last accessed: 01/09/2023, 1991.

Kadioglu, S. Y., Nourgaliev, R. R., and Mousseau, V. A.: A Comparative Study of the Harmonic and Arithmetic Averaging of Diffusion Coefficients for Non-linear Heat Conduction Problems, Tech. rep., Idaho National Laboratory, Idaho Falls, Idaho 83415, https://doi.org/10.2172/928087, 2008.

Kuipers Munneke, P., van den Broeke, M. R., King, J. C., Gray, T., and Reijmer, C. H.: Near-surface climate and surface energy budget of Larsen C ice shelf, Antarctic Peninsula, The Cryosphere, 6, 353–363, https://doi.org/10.5194/tc-6-353-2012, 2012.

Lejeune, Y., Dumont, M., Panel, J.-M., Lafaysse, M., Lapalus, P., Le Gac, E., Lesaffre, B., and Morin, S.: 57 years (1960–2017) of snow and meteorological observations from a mid-altitude mountain site (Col de Porte, France, 1325 m of altitude), Earth Sys. Sci. Data, 11, 71–88, https://doi.org/10.5194/essd-11-71-2019, 2019.

Lide, D. R.: CRC handbook of chemistry and physics, 87 edn., Taylor and Francis, Boca Raton, FL, 2006.

Liston, G. E. and Elder, K.: A Distributed Snow-Evolution Modeling System (SnowModel), J. Hydrometeorol., 7, 1259 – 1276, https://doi.org/10.1175/JHM548.1, 2006.

Martin, E. and Lejeune, Y.: Turbulent fluxes above the snow surface, Ann. Glaciol., 26, 179–183, https://doi.org/10.3189/1998AoG26-1-179-183, 1998.

Menard, C. B., Essery, R., Krinner, G., Arduini, G., Bartlett, P., Boone, A., Brutel-Vuilmet, C., Burke, E., Cuntz, M., Dai, Y., Decharme, B., Dutra, E., Fang, X., Fierz, C., Gusev, Y., Hagemann, S., Haverd, V., Kim, H., Lafaysse, M., Marke, T., Nasonova, O., Nitta, T., Niwano, M., Pomeroy, J., Schädler, G., Semenov, V. A., Smirnova, T., Strasser, U., Swenson, S., Turkov, D., Wever, N., and Yuan, H.: Scientific and Human Errors in a Snow Model Intercomparison, Bull. Am. Meteorol. Soc., 102, E61 – E79, https://doi.org/10.1175/BAMS-D-19-0329.1, 2021.

Meyer, C. R. and Hewitt, I. J.: A continuum model for meltwater flow through compacting snow, The Cryosphere, 11, 2799–2813, https://doi.org/10.5194/tc-11-2799-2017, 2017.

Miller, N. B., Shupe, M. D., Cox, C. J., Noone, D., Persson, P. O. G., and Steffen, K.: Surface energy budget responses to radiative forcing at Summit, Greenland, The Cryosphere, 11, 497–516, https://doi.org/10.5194/tc-11-497-2017, 2017.

Morin, S., Domine, F., Arnaud, L., and Picard, G.: In-situ monitoring of the time evolution of the effective thermal conductivity of snow, Cold Regions Sci. Tech., 64, 73–80, https://doi.org/10.1016/j.coldregions.2010.02.008, international Snow Science Workshop 2009 Davos, 2010.

Oerlemans, J., Giesen, R., and Van Den Broeke, M.: Retreating alpine glaciers: increased melt rates due to accumulation of dust (Vadret da Morteratsch, Switzerland), J. Glaciol., 55, 729–736, https://doi.org/10.3189/002214309789470969, 2009.

Pepper, D. and Heinrich, J.: The Finite Element Method, Taylor and Francis Group, Boca Raton, FL, 2005.

Potocki, M., Mayewski, P. A., Matthews, T., Perry, L. B., Schwikowski, M., Tait, A. M., Korotkikh, E., Clifford, H., Kang, S., Sherpa, T. C., Singh, P. K., Koch, I., and Birkel, S.: Mt. Everest's highest glacier is a sentinel for accelerating ice loss, npj Clim. Atmos. Sci., 5, 7, https://doi.org/10.1038/s41612-022-00230-0, 2022.

Sauter, T., Arndt, A., and Schneider, C.: COSIPY v1.3 – an open-source coupled snowpack and ice surface energy and mass balance model, Geosci. Model Dev., 13, 5645–5662, https://doi.org/10.5194/gmd-13-5645-2020, 2020.

Schmidt, L. S., Aðalgeirsdóttir, G., Guðmundsson, S., Langen, P. L., Pálsson, F., Mottram, R., Gascoin, S., and Björnsson, H.: The importance of accurate glacier albedo for estimates of surface mass balance on Vatnajökull: evaluating the surface energy budget in a regional climate model with automatic weather station observations, The Cryosphere, 11, 1665–1684, https://doi.org/10.5194/tc-11-1665-2017, 2017.

Tubini, N., Gruber, S., and Rigon, R.: A method for solving heat transfer with phase change in ice or soil that allows for large time steps while guaranteeing energy conservation, The Cryosphere, 15, 2541–2568, https://doi.org/10.5194/tc-15-2541-2021, 2021.

Ubbiali, S., Schär, C., Schlemmer, L., and Schulthess, T. C.: A Numerical Analysis of Six Physics-Dynamics Coupling Schemes for Atmospheric Models, J. Adv. Model. Earth Sys., 13, e2020MS002 377, https://doi.org/10.1029/2020MS002377, 2021.

van Kampenhout, L., Lenaerts, J. T. M., Lipscomb, W. H., Sacks, W. J., Lawrence, D. M., Slater, A. G., and van den Broeke, M. R.: Improving the Representation of Polar Snow and Firn in the Community Earth System Model, J. Adv. Model. Earth Sys., 9, 2583–2600, https://doi.org/10.1002/2017MS000988, 2017.

van Pelt, W. J. J., Oerlemans, J., Reijmer, C. H., Pohjola, V. A., Pettersson, R., and van Angelen, J. H.: Simulating melt, runoff and refreezing on Nordenskiöldbreen, Svalbard, using a coupled snow and energy balance model, The Cryosphere, 6, 641–659, https://doi.org/10.5194/tc-6-641-2012, 2012.

Vernay, M., Lafaysse, M., Monteiro, D., Hagenmuller, P., Nheili, R., Samacoïts, R., Verfaillie, D., and Morin, S.: The S2M meteorological and snow cover reanalysis over the French mountainous areas: description and evaluation (1958–2021), Earth Sys. Sci. Data, 14, 1707–1733, https://doi.org/10.5194/essd-14-1707-2022, 2022.

Versteeg, H. and Malalasekera, W.: An Introduction to Computational Fluid Dynamics, Pearson Education Limited, Essex CM20 2JE, England, 2007.

Vionnet, V., Brun, E., Morin, S., Boone, A., Faroux, S., Le Moigne, P., Martin, E., and Willemet, J.-M.: The detailed snowpack scheme Crocus and its implementation in SURFEX v7.2, Geosci. Model Dev., 5, 773–791, https://doi.org/10.5194/gmd-5-773-2012, 2012.

Wang, X. and Tchelepi, H. A.: Trust-region based solver for nonlinear transport in heterogeneous porous media, J. Comput. Phys., 253, 114–137, https://doi.org/10.1016/j.jcp.2013.06.041, 2013.

Westermann, S., Ingeman-Nielsen, T., Scheer, J., Aalstad, K., Aga, J., Chaudhary, N., Etzelmüller, B., Filhol, S., Kääb, A., Renette, C., Schmidt, L. S., Schuler, T. V., Zweigel, R. B., Martin, L., Morard, S., Ben-Asher, M., Angelopoulos, M., Boike, J., Groenke, B., Miesner, F., Nitzbon, J., Overduin, P., Stuenzi, S. M., and Langer, M.: The CryoGrid community model (version 1.0) – a multi-physics toolbox for climate-driven simulations in the terrestrial cryosphere, Geosci. Model Dev., 16, 2607–2647, https://doi.org/10.5194/gmd-16-2607-2023, 2023.

Wever, N., Rossmann, L., Maaß, N., Leonard, K. C., Kaleschke, L., Nicolaus, M., and Lehning, M.: Version 1 of a sea ice module for the physics-based, detailed, multi-layer SNOWPACK model, Geoscientific Model Development, 13, 99–119, https://doi.org/10.5194/gmd-13-99-2020, 2020.

Zhang, F.: The Schur complement and its applications, vol. 4, Springer Science & Business Media, 2006.